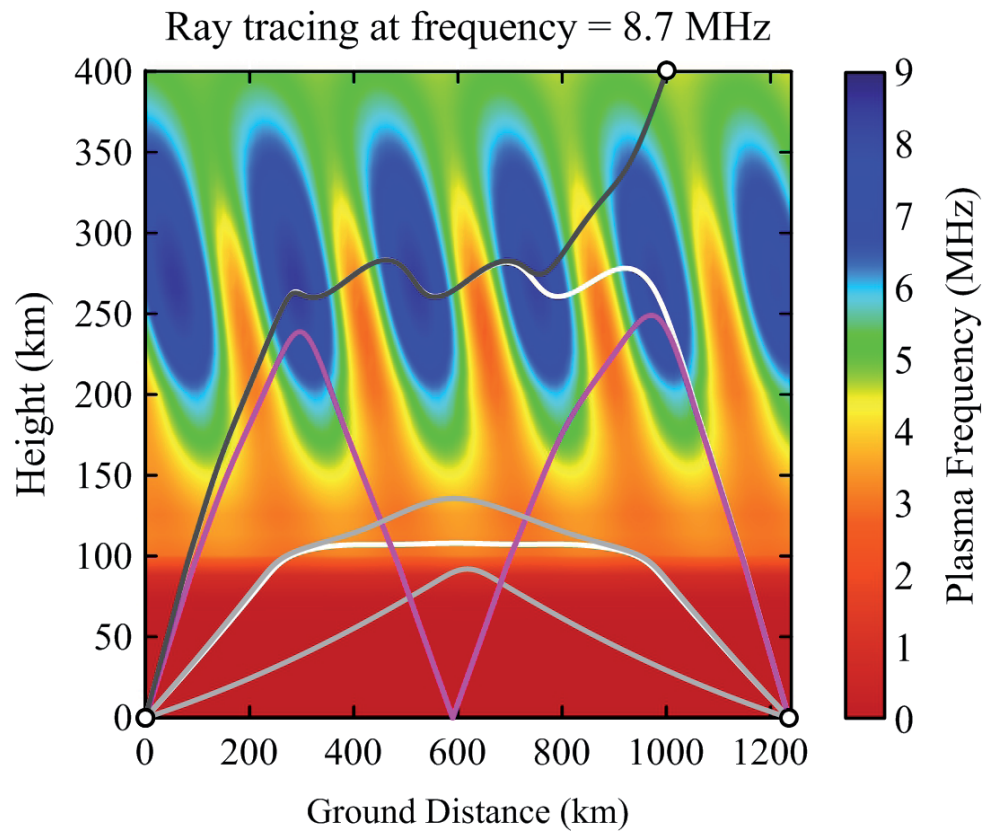
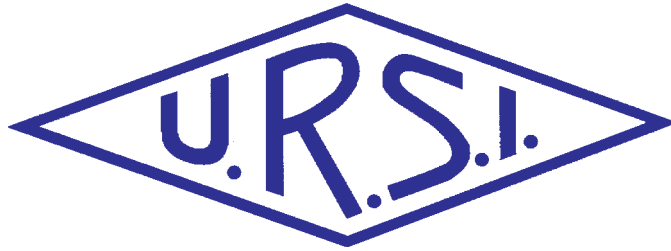


INTERNATIONAL
UNION OF
RADIO SCIENCE

UNION
RADIO-SCIENTIFIQUE
INTERNATIONALE



No 361
June 2017

Contents

Radio Science Bulletin Staff	4
URSI Officers and Secretariat.....	7
Editor’s Comments	9
President’s Message	11
Special Issue on the URSI AP-RASC 2016 Student Paper Competition	12
Application of the Optimization Method to the Point-to-Point Radio Wave Ray-Tracing Problem.....	14
Suppression of Multi-Path Couplings in Scaled-Down Experiment for Cross-Borehole Pulse Radar	20
RF Output-Power Enhancement by Optical-Pulse Compression in Photonic- Based RF Generation.....	26
Survey of Emerging Information Teleportation Networks and Protocols.....	34
URSI France 2017 Workshop on Radio Science for Humanity - Journées scientifiques URSI-France 2017 Radiosciences au service de l’humanité (Part 2)	55
Copernicus, A Major European Cooperation Program: From the Early Concept to Operational Services	55
Call for Papers AT-RASC 2018.....	62
In Memoriam: Michael C. Sexton	63
Call for Papers FEM 2018.....	64
Book Review	65
Et Cetera	68
Ethically Speaking	69
Solution Box.....	71
Early Career Representative Column.....	75
Women in Radio Science	80
Education Column	83
Call for papers 2018 IEEE AP-S & USNC-URSI Radio Science Meeting.....	85
D. V. Giri Receives Indian Awards	86
Clerk Maxwell Foundation Newsletter	86
Call for Papers NRSC 2018.....	87
3rd Indian URSI Regional Conference on Radio Science	88
Report on the Egyptian 34th National Radio Science Conference (NRSC2017)	92
URSI Conference Calendar.....	98
Information for Authors.....	99
Become An Individual Member of URSI.....	100

(Cover) The results of point-to-point ray tracing calculations using the nudged elastic-band method at a frequency of 8.7 MHz between Kaliningrad and Tromsö for daytime summer solstice. The white solid lines are for the high ray. The grey solid line is for the low ray. The black solid and dashed line is for the trans-ionospheric ray. The pink solid line is for the multi-hop ray. The electron density given by the IRI-2007 model was perturbed by TIDs. See the paper by I. A. Nosikov, M. V. Klimenko, P. F. Bessarab, and G. A. Zhabankov in the Special Section on the URSI AP-RASC 2016 Student Paper Competition, pp. 14-19.

The International Union of Radio Science (URSI) is a foundation Union (1919) of the International Council of Scientific Unions as direct and immediate successor of the Commission Internationale de Télégraphie Sans Fil which dates from 1914.

Unless marked otherwise, all material in this issue is under copyright © 2017 by Radio Science Press, Belgium, acting as agent and trustee for the International Union of Radio Science (URSI). All rights reserved. Radio science researchers and instructors are permitted to copy, for non-commercial use without fee and with credit to the source, material covered by such (URSI) copyright. Permission to use author-copyrighted material must be obtained from the authors concerned.

The articles published in the Radio Science Bulletin reflect the authors' opinions and are published as presented. Their inclusion in this publication does not necessarily constitute endorsement by the publisher.

Neither URSI, nor Radio Science Press, nor its contributors accept liability for errors or consequential damages.

Radio Science Bulletin Staff

Editor

W. R. Stone

Stoneware Limited
840 Armada Terrace
San Diego, CA 92106, USA
Tel: +1-619 222 1915, Fax: +1-619 222 1606
E-mail: r.stone@ieee.org

Editor-in-Chief

P. Lagasse

URSI Secretariat
Ghent University - INTEC
Technologiepark - Zwijnaarde 15
B-9052 Gent, BELGIUM
Tel: +32 9-264 33 20, Fax: +32 9-264 42 88
E-mail: lagasse@intec.ugent.be

Production Editors

I. Lievens

I. Heleu

URSI Secretariat / Ghent University - INTEC
Technologiepark - Zwijnaarde 15
B-9052 Gent, BELGIUM
Tel: +32 9-264.33.20, Fax: +32 9-264.42.88
E-mail: ingeursi@intec.ugent.be, info@ursi.org

Senior Associate Editors

A. Pellinen-Wannberg

Department of Physics
Umea University
BOX 812
SE-90187 Umea, SWEDEN
Tel: +46 90 786 74 92, Fax: +46 90 786 66 76
E-mail: asta.pellinen-wannberg@umu.se

O. Santolik

Institute of Atmospheric Physics
Academy of Sciences of the Czech Republic
Bocni II
1401, 141 31 Prague 4, CZECH REPUBLIC
Tel: +420 267 103 083, Fax +420 272 762 528
E-mail os@ufa.cas.cz, santolik@gmail.com

Associate Editors, Commissions

Commission A

P. Tavella

INRIM
Strada delle Cacce 91
10135 Torino, ITALY
Tel: +39 011 3919235, Fax: +39 011 3919259
E-mail: tavella@inrim.it

P. M. Duarte Cruz

Instituto de Telecomunicações
Campus Universitário de Santiago
P-3810-193 Aveiro, PORTUGAL
Tel: +351 234377900
E-mail: pcruez@av.it.pt

Commission B

K. Kobayashi

Dept. of Electrical, and Communication Engineering
Chuo University
1-13-27 Kasuga, Bunkyo-ku
Tokyo, 112-8551, JAPAN
Tel: +81 3 3817 1846/69, Fax: +81 3 3817 1847
E-mail: kazuya@tamacc.chuo-u.ac.jp

L. Li

School of EECS
Peking University
Room 2843N, Science Building#2
Beijing 100871, CHINA CIE
Tel: +86-10-62754409-2, Fax: +86-10-62754409
E-mail: lianlin.li@pku.edu.cn

Commission C

S. E. El-Khamy

Dept. of Electrical Engineering
Alexandria University - Faculty of Engineering
Abou-Keer Street
Alexandria 21544, EGYPT
Tel: +2010-1497360, Fax: +203 5971853
E-mail: elkhamy@ieee.org, said.elkhamy@gmail.com

A. I. Zaghloul

Ece, Virginia Tech
7054 Haycock Rd
22043 Falls Church, USA
Tel: +1-703-538-8435, Fax: +1-703-538-8450
E-mail: amirz@vt.edu

Commission D

G. Gradoni

School of Mathematical Sciences
University of Nottingham
University Park
Nottingham NG7 2RD, UNITED KINGDOM
Tel: +44(0)7745368300, Fax: +44(0)1159514951
E-mail: gabriele.gradoni@gmail.com, gabriele.gradoni@nottingham.ac.uk

Commission E

F. Gronwald

Hamburg University of Technology
Harburger Schloss Strasse 20
21079 Hamburg, GERMANY
Tel: +49-40-42878-2177
E-mail: gronwald@tuhh.de

G. Gradoni

School of Mathematical Sciences
University of Nottingham
University Park
Nottingham NG7 2RD, UNITED KINGDOM
Tel: +44(0)7745368300, Fax: +44(0)1159514951
E-mail: gabriele.gradoni@gmail.com, gabriele.gradoni@nottingham.ac.uk

Commission F

V. Chandrasekar

Engineering B117
Colorado State University
Fort Collins, Colorado 80523, USA
Tel: +1 970 491 7981, Fax: +1 970 491 2249
E-mail: chandra@engr.colostate.edu, chandra.ve@gmail.com

M. Kurum

Department of Electrical and Computer Engineering
Mississippi State University
406 Hardy Rd., Simrall Bldg., Room: 236
Mississippi State, MS 39762, USA
Tel: +1 662 325 2148
E-mail: kurum@ece.msstate.edu, mkurum@gmail.com

Commission G

P. Doherty

Institute for Scientific Research
Boston College
140 Commonwealth Avenue
Chestnut Hill, MA 02467, USA
Tel: +1 617 552 8767, Fax: +1 617 552 2818
E-mail: Patricia.Doherty@bc.edu

Commission H

J. Lichtenberger

Eötvös University
Pazmany Peter Setany 1/a
H-1111 Budeapest
HUNGARY
Tel: +36 1 209 0555 x6654, Fax +36 1 372 2927
E-mail lityi@sas.elte.hu

W. Li

UCLA
7127 Math Sciences Bldg
405 Hilgard Avenue
Los Angeles, CA, 90095, USA
E-mail: moonli@atmos.ucla.edu

Commission J

J. W. M. Baars

Mm-astronomy
Max Planck Institute for Radio Astronomy
Auf dem Hügel 69
53121 Bonn, GERMANY
Tel: +49-228-525303
E-mail: jacobbaars@arcor.de

Commission K

P. Mojabi

Room E3-504B, EITC Building
Electrical and Computer Engineering Department
University of Manitoba
Winnipeg, R3T5V6, CANADA
Tel: +1 204 474 6754, Fax: +1 204 261 4639
E-mail: Puyan.Mojabi@umanitoba.ca

Associate Editors, Columns

Book Reviews

G. Trichopoulos

Electrical, Computer & Energy Engineering ISTB4 555D
Arizona State University
781 E Terrace Road, Tempe, AZ, 85287 USA
Tel: +1 (614) 364-2090
E-mail: gtrichop@asu.edu

Solution Box

Ö. Ergül

Department of Electrical and Electronics Engineering
Middle East Technical University
TR-06800, Ankara, Turkey
E-mail: ozgur.ergul@eee.metu.edu.tr

Historical Papers

J. D. Mathews

Communications and Space Sciences Lab (CSSL)
The Pennsylvania State University
323A, EE East
University Park, PA 16802-2707, USA
Tel: +1(814) 777-5875, Fax: +1 814 863 8457
E-mail: JDMathews@psu.edu

Telecommunications Health & Safety

J. C. Lin

University of Illinois at Chicago
851 South Morgan Street, M/C 154
Chicago, IL 60607-7053 USA
Tel: +1 312 413 1052, Fax: +1 312 996 6465
E-mail: lin@uic.edu

Et Cetera

T. Akgül

Dept. of Electronics and Communications Engineering
Telecommunications Division
Istanbul Technical University
80626 Maslak Istanbul, TURKEY
Tel: +90 212 285 3605, Fax: +90 212 285 3565
E-mail: tayfunakgul@itu.edu.tr.

Historical Column

G. Pelosi

Department of Information Engineering
University of Florence
Via di S. Marta, 3, 50139 Florence, Italy
E-mail: giuseppe.pelosi@unifi.it

Women in Radio Science

A. Pellinen-Wannberg

Department of Physics and Swedish Institute of Space
Physics
Umeå University
S-90187 Umeå, Sweden
Tel: +46 90 786 7492
E-mail: asta.pellinen-wannberg@umu.se

Early Career Representative Column

S. J. Wijnholds

Netherlands Institute for Radio Astronomy
Oude Hoogeveensedijk 4
7991 PD Dwingeloo, The Netherlands
E-mail: wijnholds@astron.nl

Ethically Speaking

R. L. Haupt

Colorado School of Mines
Brown Building 249
1510 Illinois Street, Golden, CO 80401 USA
Tel: +1 (303) 273 3721
E-mail: rhaupt@mines.edu

Education Column

Madhu Chandra

Microwave Engineering and Electromagnetic Theory
Technische Universität Chemnitz
Reichenhainerstrasse 70
09126 Germany
E-mail: madhu.chandra@etit.tu-chemnitz.de

A. J. Shockley

E-mail: aj4317@gmail.com

URSI Officers and Secretariat

Current Officers triennium 2014-2017



President

P. S. Cannon
Gisbert Kapp Building
University of Birmingham
Edgbaston, Birmingham, B15 2TT,
UNITED KINGDOM
Tel: +44 (0) 7990 564772
Fax: +44 (0)121 414 4323
E-mail: p.cannon@bham.ac.uk
president@ursi.org



Vice President

M. Ando
Dept. of Electrical & Electronic Eng.
Graduate School of Science and Eng.
Tokyo Institute of Technology
S3-19, 2-12-1 O-okayama, Meguro
Tokyo 152-8552
JAPAN
Tel: +81 3 5734-2563
Fax: +81 3 5734-2901
E-mail: mando@antenna.ee.titech.ac.jp



Past President

P. Wilkinson
Bureau of Meteorology
P.O. Box 1386
Haymarket, NSW 1240
AUSTRALIA
Tel: +61 2-9213 8003
Fax: +61 2-9213 8060
E-mail: p.wilkinson@bom.gov.au



Vice President

Y. M. M. Antar
Electrical Engineering Department
Royal Military College
POB 17000, Station Forces
Kingston, ON K7K 7B4
CANADA
Tel: +1-613 541-6000 ext.6403
Fax: +1-613 544-8107
E-mail: antar-y@rmc.ca



Secretary General

P. Lagasse
URSI Secretariat
Ghent University - INTEC
Technologiepark - Zwijnaarde 15
B-9052 Gent
BELGIUM
Tel: +32 9-264 33 20
Fax: +32 9-264 42 88
E-mail: lagasse@intec.ugent.be



Vice President

U. S. Inan
Director, STAR Laboratory
Electrical Eng. Dept
Stanford University
Packard Bldg. Rm. 355
350 Serra Mall
Stanford, CA 94305, USA
Tel: +1-650 723-4994
Fax: +1-650 723-9251
E-mail: inan@stanford.edu
uinan@ku.edu.tr



Vice President

S. Ananthkrishnan
Electronic Science Department
Pune University
Ganeshkhind, Pune 411007
INDIA
Tel: +91 20 2569 9841
Fax: +91 20 6521 4552
E-mail: subra.anan@gmail.com

URSI Secretariat



Secretary General

P. Lagasse
URSI Secretariat
Ghent University - INTEC
Technologiepark - Zwijnaarde 15
B-9052 Gent
BELGIUM
Tel: +32 9-264 33 20
Fax: +32 9-264 42 88
E-mail: lagasse@intec.ugent.be



Assistant Secretary General AP-RASC

K. Kobayashi
Dept. of Electr and Commun. Eng,
Chuo University
1-13-27 Kasuga, Bunkyo-ku
Tokyo, 112-8551
JAPAN
Tel: +81 3 3817 1846/69
Fax: +81 3 3817 1847



Assistant Secretary General

P. Van Daele
INTEC- IBBT
Ghent University
Technologiepark - Zwijnaarde 15
B-9052 Gent
BELGIUM
Tel: +32 9 331 49 06
Fax +32 9 331 48 99
E-mail peter.vandaele@intec.Ugent.be



Executive Secretary

I. Heleu
URSI Secretariat
Ghent University - INTEC
Technologiepark - Zwijnaarde 15
B-9052 Gent
BELGIUM
Tel. +32 9-264.33.20
Fax +32 9-264.42.88
E-mail info@urisi.org



Assistant Secretary General Publications & GASS

W. R. Stone
840 Armada Terrace
San Diego, CA 92106
USA
Tel: +1-619 222 1915
Fax: +1-619 222 1606
E-mail: r.stone@ieee.org



Administrative Secretary

I. Lievens
URSI Secretariat
Ghent University - INTEC
Technologiepark - Zwijnaarde 15
B-9052 Gent
BELGIUM
Tel: +32 9-264.33.20
Fax: +32 9-264.42.88
E-mail: ingeursi@intec.ugent.be



Assistant Secretary General AT-RASC

P. L. E. Uslenghi
Dept. of ECE (MC 154)
University of Illinois at Chicago 851
S. Morgan Street
Chicago, IL 60607-7053
USA
Tel: +1 312 996-6059
Fax: +1 312 996 8664
E-mail: uslenghi@uic.edu



W. Ross Stone

Stoneware Limited
840 Armada Terrace
San Diego, CA 92106, USA
Tel: +1-619 222 1915, Fax: +1-619 222 1606
E-mail: r.stone@ieee.org

Special Section on the URSI AP-RASC2016 Student Paper Competition

We have a special section consisting of papers invited from three of the awardees from the URSI AP-RASC 2016 Student Paper Competition. There is a separate Foreword describing the papers, so I won't go into details. However, these three papers are of excellent quality and deal with very interesting topics: a new optimization method for ray-tracing in the ionosphere, improvements in cross-borehole pulse radar, and a method to enhance RF power output using optical pulse compression in photonic-based RF generation. With these as examples of what our students are doing, URSI's future looks bright!

Second Part of Special Section on Radio Science for Humanity: URSI-France 2017 Workshop

The second part of the special section on the URSI-France 2017 Workshop (the first part appeared in the March issue) is one paper. However, it is a very interesting paper: it provides an overview of the Copernicus program. This includes the scientific, organizational, and funding aspects, as well as the plans for the future.

Quantum Communications

Quantum communications is a fascinating topic. In many cases, it involves what Einstein referred to as "spooky action at a distance." Tremendous advances have been made in quantum communications and quantum teleportation in the last few years. Ronald Meyers, Arnold Tunick, Keith Deacon, and Philip Hemmer have provided us with a comprehensive survey of the work on networks

and protocols in this field. Their paper is written so that someone who is new to the field can understand it, and can gain an appreciation for the various approaches being taken. They have provided an insightful overview of an important area of research, and supported it with a comprehensive introduction to the relevant literature for those wishing to learn more about a particular aspect.

Our Other Contributions

Paul Cannon shares his final comments from his term as URSI President in his President's Message in this issue. Read them: they are addressed to the people who are the future of URSI.

There are certain books that set the standard in their fields. Jacob Baars provides a comprehensive review of the newest edition of the standard for books on *Interferometry and Synthesis in Radio Astronomy*. Best of all, the book is available for free!

Be sure to take a look at Tayfun Akgul's Et Cetera column: you will enjoy it.

In Stefan Wijnholds' ECR Column, Chat Hull provides some very useful advice regarding how to prepare and present a paper. I urge everyone to read this before presenting their next paper: it will definitely improve our conferences!

Madhu Chandra is starting a new Education Column in this issue. He is looking for contributions and suggestions, and he offers a quiz.

Randy Haupt and Amy Shockley have some interesting observations regarding thinking about boxes in the Ethically Speaking column.

The Solution Box deals with two problems involving photonic crystals. Şirin Yazar, Barışcan Karaosmanoğlu,

and Özgür Ergül present one set of solutions, but there may well be better solutions available. They are looking for suggestions – and what they have is interesting on its own.

Asta Pellinen-Wannberg brings us the story of Yuka Sato. She shares her experiences as a woman radio scientist in Japan. I think you will enjoy her story.

The Radio Science Bulletin on Xplore

With this issue, the link that you will receive in the e-mail announcing the issue will connect you to the *Radio Science Bulletin* on IEEE Xplore. Currently, each issue of the *Bulletin* appears on Xplore as a collection of the individual articles, columns, calls for papers, etc. that make up the issue. If you want to download a PDF of the full issue, you can still do that from the URSI Web site. We are working on making the full PDF available on the Xplore site, as well.

AT-RASC 2018 is Coming!

AT-RASC 2018 will be held May 28-June 1, 2018, in the same venue as in 2015: the ExpoMeloneras Convention Centre, Gran Canaria, in the Canary Islands, Spain. As I've written before, this is an amazingly beautiful location for a conference, and it also has a very good conference facility. The deadline for paper submission is **January 10, 2018**. Details are available at the Web site: www.at-rasc.org. There is a program for young scientists and a student paper competition. Note that some of the best flights (in terms of price and schedule) to Gran Canaria are offered by charter airlines, rather than by the major carriers. Information on those will be made available on the AT-RASC Web site. I urge you to start planning now to attend.



President's Message



P. S. Cannon
Gisbert Kapp Building
University of Birmingham
Edgbaston, Birmingham, B15 2TT, UK
E-mail: p.cannon@bham.ac.uk

This is my final opportunity to write in the *RSB* as URSI President, and I want to use the opportunity to write about our Young Scientists.

URSI invests considerable resources – that means money and time – in its Young Scientist program. If we have chosen well, the Young Scientists attending our flagship meetings are the scientific leaders of the future, and I hope of URSI, as well. Being a Young Scientist can kick-start a career, and notably a number of our General Lecturers were once URSI Young Scientists.

If you are fortunate enough to be selected as a Young Scientist at an URSI flagship meeting, then please use the opportunity to listen and contribute to both the scientific sessions and the running of your Commission. Please also talk to other Young Scientists, and indeed, the old scientists. Try to meet the Early Career Representatives (ECRs) from each Commission, and tell them how you would like to see URSI develop. Don't forget you can contact the ECRs after the meeting by e-mail (contact details can be found on the URSI Web site).

In times of financial uncertainty, we humans become increasingly factional; you can see this in history, and there are worrying trends today. However, thankfully, science continues on a path of globalization. We do, though, have

a long way to go in this respect. If we consider the world to be represented by a village of 100 people, 60 will be from Asia, 14 will be from Africa, 11 will be from Europe, nine will be from South America, and only five will be from North America. Quite clearly, this distribution is not represented in a typical scientific conference, and we all know the historical and economic reasons for this.

URSI does not pretend to be able to change the world on its own, but we can all make our own small contributions. It is the Young Scientists, near the start of their careers, who can make the biggest difference. You may say, as a Young Scientist what can I do? The answer is of course different for each of you, but I would like to leave you with two thoughts.

The first is to choose research topics that matter. The important thing is not to be tempted to dot "I's" and cross "T's." Secondly, and perhaps more importantly, you URSI Young Scientists have been gifted good brains and, through this scheme, opportunity. Don't squander those gifts: use them to help your fellow countrymen and women – and all of us. It is my hope that many of the Young Scientists attending the GASS will stay with URSI, and that we will see them again at the Atlantic and Asia meetings of URSI in 2018 and 2019. Hopefully, we will also see them at the next General Assembly in 2020, when they will be less "young."

Special Issue on the URSI AP-RASC 2016 Student Paper Competition

The 2016 URSI Asia-Pacific Radio Science Conference (URSI AP-RASC 2016) was held at the Grand Hilton Seoul Hotel, Seoul, South Korea, August 21-25, 2016 [1, 2]. This special issue provides a collection of invited papers by the recipients of the awards from the URSI AP-RASC 2016 Student Paper Competition.

According to the tradition of the AP-RASC conferences, the Student Paper Competition (SPC) was organized at URSI AP-RASC 2016 jointly by URSI and the South Korea National Committee of URSI. In order to review the Student Paper Competition applications and select the recipients, the URSI AP-RASC 2016 Young Scientist Program Committee was formed, as follows:

Chair: Peter Van Daele, URSI Assistant Secretary-General (Ghent University)

Co-Chairs: Paul S. Cannon, URSI President (University of Birmingham); Jeong-Hae Lee (Hongik University); Ikmo Park (Ajou University)

Members:

Commission A: Yasuhiro Koyama, Chair, URSI Commission A (National Institute of Information and Communications Technology); Jeong Hwan Kim (Korea Research Institute of Standards and Science)

Commission B: Kazuya Kobayashi, Vice Chair, URSI Commission B (Chuo University); Ikmo Park (Ajou University)

Commission C: Amir I. Zaghloul, Vice Chair, URSI Commission C (Virginia Polytechnic Institute and State University); Jungwoo Lee (Seoul National University)

Commission D: Günter Steinmeyer, Chair, URSI Commission D (Max Born Institute); Jae-Sung Rieh (Korea University)

Commission E: Frank Gronwald, Vice Chair, URSI Commission E (Technische Universität Hamburg-Harburg); Wansoo Nah (Sungkyunkwan University)

Commission F: V. Chandrasekar, Vice Chair, URSI Commission F (Colorado State University); Yisok Oh (Hongik University)

Commission G: Iwona Stanislawska, Chair, URSI Commission G (Space Research Centre, Polish Academy of Sciences); Dong-Hun Lee (Kyung Hee University)

Commission H: Wen Li, ECR, URSI Commission H (University of California, Los Angeles); Jin Joo Choi (Kwangwoon University)

Commission J: Richard Bradley, Vice Chair, URSI Commission J (Technology Center, National Radio Astronomy Observatory); Jongsoo Kim (Korea Astronomy and Space Science Institute)

Commission K: Samyoung Chung, Vice Chair, URSI Commission K (National Radio Research Agency)

The Young Scientist Program Committee (YSPC) selected five finalists from among 43 Student Paper Competition applicants before the conference. All the Student Paper Competition finalists were given free registration for the conference, free accommodations, and free tickets for the banquet. The Student Paper Competition special session was organized on August 22, where all the finalists made oral presentations. The Young Scientist Program Committee further carefully evaluated the presentations by the finalists, and selected the three winners (first, second, and third prizes). The selection results were the following:

First Prize winner: Igor A. Nosikov, Immanuel Kant Baltic Federal University, Russia

Second Prize winner: Ahmed Soliman, California Institute of Technology, USA

Third Prize winner: Hengxin Ruan, Peking University, China

Non-winning finalist: Jae-Hyoung Cho, Korea Institute of Science and Technology and Yonsei University, South Korea

Non-winning finalist: Takashi Yamaguchi, Doshisha University, Japan

The award ceremony was held during the banquet on August 24, where the first, second, and third prize winners received certificates, with prize monies of US\$1,000, US\$750, and US\$500, respectively. The two non-winning finalists each received a certificate. Figure 1 shows a group photo of the five Student Paper Competition recipients.

The following three invited papers by the Student Paper Competition recipients appear in this special issue of the *Radio Science Bulletin*:

1. “Application of the Optimization Method to the Point-to-Point Radio Wave Ray Tracing Problem”
Igor A. Nosikov, Maxim V. Klimenko, Pavel F. Bessarab, and Gennady A. Zhabankov
2. “Suppression of Multipath Couplings in Scaled-Down Experiment for Cross-Borehole Pulse Radar”
Jae-Hyoung Cho, Ji-Hyun Jung, Jong-Gwan Yook, and Se-Yun Kim
3. “RF Output Power Enhancement by Optical Pulse Compression in Photonic-Based RF Generation”
Takashi Yamaguchi, Hiroki Morimoto, and Hiroyuki Toda

We were happy that the URSI AP-RASC 2016 Student Paper Competition was a great success. This success was due to the constant efforts by the South Korea National Committee of URSI during the course of preparations of the conference. We were particularly thankful to the URSI AP-RASC 2016 Young Scientist Program Committee for their hard work. In addition, Genicom Co., Ltd., did an outstanding job as the Conference Secretariat. Finally, we

would like to express our appreciation to the Student Paper Competition recipients who contributed to this special issue.

References

1. URSI AP-RASC 2016 Web site, <http://aprasc2016.org/>
2. URSI AP-RASC 2016 final program, http://www.ursi.org/content/AP-RASC/AP-RASC2016/URSI_AP-RASC_2016_Program.pdf

Guest Editors:
Kazuya Kobayashi
General Co-Chair, URSI AP-RASC 2016
Chuo University, Japan
E-mail: kazuya@tamacc.chuo-u.ac.jp

Ikmo Park
Co-Chair, URSI AP-RASC 2016 Young Scientist
Program Committee
Ajou University, South Korea
E-mail: ipark@ajou.ac.kr



Figure 1. The recipients of the URSI AP-RASC 2016 Student Paper Competition (r-l): Jeong-Hae Lee, Co-Chair, URSI AP-RASC 2016 Young Scientist Program Committee; Sangwook Nam, President, South Korea National Committee of URSI and URSI AP-RASC 2016 General Chair; Paul S. Cannon, URSI President; Igor A. Nosikov, first prize winner; Ahmed Soliman, second prize winner; Hengxin Ruan, third prize winner; Jae-Hyoung Cho, non-winning finalist; Takashi Yamaguchi, non-winning finalist; Kazuya Kobayashi, URSI Assistant Secretary General (AP-RASC) and URSI AP-RASC 2016 General Co-Chair; Piergiorgio L. E. Uslenghi, URSI Assistant Secretary General (AT-RASC) and URSI AP-RASC 2016 General Co-Chair; Peter Van Daele, URSI Assistant Secretary General and Chair, URSI AP-RASC 2016 Young Scientist Program Committee.

Application of the Optimization Method to the Point-to-Point Radio Wave Ray-Tracing Problem

I. A. Nosikov^{1,2}, M. V. Klimenko^{1,2}, P. F. Bessarab^{3,4}, and G. A. Zhbankov⁵

¹Immanuel Kant Baltic Federal University
236041, Kaliningrad, Russia
E-mail: igor.nosikov@gmail.com

²West Department of Pushkov Institute of Terrestrial Magnetism,
Ionosphere and Radio Wave Propagation, RAS
236017, Kaliningrad, Russia
E-mail: maksim.klimenko@mail.ru

³Science Institute of the University of Iceland
107 Reykjavik, Iceland
E-mail: bessarab@hi.is

⁴ITMO University
St. Petersburg 197101, Russia

⁵Southern Federal University
344006, Rostov-on-Don, Russia
E-mail: gzhbankov@sfnu.ru

Correspondence to: I. A. Nosikov
Tel: +74012215606; Fax: +74012215606
E-mail: igor.nosikov@gmail.com

Abstract

Point-to-point ray tracing is an important problem in many fields of science. In direct variational methods, some trajectory is transformed to an optimal trajectory. While these methods are routinely used in calculations of pathways of seismic waves, chemical reactions, diffusion processes, etc., these approaches are not widely known in ionospheric point-to-point ray tracing. A two-dimensional representation of the optical path functional is developed, and used to gain insight into the fundamental difference between high and low ionospheric rays. We conclude that high and low rays are minima and saddle points of the optical path functional, respectively. An optimization method for point-to-point ionospheric ray tracing, based on the direct variational principle for the optical path, is proposed. This is applied to calculations of high, trans-ionospheric, and multi-hop rays.

Keywords: point-to-point ray tracing; ionospheric radio; Fermat's principle; nudged elastic-band method

1. Introduction

The point-to-point radio wave ray-tracing problem essentially involves two steps. The first step is related to the choice of the environment model describing the ionospheric parameters. Another important issue concerns the methods for the ionospheric ray tracing, where the positions of the receiver and transmitter are fixed (Figure 1). The accuracy of both steps has a direct impact on the agreement between modeled and experimental oblique-sounding ionograms.

There are essentially two approaches for radio wave point-to-point ray tracing. The most traditional approach is the numerical solution of the eikonal equation, combined with the shooting method. This is also known as the homing-in approach [1-12], where the directions at which the rays are sent out are iteratively refined so as to achieve the desired landing point. The shooting method is widely used to calculate radio-wave paths in the ionosphere, although it

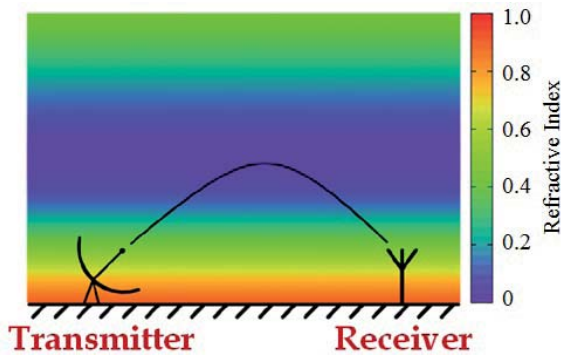


Figure 1. A schematic representation of the ray-tracing problem with boundary conditions. A radio ray emitted from the transmitter to the receiver is shown with a black line.

has some disadvantages [13]. Another approach is based on optimization of the optical path (Fermat's principle) [14]. In this approach, the initially defined radio-wave trajectory is transformed to an optimal trajectory, while its endpoints are kept fixed according to the boundary conditions.

In this paper, we discuss the following issues: 1) The use of an optimization method for finding radio-wave paths with fixed endpoints based on the direct variational principle for the optical path; 2) Application of the optimization method to both low and high ionospheric radio-wave trajectories; 3) Advantages of the optimization method in comparison to the shooting method.

2. Optimization Method

The optimization method for point-to-point ray tracing based on the direct variational principle for the optical path is widely used in seismology, as previously mentioned [15, 16]. There, it is known as the bending method [17] and the pseudo-bending method [18- 20]. However, it is hardly known in ionospheric radiophysics. The direct variational method for point-to-point ionospheric ray tracing was proposed by [21], which derived ordinary differential equations for the radio ray and solved them using a Galerkin technique. Coleman [3] developed an alternative approach, involving discretization of the optical-path functional. However, the direct minimization method fails to converge on the low rays [3]. The low rays do not satisfy the Jacobi test for a minimum of the optical-path functional, and therefore cannot be found by a direct minimization procedure. This problem can be solved with the Newton-Raphson method, as advocated by Coleman [3]. However, the Newton-Raphson method converges to any stationary point of an object function, and does not discriminate among minima, maxima, and saddle points of all orders.

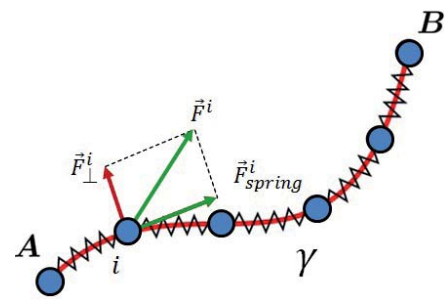


Figure 2. The principles of the nudged elastic-band method. The red line represents a trajectory discretized by a number of points (blue dots). Force vectors acting at each ray point are shown with red and green arrows.

2.1 Fermat's Principle

In an isotropic medium, the optical path of the radio-wave ray is defined by the following equation:

$$S[\gamma] = \int_A^B n(\vec{r}) dl. \quad (1)$$

Integration is performed along the curve γ , which joins boundary points A and B . $n(\vec{r})$ is the refractive index at point $\vec{r} = (x, y, z)$. dl is the length element along γ . According to Fermat's principle, the optical path of the radio wave satisfies the equation

$$\delta S = 0. \quad (2)$$

This problem of the calculus of variations can be transformed to the optimization problem in multidimensional space by representing the curve by a polygonal line connecting N points, and using the trapezoidal rule or Simpson's rule to compute the integral in Equation (1). The set of points corresponding to the minimum of the optical path gives the discrete representation of the radio-wave trajectory. The negative gradient of the optical path with respect to \vec{r} , which has the meaning of the force acting on the point in the multidimensional configuration space, can be used to guide the minimization:

$$F = -\nabla S = (\vec{F}^2, \vec{F}^3, \dots, \vec{F}^{N-1}). \quad (3)$$

2.2 Nudged Elastic-Band Method

In our investigations [22-24], the nudged elastic-band (NEB) method is applied to a point-to-point ionospheric ray-tracing problem. The method was originally developed to identify minimum-energy paths of chemical reactions [25], and it is widely used in various fields of science [26-28]. The use of the force defined in Equation (3) in the minimization procedure, such as the steepest-descent method or the conjugate-gradient method, can lead to a problem connected with the discrete representation of the path γ . The minimum of the optical path can correspond to a highly nonuniform distribution of the points where there are several localization centers with very low density of points in between them. As a result, the information about the radio wave's trajectory in some critical regions may be lost (see, for example, [22]). The remedy to this problem lies in force projection and the inclusion of elastic forces, which is the basis of the nudged elastic-band (NEB) method. According to the nudged elastic-band method, the force acting on each point, i , on the path γ is defined as

$$\bar{F}^i = \bar{F}_\perp^i + \bar{F}_{spring}^i. \quad (4)$$

Here, \bar{F}_\perp^i is a transverse component of $-\nabla S$, while \bar{F}_{spring}^i is the parallel component of the artificial spring force acting between the points. We previously proposed a method of transverse displacements using only projected forces, \bar{F}_\perp^i for the isotropic medium [22]. \bar{F}_\perp^i defines the transverse displacement of the path, while the spring force controls the distribution of the points along the path. If the same value of the spring constant is used for all springs connecting the points, the method ensures the uniform distribution of the

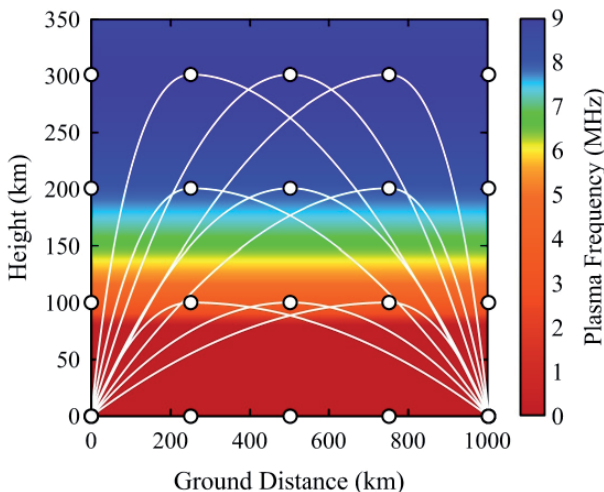


Figure 3. The three-point representation of the radio wave's trajectory. Two points are fixed according to the boundary conditions, and the third point defines the position of the apex (white dots), with spline interpolation in between the points (white solid lines).

points along the path after convergence has been achieved, providing good resolution of all parts of the path [23]. Since the spring force acts only along the path, it does not affect the position of the path in space. A summary of the nudged elastic-band method is schematically presented in Figure 2.

3. New Results

3.1 Analysis of Low and High Rays: Optical Path Maps

We develop a two-dimensional representation of the optical path as a function of control parameters defining the radio-wave trajectory, and we use it to gain a deeper insight into the problem of determining the high and low rays. The optical path given by the discretized functional (see Equation (1)) is a function of many variables defining the position of each vertex of the polygonal representation of the radio wave's trajectory. In order to visualize this as a two-dimensional map, we use a reduced description of the model in terms of only two essential variables. This is accomplished by choosing a three-point representation of the radio wave's trajectory, where two points are fixed

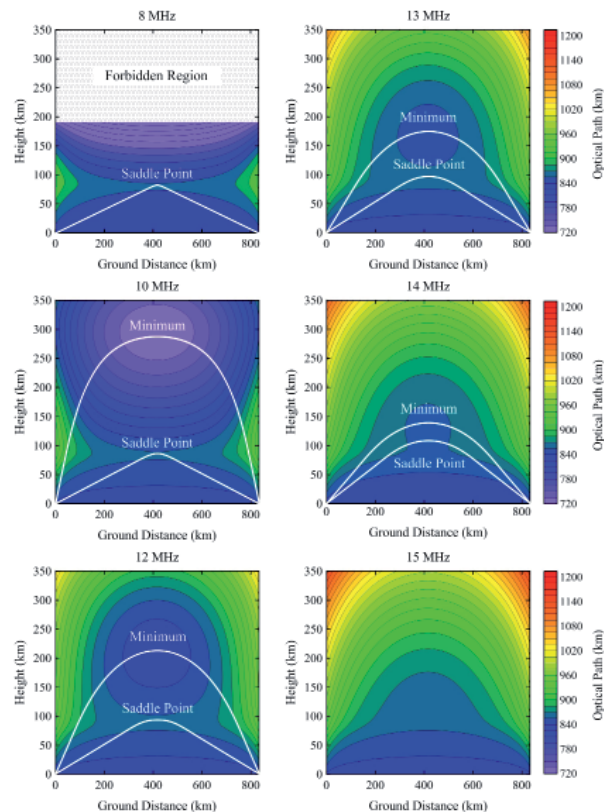


Figure 4. Contour maps of the optical path for various frequencies in a range of 8 MHz to 15 MHz in the parabolic-layer ionosphere. The high ray, obtained with the nudged elastic-band method, and the low ray, obtained by the numerical solution of the Euler-Lagrange equation, are shown with white solid lines.

according to the boundary conditions and the third point defines the position of the apex. Spline interpolation is performed in between the points (see Figure 3). With this representation, the radio wave's trajectory is completely defined by two variables, the coordinates of the apex point, and a contour map of the optical path can be constructed. These two-dimensional maps of the optical path are consistent with detailed calculations of the trajectories using the full set of variables, and they give a qualitative insight into the distribution of the optical path.

The resulting contour map of the optical path obtained for six values of the frequency in a range of 8 MHz to 15 MHz is shown in Figure 4. Radio-wave trajectories are also shown, where the high rays were obtained with the nudged elastic-band method, and the low rays were obtained by solving the Euler-Lagrange equation. Our results showed that the high rays corresponded to minima of the optical path, which led to the robust determination of the rays with the minimization approach. However, the low rays corresponded to saddle points of the optical-path functional, which were difficult to locate. The difficulty arises from the need to minimize the optical path with respect to all but one degree of freedom, for which a maximization should be carried out. It is not known a priori which degree of freedom should be treated differently. In particular, implementation of the nudged elastic-band method and the dimer method [29] will extend the applicability of the optimization approach in the field of HF radio-wave trajectory calculations.

3.2 Identification of High, Trans-Ionospheric, and Multi-Hop Rays

Point-to-point ionospheric ray tracing reduces to the identification of all high and low rays connecting the receiver and transmitter. As an example, we here focus on the radio-wave ray tracing in the region between Kaliningrad and Tromsø at 8.7 MHz. The electron density was given by the IRI-2007 model [30] for 12:00 UT on June 22, 2014, with settings simplified for traveling ionospheric disturbances (TIDs). The results obtained with the homing-in approach [10, 11] are presented in Figure 5.

Five radio-wave rays were found: two high rays, two low rays, and one multi-hop ray, which are consistent with a well-defined two-layer structure in the vertical electron-density profile. These solutions served as a reference for the nudged elastic-band calculations. Both high rays could be calculated with the nudged elastic-band method by setting the initial guesses for the radio-wave trajectory at the altitudes of the F2- and E-layer peaks.

As an example, we also obtained the trans-ionospheric ray that is shown in Figure 5. The results were in good agreement with the solutions given by the homing-in approach. However, the direct minimization method failed to converge on the low and multi-hop rays. The low rays

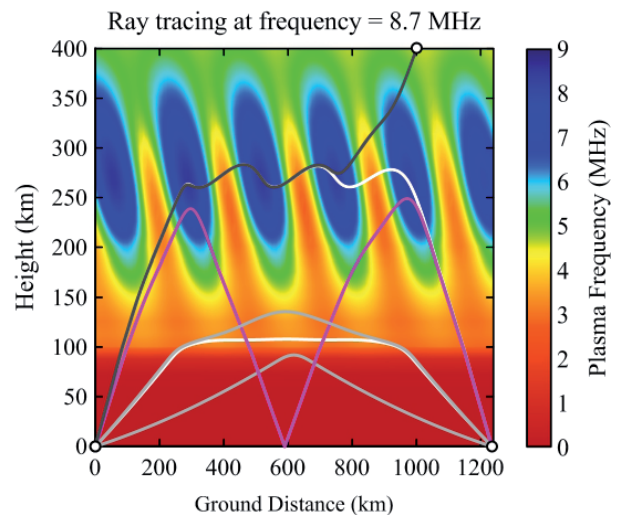


Figure 5. The results of point-to-point ray tracing calculations using the nudged elastic-band method at a frequency of 8.7 MHz between Kaliningrad (54.57°N, 20°E) and Tromsø (65.65°N, 18.57°E) for daytime summer solstice on 22.06.2014. The white solid lines are for the high ray. The grey solid line is for the low ray. The black solid and dashed line is for the trans-ionospheric ray. The pink solid line is for the multi-hop ray. The electron density given by the IRI-2007 model was perturbed by TIDs.

corresponded to a saddle point of the optical-path functional, and therefore could not be found by a direct minimization procedure. The low rays as well as the multi-hop ray could still be found with the proposed technique if the trajectory was divided at the apex, and separate calculations were performed for each segment of the radio ray. However, this scheme is only possible if the position of the apex is known.

4. Discussion

The most traditional approach for radio-wave point-to-point ray tracing is a homing-in approach. However, such an approach may suffer from convergence problems when applied to a realistic three-dimensional ionosphere [13]. The direct variational method has advantages compared to the homing-in approach, since it automatically satisfies the boundary conditions. High, trans-ionospheric, and multi-hop rays were calculated for the ionospheric medium predicted by the International Reference Ionosphere (IRI) model, where the electron density was perturbed by traveling ionospheric disturbances (TIDs). The results obtained with the nudged elastic-band method were in good agreement with those given by the homing-in approach.

However, low rays needed special treatment, since they corresponded to a saddle point of the optical-path functional [24], and therefore could not be found by direct minimization of the optical-path functional [3]. The problem of low-ray identification by the direct variational method was also discussed. For that reason, a two-dimensional

representation of the optical path surface was introduced and used to gain insight into the nature of low rays, which are particularly difficult to calculate, and to discuss a scheme for their identification. This problem can be solved with the Newton-Raphson method, as advocated by Coleman [3]. However, the Newton-Raphson method converges to any stationary point of an object function, and does not discriminate among minima, maxima, and saddle points of all orders.

However, our preliminary analysis suggests that the definite identification of the low rays is equivalent to the first-order saddle-point search, for which several methods have been developed. The method that is very efficient and commonly used is actually the nudged elastic-band method. Originally, the nudged elastic-band method was introduced to calculate lowest-lying paths between minima of a multidimensional surface. A saddle point is extracted from the position of maxima along such paths. Therefore, the low ionospheric rays can be found by applying the nudged elastic-band method in its original context. An optimal path needs to be found in a space of radio-ray trajectories. The final, relaxed path obtained from a nudged elastic-band calculation lies lowermost on the multidimensional optical-path surface so that the maximum along the path is precisely a saddle point corresponding to a low ray. Calculation of the low rays using this approach is a subject of future research.

5. Summary

In this paper, we applied the nudged elastic-band method to a point-to-point ionospheric ray-tracing problem. Although the method was originally developed for calculations of mechanisms and pathways of chemical reactions, it proved to be well-suited for the identification of radio-ray trajectories in realistic ionospheric media, especially when the positions of the receiver and transmitter were fixed. All high rays could be found, given that some sampling of the initial conditions for the radio-wave trajectory was performed.

Care needs to be taken when calculating the low rays. Although both high and low rays are stationary radio-wave trajectories, our analysis showed that the former correspond to the minima of the optical-path functional, while the latter correspond to the saddle points, which are difficult to locate. A better strategy is to again exploit the nudged elastic-band method, but in a different context. The nudged elastic-band method was originally designed to identify saddle points on a multidimensional surface. In order to locate a low ionospheric ray, the nudged elastic-band method needs to be applied to a path in a space of radio-ray trajectories. The final, relaxed path lies lowermost on the multidimensional optical-path surface, so that the maximum along the path is precisely a saddle point corresponding to a low ray. Formulation of new methods for finding low rays can be based on conclusions drawn from the present work, and will be addressed in a future study.

6. Acknowledgments

The authors thank F. S. Bessarab and V. V. Klimenko for fruitful discussions. This study was financially supported by grants from the RFBR No. 16-35-00590. This work was supported by the Russian Science Foundation (project No. 17-77-20009), the program “5-100” to improve competitiveness of Immanuel Kant Baltic Federal University.

7. References

1. R. M. Jones and J. J. Stephenson, “A Versatile Three-Dimensional Ray Tracing Computer Program for Radio Waves in the Ionosphere,” NASA STI/Recon Technical Report, **76**, October 1975, 25476.
2. C. J. Coleman, “A Ray Tracing Formulation and Its Application to Some Problems in Over-The-Horizon Radar,” *Radio Science*, **33**, 4, August 1998, pp. 1187-1197.
3. C. J. Coleman, “Point-to-Point Ionospheric Ray Tracing by a Direct Variational Method,” *Radio Science*, **46**, 5, October 2011, RS5016.
4. H. J. Strangeways, “Effects of Horizontal Gradients on Ionospherically Reflected or Transionospheric Paths Using a Precise Homing-in Method,” *Journal of Atmospheric and Solar-Terrestrial Physics*, **62**, 15, October 2000, pp. 1361-1376.
5. N. Y. Zaalov, E. M. Warrington, and A. J. Stocker, “The Simulation of Off-Great Circle HF Propagation Effects Due to Presence of Patches and Arc of Enhanced Electron Density Within the Polar Cap Ionosphere,” *Radio Science*, **38**, 3, June 2003, pp. 1052-1058.
6. X. Huang, B. W. Reinisch, “Real-Time HF Ray Tracing Through a Tilted Ionosphere,” *Radio Science*, **41**, 5, August 2006, RS5547.
7. X. Huang, B. W. Reinisch, G. S. Sales, et al., “Comparing TID Simulations Using 3D Ray Tracing and Mirror Reflection,” *Radio Science*, **51**, 4, April 2016, pp. 337-343.
8. D. V. Blagoveshchensky, M. Yu. Andreyev, V. S. Mingalev, et al., “Physical and Model Interpretation of HF Radio Propagation on the St. Petersburg-Longyearbyen (Svalbard) Path,” *Advances in Space Research*, **43**, 12, June 2009, pp. 1974-1985.
9. G. V. Kotovich, V. P. Grozov, A. G. Kim, et al., “Application of the Theoretical Reference Ionosphere Model for Calculating HF-Radiowave Propagation Characteristics,” *Geomagnetism and Aeronomy*, **50**, 4, August 2010, pp. 504-508.

10. G. A. Zhibankov, A. T. Karpachev, V. A. Telegin, and K. G. Tsybulya, "Specific Propagation of Radiowaves from the Intercosmos-19 Satellite in the Region of the Nighttime Equatorial Anomaly Crest," *Geomagnetism and Aeronomy*, **50**, 1, March 2010, pp. 119-126.
11. A. T. Karpachev, M. V. Klimenko, V. V. Klimenko, et al., "Latitudinal Structure of the Equatorial F3 Layer Based on Intercosmos-19 Topside Sounding Data," *Journal of Atmospheric and Solar-Terrestrial Physics*, **77**, March 2012, pp. 186-193.
12. A. Settimi, M. Pezzopane, and M. Pietrella, et al. "Testing the IONORT-ISP System: A Comparison Between Synthesized and Measured Oblique Ionograms," *Radio Science*, **48**, 2, March 2013, pp. 167-179.
13. N. N. Kalitkin, *Numerical Methods*, Moscow, Nauka, 1978, p. 508 (in Russian).
14. Y. A. Kravtsov and Y. I. Orlov, *The Geometric Optics of Nonhomogeneous Media*, Moscow, Russia, Science, 1980, p. 304 (in Russian).
15. D. Zhao, A. Hasegawa, and S. Horiuchi, "Tomographic Imaging of P and S Wave Velocity Structure Beneath Northeastern Japan," *Journal of Geophysical Research: Solid Earth*, **97**, B13, December 1992, pp. 19909-19928.
16. K. Koketsu and S. Sekine, "Pseudo-Bending Method for Three-dimensional Seismic Ray Tracing in a Spherical Earth with Discontinuities," *Geophysical Journal International*, **132**, 2, February 1998, pp. 339-346.
17. V. Pereyra, W. H. K. Lee, and H. B. Keller, "Solving Two-Point Seismic Ray Tracing Problems in a Heterogeneous Medium," *Bulletin of the Seismological Society of America*, **70**, 1, February 1980, pp. 79-99.
18. J. Um and C. Thurber, "A Fast Algorithm for Two-Point Seismic Ray Tracing," *Bulletin of the Seismological Society of America*, **77**, 3, June 1987, pp. 972-986.
19. W. A. Prothero, W. J. Taylor, and J. A. Eickemeyer, "A Fast, Two-Point, Three-Dimensional Ray Tracing Algorithm Using a Simple Step Search Method," *Bulletin of the Seismological Society of America*, **79**, 3, June 1988 pp. 1190-1198.
20. T. J. Moser, G. Nolet, and R. Snieder, "Ray Bending Revisited," *Bulletin of the Seismological Society of America*, **82**, 1, February 1992, pp. 259-288.
21. J. Smilauer, "The Variational Method Ray Path Calculation in an Isotropic, Generally Inhomogeneous Ionosphere," *Journal of Atmospheric and Solar-Terrestrial Physics*, **32**, 1, January 1970, pp. 83-96.
22. I. A. Nosikov, P. F. Bessarab, and M. V. Klimenko, "Method of Transverse Displacements Formulation for Calculating the HF Radio Wave Propagation Paths. Statement of the Problem and Preliminary Results," *Radiophysics and Quantum Electronics*, **59**, 1, July 2016, pp. 1-12.
23. I. A. Nosikov, M. V. Klimenko, P. F. Bessarab, and G. A. Zhibankov, "Application of the Nudged Elastic Band Method to the Point-to-Point Radio Wave Ray Tracing in IRI Modeled Ionosphere," *Advances in Space Research*, available online 19 December 2016 (in Press).
24. I. A. Nosikov, M. V. Klimenko, P. F. Bessarab, and G. A. Zhibankov, "Investigation of Optical Path Functional for High and Low Ionospheric Radio Rays," URSI Asia-Pacific Radio Science Conference (URSI AP-RASC), August 2016, Seoul, Korea, pp. 1317-1320.
25. H. Jónsson, G. Mills, and K. W. Jacobsen, "Nudged Elastic Band Method for Finding Minimum Energy Paths of Transitions," in *Classical and Quantum Dynamics in Condensed Phase Simulations*, Singapore, World Scientific Publishing Co., 1998, pp. 345-404.
26. G. Henkelman and H. Jónsson, "Multiple Time Scale Simulations of Metal Crystal Growth Reveal the Importance of Multiatom Surface Processes," *Physical Review Letters*, **90**, 11, March 2003, 116101.
27. L. Xu, G. Henkelman, C. T. Campbell, and H. Jónsson, "Small Pd Clusters, Up to the Tetramer at Least, Are Highly Mobile on the MgO (100) Surface," *Surface Physical Review Letters*, **95**, 14, September 2005, 146103.
28. P. F. Bessarab, V. M. Uzdin, and H. Jónsson, "Effect of Hydrogen Adsorption on the Magnetic Properties of a Surface Nanocluster of Iron," *Physical Review B*, **88**, 21, December 2013, 214407.
29. G. Henkelman, G. Jóhannesson, and H. Jónsson, "Methods for Finding Saddle Points and Minimum Energy Paths," in S. D. Schwartz (ed.), *Theoretical Methods in Condensed Phase Chemistry, (Progress in Theoretical Chemistry and Physics, Volume 5)*, Netherlands, Springer, 2002.
30. D. Bilitza and B. W. Reinisch, "International Reference Ionosphere 2007: Improvements and New Parameters," *Advances in Space Research*, **42**, 4, August 2008, pp. 599-609.

Suppression of Multi-Path Couplings in Scaled-Down Experiment for Cross-Borehole Pulse Radar

Jae-Hyoung Cho¹, Ji-Hyun Jung², Jong-Gwan Yook³, and Se-Yun Kim⁴

¹Imaging Media Research Center
Korea Institute of Science and Technology
and Yonsei University
Seoul, Korea
E-mail: cjh78@imrc.kist.re.kr

²Radar SW Team
Hanwha Thales
Gyeonggi-do, Korea
E-mail: jh82.jung@hanwha.com

³Electrical and Electronic Engineering Department
Yonsei University
Seoul 120-749, Korea
E-mail: jgyook@yonsei.ac.kr

⁴Imaging Media Research Center
Korea Institute of Science and Technology
Seoul, Korea
E-mail: ksy@imrc.kist.re.kr

Abstract

A scaled-down experiment using cross-borehole pulse radar was performed in a laboratory to extract a more precise decision rule for detecting an intrusive manmade tunnel in Korea. To minimize the total size, a scaled-down model of an air-filled tunnel in underground rock was replaced by a cylindrical ceramic rod in pure water. When the upper arm of a sleeve-dipole antenna of the scaled-down cross-borehole pulse radar was directly connected to a coaxial cable, the measured B-scan data were contaminated by unwanted striped patterns that were generated by multipath coupling. Such multipath coupling between the sleeve-antenna pair was generated by the glass-tube-guided waves. To suppress the glass-tube-guided waves, the coaxial cable was clad in ferrite cores. As the total length of the ferrite-core cladding was increased up to 150 mm, the unwanted multipath couplings were gradually suppressed, and the target signature could be more clearly recognized.

Keywords: bistatic pulse radar; ferrite core; multipath coupling; sleeve dipole antenna; tube-guided wave

1. Introduction

The detection of a deeply located intrusive tunnel in Korea is considered one of the most attractive missions in geophysical exploration [1-6]. To detect such a small tunnel – its cross section is 2 m by 2 m – several borehole radar systems have been operated during the past three decades. We recently developed two different types of borehole pulse radar systems. One type is the monostatic pulse radar, which uses only a single borehole. This single-borehole radar has been widely used to save the time and cost of drilling boreholes. However, the signal generated by the reflection from the tunnel was relatively weaker than the direct coupling from the transmitter to the receiver [7]. In addition, the borehole-guided wave was generated along the coaxial cable connected to the upper arm of the antenna in the borehole [8]. Underground rock in Korea is highly inhomogeneous. Hence, all of the measured B-scan data were contaminated by an unwanted striped pattern because the borehole-guided wave was reflected back from the boundaries of different rocks. A ferrite cladding along the coaxial cable connected to the upper arm of the dipole antenna effectively suppressed the unwanted striped pattern [9].

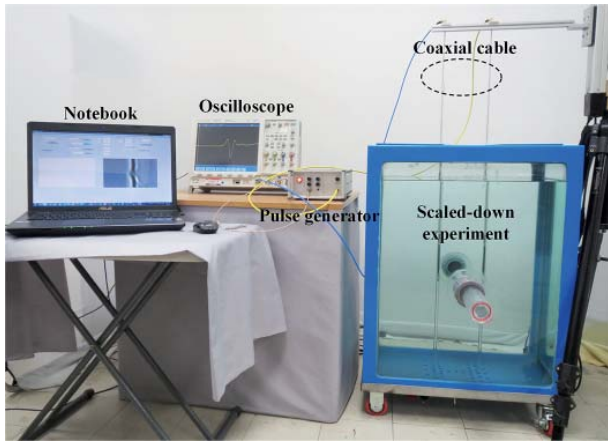


Figure 1a. The configuration of the scaled-down experiment for a cross-borehole pulse radar system.

The other type of borehole pulse radar system is the bistatic pulse radar, in which transmitting and receiving antennas are inserted into two separate boreholes, one by one. The detection principle of the cross-borehole pulse radar is the relatively fast propagation of the pulse at the depth of an air-filled tunnel. In addition, the tunnel boundary causes severe attenuation, while multiple reflections inside the tunnel distort signal shapes. In particular, most underground rock in Korea includes many faults, layers, lodes, etc. Such underground inhomogeneity hinders the clear understanding of the physical mechanism of how the tunnel signature is affected by the parameters involved. For precise and concise investigations on tunnel signatures in various situations, a scaled-down experiment in a well-controlled laboratory may be an attractive solution, with a low cost and a high degree of flexibility in measurement situations [10-18].

In scaled-down experiments, a sleeve-dipole antenna has usually been used for appropriately inserting and pulling the antenna inside a thin, long glass tube. In our previous work [19], the scaled-down experiment was performed to find an enhanced rule for detecting a manmade tunnel by employing a cross-borehole frequency-swept radar system. The sleeve-dipole antenna, fed by a coaxial cable passing through its upper arm, was improved to provide its wideband symmetric near-field radiation pattern using additional ferrite-clad wire [19]. Unlike the frequency-swept cross-borehole radar, the cross-borehole pulse radar system should be analyzed in the time domain, using the reasonable shortest and fastest path. It should be noted that to minimize the total size, a scaled-down model of an air-filled tunnel in underground rock is replaced by a cylindrical ceramic rod in pure water. The measured B-scan data are contaminated by an unwanted striped pattern. Such multipath coupling between the sleeve-antenna pair is generated by the glass-tube-guided waves. To suppress the glass-tube-guided waves, the coaxial cable connected to the upper end of the sleeve dipole antenna was clad in ferrite cores. The total length of the ferrite-core cladding was changed from 25 mm to 150 mm. Our experimental results illustrate that the unwanted multipath couplings

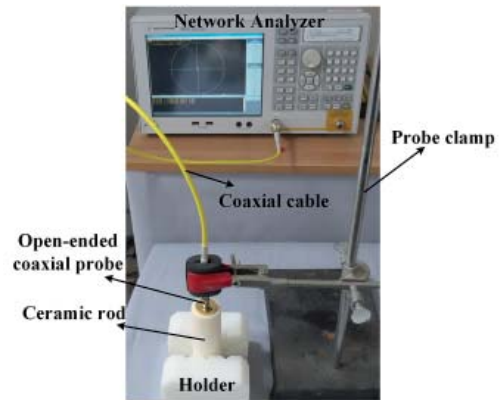


Figure 1b. A photograph of the open-ended coaxial probe for measuring the permittivity of the ceramic rod.

were gradually suppressed according to the total length of the ferrite-core cladding.

2. Scaled-Down Experiment

Figure 1a presents the configuration of a scaled-down experiment using the cross-borehole pulse radar system in our laboratory. The main frame of the experiment was made of polyvinylchloride (PVC) with a size of 600 mm × 350 mm × 800 mm. Two thin and long Pyrex glass tubes were filled with air. The outer and inner diameters of those tubes were 13 mm and 11 mm, respectively. In the field experiment, a Gaussian impulse that had a 10 ns FWHM (full-width half maximum), with a maximum frequency of 100 MHz, was adopted. For our scaled-down experiment, we used a conventional impulse generator (AVH-HV1-C-T1) with a 630 ps FWHM, manufactured by Avtech Electrosystems, with a maximum frequency of 2 GHz.

The pure water was used as a background medium because of the high scaled-down ratio and flexibility of the experimental situation. Considering the lower and upper limits of the dielectric constant of the background rock in the field experiment, the ratio of the refractive index of the background rock to that of the air inside the tunnel was in the range of 2.41 to 3.46. To satisfy a one-to-one correspondence between the field and the scaled-down experiments, the air-filled tunnel in the real site was implemented by a circular ceramic rod in our scaled-down experiment. The permittivity of the ceramic rod was measured by our open-ended coaxial-probe method, as shown in Figure 1b [20, 21]. The ratio of the refractive index, 3.11, was achieved in our scaled-down experiment because the permittivity of our ceramic rod was 8.3 at 2 GHz. At the maximum frequency of 100 MHz in the field experiment, the wavelength in different background rocks was in the range between 0.87 m to 1.25 m. Since the wavelength corresponding to the scaled-down experiment was 16.7 mm, the total scaling-down factor could be realized in the range between 52 and 75. The tempered glass, for easily looking inside,

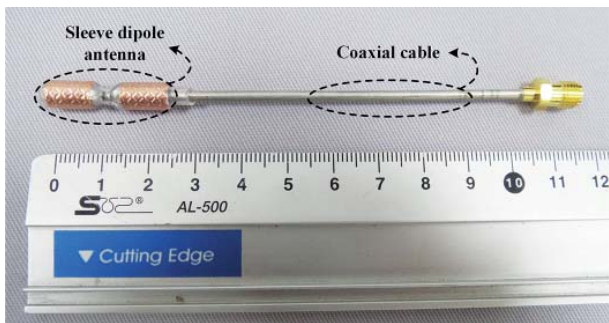


Figure 2. A photograph of the sleeve-dipole antenna fed by a coaxial cable without ferrite cladding.

were used to cover the four side boundaries of the water tank. In this scaled-down experiment, the air-filled tunnel in the real site was implemented by a circular ceramic rod. The target holder mounting the ceramic rod was located at the central position in depth.

Figure 2 shows a photograph of the sleeve-dipole antenna fed by a coaxial cable without ferrite cladding. The lengths of the sleeve-dipole antenna's arms were 10 mm. The lower and upper arms of each antenna were connected to the inner and outer conductors of the coaxial cable, respectively. Two identical sleeve-dipole antennas were used, here. The transmitting and receiving antennas, inserted into the corresponding glass tubes, were connected to port 1 and port 2 of the pulse generator and the oscilloscope, respectively. The distance between the antenna pair was 200 mm. For measurements and data acquisition, the digital sampling oscilloscope (DSO7104A), manufactured by Keysight technologies, was used.

3. Multi-Path Couplings Between the Sleeve-Dipole Antenna Pair

Since the coaxial cable exists above the upper arm of each antenna, the glass-tube-guided wave may be generated along the coaxial cable and propagates through the air in the glass tube. Such multipath coupling signals are transmitted and received through the air. It may then be possible that one of such multi-path coupling signals will arrive earlier than the signal transmitted through the ceramic rod in the water. Figure 3 depicts the possible paths between the sleeve-dipole antenna pair in the scaled-down experiment. The black solid line is the desired path, which helps us to detect the ceramic rod in the water. As one of multipath couplings, the broken line in Figure 3 denotes the path along which an electromagnetic pulse radiated from the transmitting antenna propagates upwardly inside the glass tube, and then changes its course along the air-water interface, and finally propagates downwardly until arriving at the receiving antenna. The total length of the broken line is much longer than that of the direct path. However, the total time of the pulse propagation along the broken line is significantly reduced because the pulse in this path propagates through air. Hence, the pulse along the broken path can arrive at the receiver earlier than the pulse along the direct path, as the depth of both antennas approaches the air-water boundary. The broken-dotted line in Figure 3 denotes another multipath coupling, which includes the reflection at the PVC cover of the water tank instead of the propagation along the air-water interface.

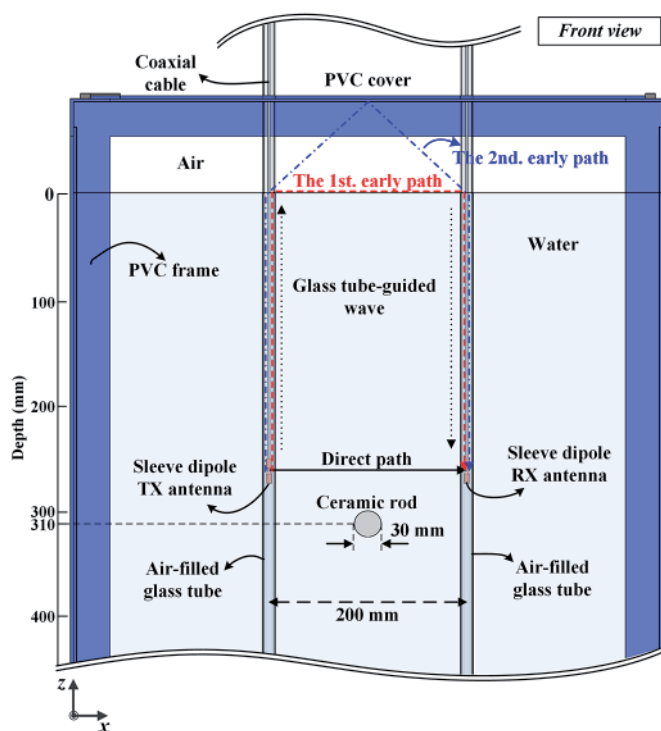


Figure 3. Possible multipath couplings between the sleeve-dipole antenna pair in the scaled-down experiment of a cross-borehole pulse radar.

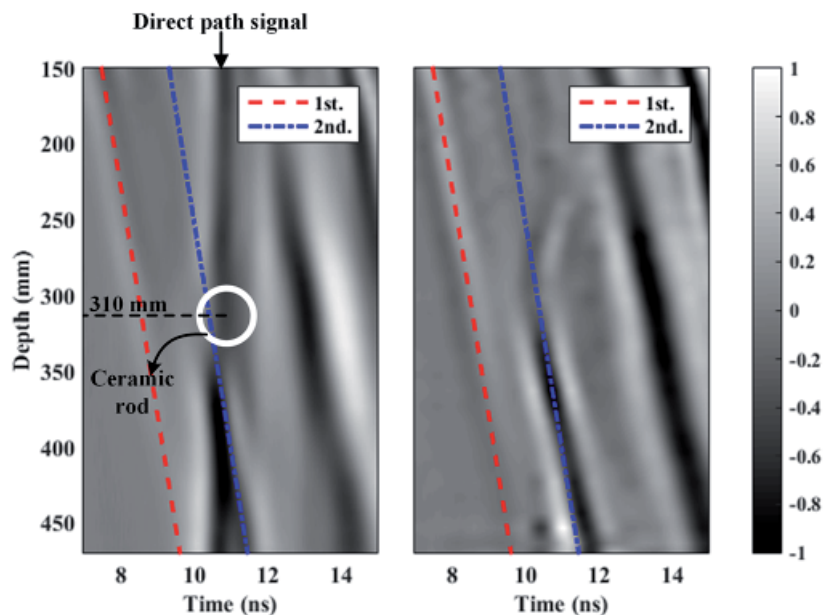


Figure 4. (a - left) The measured B-scan results after normalization, overlapping the arrival times of the possible multipaths. (b - right) The normalized differential B-scan data.

Figure 4a illustrates the B-scan data acquired by simultaneously pulling up the antenna pair from 470 mm to 150 mm in equal intervals along the z direction. It should be noted that zero depth means that the feeder of the sleeve-dipole antenna was located at the air-water interface. The horizontal and vertical axes mean time in ns and depth in mm, respectively. To enhance the signature of the ceramic rod, the normalized differential B-scan data as shown in Figure 4b were constructed by taking the difference between two adjacent A-scan data among the B-scan data in Figure 4a. As a scaled-down model of the intrusive man-made tunnel, the center of the ceramic rod was located at 310 mm in depth. As expected, one could not succeed in achieving target recognition from the B-scan data in Figure 4, because the measured data were significantly contaminated by the unwanted stripe patterns. This stripe patterns were generated by the multipath couplings, as shown in Figure 3. The broken and broken-dotted lines in Figure 4 denote the multipath coupling along the same corresponding lines in Figure 3. As the depth of the antenna pair approached to the air-water interface, the earliest arrival of the radiated pulse was implemented by propagation along the two multipath couplings in Figure 3. Such multipath couplings hence generated such stripe patterns, which rendered it difficult to single out the target signature in the measured B-scan data.

4. Ferrite Cladding Effects

As described in [19], the glass-tube-guided wave could be suppressed using the ferrite-cladding technique [19]. Figure 5 shows a photograph of the sleeve-dipole antenna fed by the coaxial cable, on which ferrite cores

with a total length (L) were clad. In this case, we used the commercial ferrite cores of Ni-Zn type made by Samwha electronics [22]. To hold the ferrite cores tightly on the coaxial cable, a clear heat-shrink tubing was employed, as shown in Figure 5. It may be interesting to know how short the length of the ferrite-core cladding could be made for a reasonable suppression of unwanted multipath coupling signals in measured B-scan data.

To observe the ferrite-cladding effect, several intermediate cases according to the length of the ferrite cores were also experimented with. The total length of the clad ferrite cores was gradually increased up to 150 mm in equal intervals of 25 mm. Figures 6a to 6f represent the normalized differential B-scan data for six different lengths of ferrite cladding: 25 mm, 50 mm, 75 mm, 100 mm, 125 mm, and 150 mm, respectively. Figure 6a was severely contaminated by the long-standing obliquely stripe lines due to the multipath couplings. In Figure 6, one could



Figure 5. A photograph of the sleeve-dipole antenna fed by a coaxial cable on which the total length (L) of ferrite cores was clad.

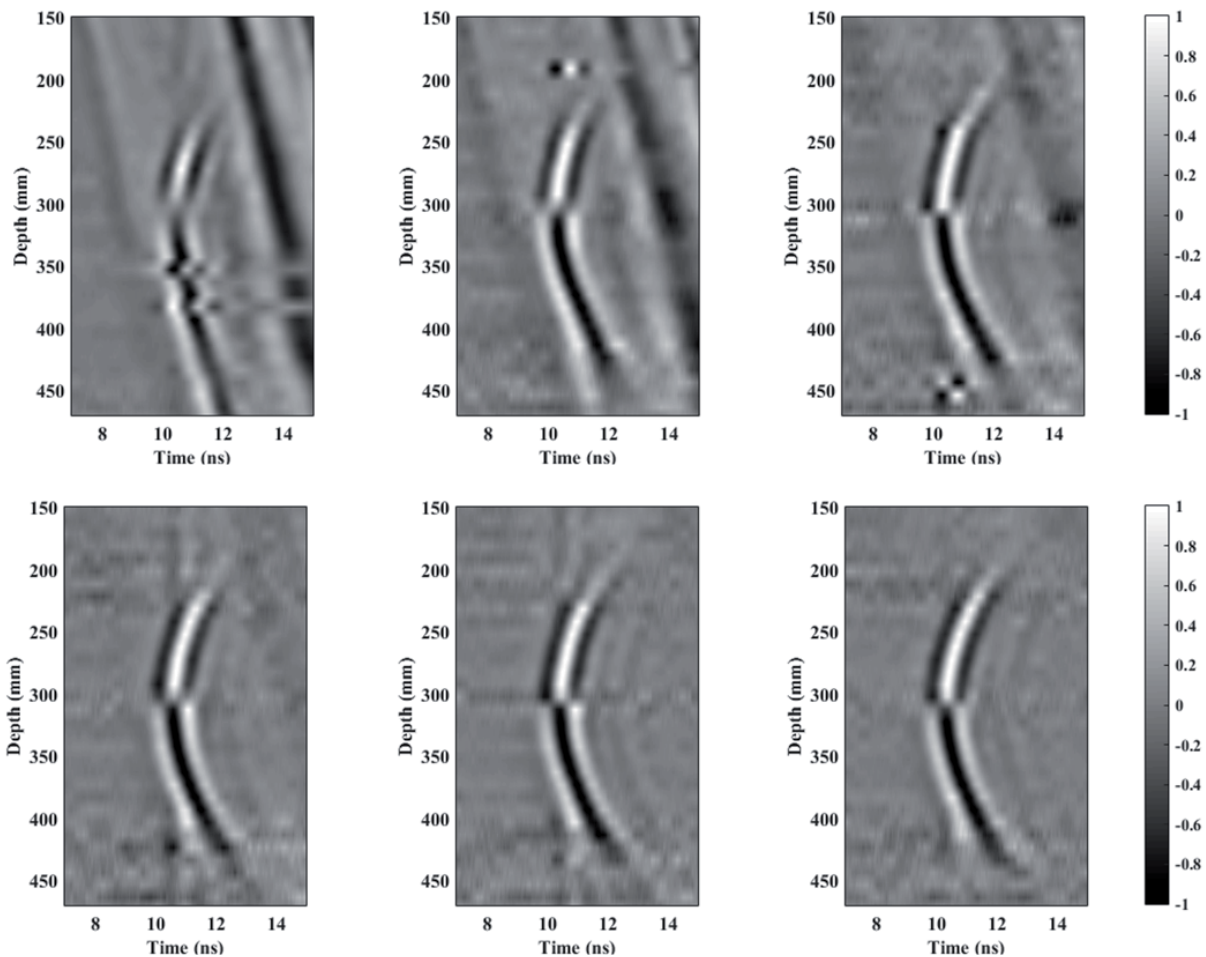


Figure 6. The normalized differential B-scan data for eight different lengths (L) of ferrite cladding on the coaxial cable: (a) $L = 25$ mm, (b) 50 mm, (c) 75 mm, (d) 100 mm, (e) 125 mm, and (f) 150 mm.

easily find such an interesting trend that the strength of the stripe lines was gradually reduced as the total length of the ferrite cladding increased. When the length of the ferrite cladding reached 150 mm, in Figure 6f, most of the stripe lines were sufficiently suppressed. This led us to find a proper way of suppressing the unwanted multipath coupling signals in the B-scan data measured by a scaled-down cross-borehole pulse radar.

5. Conclusion

In a scaled-down experiment of a cross-borehole pulse radar, multipath couplings occurred due to the generation of glass-tube-guided waves. Such multipath coupling signals contaminated the measured B-scan data. To suppress the glass-tube-guided waves, the feeding coaxial cable was clad in ferrite cores. As the total length of the ferrite-core cladding was increased up to 150 mm, the unwanted multipath signals were sufficiently suppressed to distinguish the target signature in the measured B-scan data. These results showed that ferrite cladding on the conduction cable will be a reasonable solution for considerably suppressing guided waves in the relatively thin guiding structure.

6. References

1. T. R. Owen, "Cavity Detection Using VHF Hole-to-Hole Electromagnetic Techniques," Technical Symposium on Tunnel Detection, Golden, CO, USA, July 21-23, 1981.
2. B. Duff, "A Review of Electromagnetic Methods Used for Detection of Underground Tunnels and Cavities," IEEE Antennas and Propagation Society International Symposium, Houston, TX, USA, May 23-26, 1983.
3. G. R. Olhoeft, "Interpretation of Hole-to-Hole Radar Measurements," Technical Symposium on Tunnel Detection, Golden, CO, USA, January 12-15, 1988.
4. R. J. Greenfield, "Modeling of Electromagnetic Propagation Between Boreholes," Technical Symposium on Tunnel Detection, Golden, CO, USA, January 12-15, 1988.
5. S.-Y. Kim and J.-W. Ra, "The Role of Cross Borehole Radar in the Discovery of Fourth Tunnel at the Korea DMZ," Technical Symposium on Tunnel Detection, Golden, CO, USA, April 26-29, 1993.

6. S.-W. Kim, S.-Y. Hyun, J.-H. Lee, S.-Y. Lee, J.-H. Cho, K.-T. Oh, and S.-Y. Kim, "The Development of a Pulse Borehole Radar System for Underground Cavity Detection," *Technical Report of IEICE. SANE*, **107**, 277, October 2007, pp. 93-97.
7. J.-H. Cho, J.-S. Choi, S.-W. Kim, J.-G. Yook, and S.-Y. Kim, "Switching Characteristics of Single-Borehole Monostatic Radar System for Adjacent Tunnel Detection," International Symposium on Antennas and Propagation, Jeju, Korea, October 25-28, 2011.
8. S. Ebihara, M. Sato, and H. Niitsuma, "Analysis of a Guided Wave Along a Conducting Structure in a Borehole," *Geophysical Prospecting*, **46**, 5, September 1998, pp. 489-505.
9. J.-H. Cho, J.-H. Jung, S.-W. Kim and S.-Y. Kim, "Suppression of Borehole-Guided Waves Supported by the Connection Cable of a Single-Borehole Monostatic Pulse Radar," *IEEE Transactions on Geoscience and Remote Sensing*, **51**, 6, January 2013, pp. 3431-3438.
10. S.-Y. Hyun, Y.-S. Jo, H.-C. Oh, S.-Y. Kim, and Y.-S. Kim, "The Laboratory Scaled-Down Model of a Ground-Penetrating Radar for Leak Detection of Water Pipes," *Measurement Science and Technology*, **18**, 9, July 2007, pp. 2791-2799.
11. S. Eyuboglu, H. Mahdi, and H. Al-Shukri, "Detection of Water Leaks Using Ground Penetrating Radar," International Conference on Applied Geophysics, Orlando, FL, USA, December 8-12, 2003.
12. S.-Y. Hyun, Y.-S. Jo, H.-C. Oh, and S.-Y. Kim, "An Experimental Study on a Ground-Penetrating Radar for Detecting Water-Leaks in National Symposium on Antennas Propagation and EM Theory, October 28-November 1, 2003.
13. G. S. Smith and W. R. Scott, "A Scale Model for Studying Ground Penetrating Radars," *IEEE Transactions on Geoscience and Remote Sensing*, **27**, 4, July 1989, pp. 358-363.
14. J. Schneider, J. Brew, and I. C. Peden, "Electromagnetic Detection of Buried Dielectric Targets," *IEEE Transactions on Geoscience and Remote Sensing*, **29**, 4, July 1991, pp. 555-562.
15. G. A. Ellis and I. C. Peden, "An Improved Scale Model Measurement Facility for Studying Geophysical Cross-Borehole Sensing," International Symposium on Antennas Propagation, July 18-25, 1992.
16. I. C. Peden, R. Kipp, and J. Allestad, "A Scale-Model Study of Down-Hole VHF Dipole Arrays with Application to Subsurface Exploration," *IEEE Transaction on Geoscience and Remote Sensing*, **30**, 5, September 1992, pp. 885-891.
17. I. C. Peden and J. Brew, "A Laboratory Scale Model for the Study of Subsurface Scattering in Low-Loss Media with Applications to Ground Penetrating Radar," *Applied Geophysics*, **33**, 1-3, January 1995, pp. 109-118.
18. J.-H. Cho, J.-H. Jung, and S.-Y. Kim, "Laboratory Scaled-Down Experiment of Cross-Borehole Pulse Radar Signatures for Detection of a Terminated Tunnel," *Measurement Science and Technology*, **27**, 9, August 2016, pp. 095008.
19. J.-H. Cho and S.-Y. Kim, "Wideband Symmetric Near-Field Radiation Pattern of Sleeve Dipole Antenna by Connecting Additional Ferrite-Loaded Wire," *Electronics Letters*, **51**, 8, April 2015, pp. 610-611.
20. J.-H. Jung and S.-Y. Kim, "Measured Dielectric Properties of Borehole Cores Using an Open-Ended Coaxial Probe," *Technical Report of IEICE. SANE*, **107**, 277, October 2007, pp. 99-102.
21. J.-H. Jung, J.-H. Cho and S.-Y. Kim, "Accuracy Enhancement of Wideband Complex Permittivity Measured by an Open-Ended Coaxial Probe," *Measurement Science and Technology*, **27**, 1, January 2016, pp. 015011; available: <http://www.samwha.co.kr/electronics/product/product.aspx> (last access January 6, 2017)

RF Output-Power Enhancement by Optical-Pulse Compression in Photonic-Based RF Generation

Takashi Yamaguchi, Hiroki Morimoto, and Hiroyuki Toda

Graduate School of Science and Engineering
Doshisha University
Kyotanabe, Japan
E-mail: eup1306@mail4.doshisha.ac.jp
dup0332@mail4.doshisha.ac.jp htoda@mail.doshisha.ac.jp

Abstract

In photonic-based RF generation, the RF output power is limited by the average optical power to the photodetector (PD). It is known that the RF output power is enhanced by use of a narrow optical pulse at the photodetector, whereas the average power to the photodetector is the same. In this paper, we propose to use optical-pulse compression in a standard optical fiber in order to enhance the RF output power. We use an optical two tone, or optical pulses generated with a Mach-Zehnder modulator (MZM), as an optical-pulse source. In numerical simulation of the Mach-Zehnder modulator pulse, a maximum RF gain due to optical-pulse compression of 8.0 dB is obtained. In a 20-GHz RF generation experiment with a standard single-mode fiber and a Mach-Zehnder modulator pulse, an RF gain of 6.6 dB was obtained with a fiber length of 7.5 km and a launched average power to the fiber of 20.0 dBm. Furthermore, we found that 50 GHz, 75 GHz, and 100 GHz generation with RF gain is possible with realistic optical power if non-zero dispersion-shifted fiber is used as the transmission fiber, whereas highly nonlinear fiber is necessary for 300-GHz RF generation.

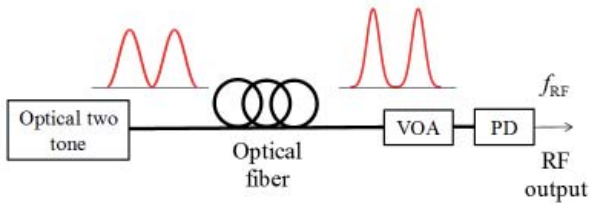
1. Introduction

Microwave and millimeter-wave generation based on photonic technology [1-3] is promising for many applications, such as an opto-electronic oscillator [4], W-band radar [5], THz-wave generation [6], and so on. In this method, the RF output power is limited by the maximum average optical power delivered to the photodetector (PD). Photodiodes with high optical-power handling [7-10] are therefore necessary if high RF output power is required. Hirata et al. reported that if the optical pulse width delivered to the photodetector was narrower whereas the average power to the photodetector was the same, the RF output power was enhanced since the fundamental frequency

component included in the photodetector's input was increased [11]. Kuo et al. theoretically analyzed this phenomenon with a phase-locked optical-frequency comb [12] and showed that the theoretical limit of the power enhancement was 6 dB when the number of comb lines was increased from two (optical two tone) to infinite. So far, generating of 100 GHz [12] and 160 GHz [13] signals were reported by using short optical pulses delivered to the photodetector.

The use of an optical-frequency comb and a spectral pulse shaper enables us to shorten the optical pulse width. However, the setup becomes complicated. Recently, we proposed a new simple approach that utilizes optical-pulse compression in a standard optical fiber [14]. The optical-pulse width can be shortened by properly adjusting the fiber's length and the power launched into the fiber in accordance with the fiber's dispersion and the pulse repetition frequency. A Mach-Zehnder modulator (MZM) is used to generate the optical pulse in order to enhance the RF power more efficiently by increasing the duty ratio of the optical pulse.

In this paper, we numerically and experimentally demonstrate RF output-power enhancement by optical-pulse compression in a standard optical fiber, with optical two tone and optical pulses generated with a Mach-Zehnder modulator. In Section 2, we describe a numerical simulation of optical-pulse propagation in an optical fiber using the generalized nonlinear Schrödinger equation (GNLSE), and calculate the gain of the RF output power due to the optical-pulse compression. In Section 3, we describe experiments on the RF output-power enhancement with narrower optical pulses and optical-pulse compression. Furthermore, we investigate the possibility of high-frequency RF generation using the scaling law of the generalized nonlinear Schrödinger equation in Section 4. Finally, we conclude our discussion in Section 5.

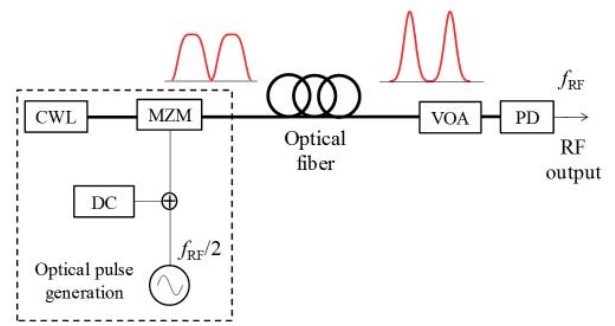


VOA: Variable optical attenuator, PD: Photo detector.

Figure 1a. The simulation model of the photonic-based RF generation with optical-pulse compression in an optical fiber. An optical two tone was used as the optical pulse source.

2. Simulation

In this section, we describe a numerical simulation for the RF output-power enhancement by optical-pulse compression. Figure 1 shows the simulation model of the photonic-based RF generation. In Figure 1a, an optical two tone with a repetition frequency of f_{RF} was used as the optical-pulse source. In Figure 1b, a Mach-Zehnder modulator generated optical pulses with a repetition frequency of f_{RF} . The Mach-Zehnder modulator pulses were generated as follows. Single-frequency continuous-wave (CW) laser light, generated by a CW laser (CWL), was intensity modulated with a Mach-Zehnder modulator. The operating point of the Mach-Zehnder modulator was set to minimum transmission with a dc bias voltage. The Mach-Zehnder modulator was then driven by an RF sine wave with a repetition frequency of $f_{RF}/2$ and the amplitude of the half-wave voltage of the Mach-Zehnder modulator. The resultant Mach-Zehnder modulator's output was carrier-suppressed return-to-zero with a frequency of f_{RF} , where the optical phase was reversed from one pulse to the next. The optical pulse was transmitted in an optical fiber in order to perform optical-pulse compression, and detected with a photodetector. A variable optical attenuator (VOA) was used to keep the average power to the photodetector constant. Finally, the RF power with the f_{RF} component was measured. We set $f_{RF} = 20$ GHz in order to simulate the experiment that will be described later.



CWL: CW laser, MZM: Mach-Zehnder modulator, VOA: Variable optical attenuator, PD: Photo detector.

Figure 1b. The simulation model of the photonic-based RF generation with optical-pulse compression in an optical fiber. A Mach-Zehnder modulator generated the optical pulses.

The electric field of the optical pulse during the fiber transmission was obtained by solving the generalized nonlinear Schrödinger equation (GNLSE),

$$\frac{\partial A}{\partial z} + \frac{i\beta_2}{2} \frac{\partial^2 A}{\partial t^2} - \frac{\beta_3}{6} \frac{\partial^3 A}{\partial t^3} + \frac{\alpha}{2} A = i\gamma |A|^2 A, \quad (1)$$

where $A, z, t, \hat{a}_2, \hat{a}_3, \hat{a}$, and γ were the electric field, transmission distance, time, second-order dispersion, third-order dispersion, loss, and nonlinear coefficient, respectively [15]. Here, we ignored higher-order effects, such as forth-order dispersion and the Raman effect. In this simulation, we supposed the use of standard single-mode fiber (SSMF) as the optical fiber so that the dispersion parameter was $D = 17$ ps/nm/km, the dispersion slope was $D_s = 0.06$ ps/nm²/km, the loss coefficient was 0.2 dB/km, the Kerr coefficient was $n_2 = 2.2 \times 10^{-20}$ m²/W, and the effective area was $A_{eff} = 80$ μ m², respectively. After the electric field of the transmitted optical pulse was obtained, the generated RF output power P_{RF} was obtained from the following equation:

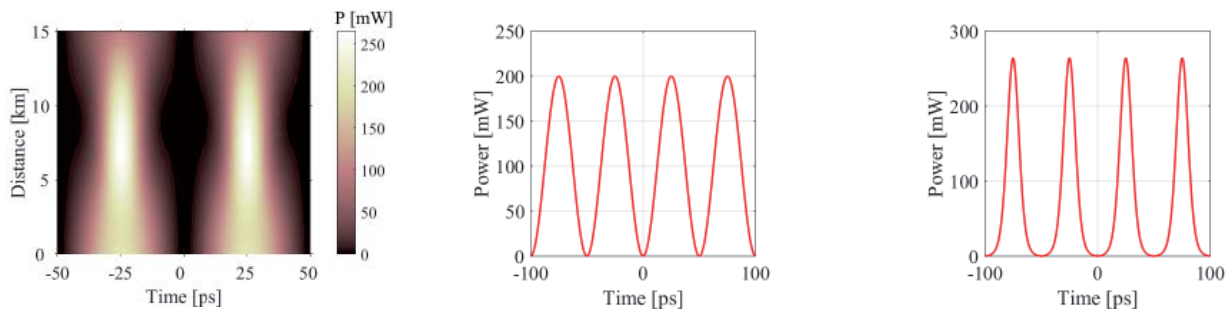


Figure 2. The calculated optical pulse in the case of an optical two tone, where the peak optical power at $z = 0$ km was 200 mW. (a) The plot shows the optical pulse's propagation, and (b) and (c) show optical-pulse waveforms at $z = 0$ km and $z = 7.0$ km, respectively.

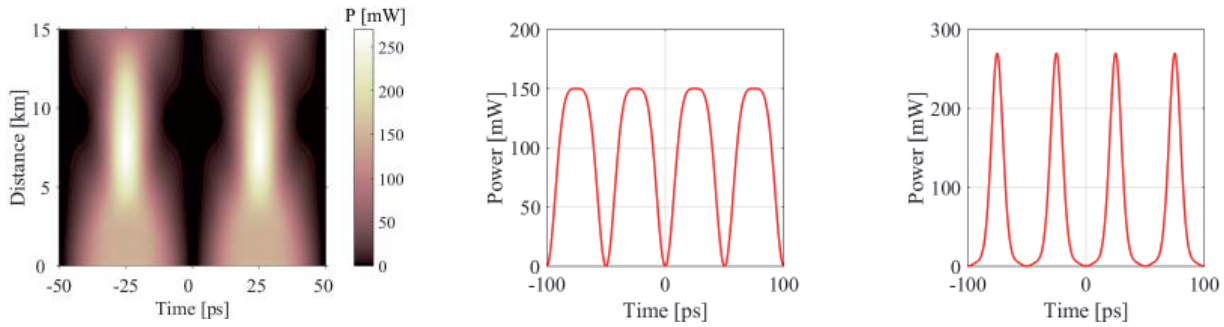


Figure 3. The calculated optical pulse for the case of a Mach-Zehnder modulator pulse where the peak optical power at $z = 0$ km was 150 mW. (a) The plot shows the optical pulse's propagation, and (b) and (c) show optical-pulse waveforms at $z = 0$ km and $z = 7.4$ km, respectively.

$$P_{RF} = ZR^2 \left| \mathfrak{F} [P(t)] \right|_{f=f_{RF}}^2, \quad (2)$$

where Z , R , $P(t)$ are the impedance of the RF circuit, the responsivity of the photodetector, and the optical intensity waveform at the photodetector, respectively, and \mathfrak{F} denotes complex Fourier transformation. Using Equation (2), we calculated the RF gain due to optical-pulse compression, which is defined as the ratio of the RF power obtained from the transmitted optical pulse to the RF power without fiber transmission.

Figure 2 shows the calculated optical pulse for the case of an optical two tone where the peak optical power at $z = 0$ km was 200 mW. Figure 2a shows the optical-pulse propagation. The optical pulse was compressed after the fiber propagation, and the pulse width was minimized at fiber length of 7.0 km. Figures 2b and 2c show the optical-pulse waveforms at $z = 0$ km and $z = 7.0$ km, respectively. The 25.0 ps optical-pulse width was compressed to 11.7 ps after the fiber transmission.

Figure 3 shows the calculated optical pulse for the case of the Mach-Zehnder modulator pulse. The peak optical power at $z = 0$ was 150 mW, where the average optical power was the same as that of the optical two tone. Figure 3a

shows the optical-pulse propagation. The optical pulse was compressed after the fiber propagation, and the pulse width was minimized at a fiber length of 7.4 km. Figures 3b and 3c show the optical-pulse waveforms at $z = 0$ km and $z = 7.4$ km, respectively. The 33.4 ps optical-pulse width at the Mach-Zehnder modulator output was compressed to be 11.5 ps after the fiber transmission.

We next calculated the optical-pulse width and the RF gain due to optical-pulse compression as a function of initial peak power to the fiber, P_0 , and the transmission distance. Figure 4 shows the results for the case of an optical two tone. Figures 4a and 4b show the optical-pulse width and the RF gain, respectively. By increasing P_0 , a narrower optical pulse could be obtained, and maximum RF gain at the optimized transmission distance was increased. RF gain was not obtained when P_0 was low, i.e., without optical-fiber nonlinearity. Figure 4c shows the maximum RF gain and the transmission distance where the RF gain was maximized as functions of P_0 . The RF gain was maximized at a transmission distance of between 3.2 km and 8.9 km, where P_0 was < 30 dBm. The maximum RF gain increased up to 5.1 dB when P_0 was 26.3 dBm at a transmission distance of 5.9 km.

Figure 5 shows the results for the case of a Mach-Zehnder modulator pulse. Figures 5a and 5b show the

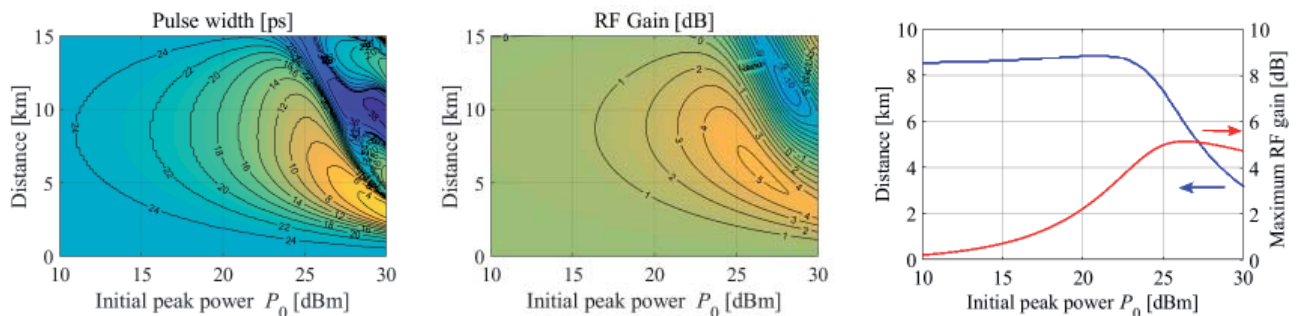


Figure 4. The calculated optical-pulse width and RF gain due to optical-pulse compression as functions of the initial peak power to the fiber, P_0 , and the transmission distance, with an optical two tone. (a) and (b) show the optical pulse width and the RF gain, respectively. (c) shows the maximum RF gain and the transmission distance where the RF gain is maximized as functions of P_0 .

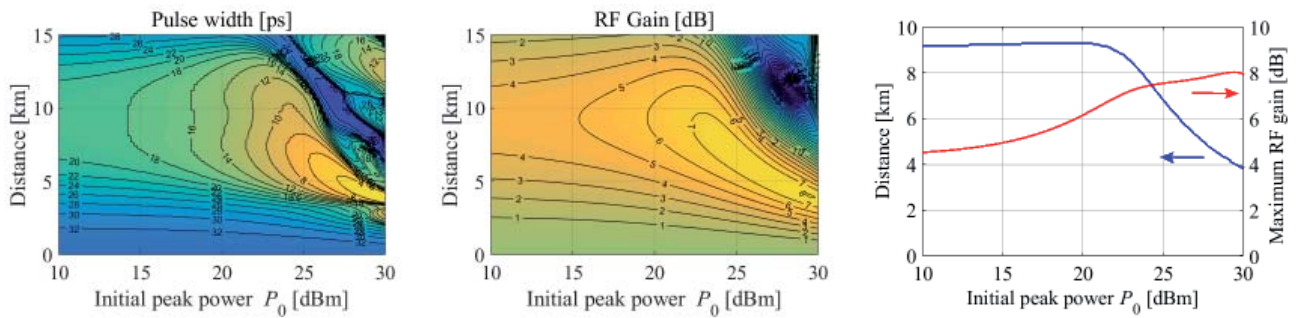


Figure 5. The calculated optical pulse width and RF gain due to optical-pulse compression as functions of the initial peak power to the fiber, P_0 , and the transmission distance, with a Mach-Zehnder modulator pulse. (a) and (b) show the optical-pulse width and the RF gain, respectively. (c) shows the maximum RF gain and the transmission distance where the RF gain is maximized as functions of P_0 .

optical-pulse width and the RF gain, respectively. By increasing P_0 , a narrower optical-pulse could be obtained, and the maximum RF gain at the optimized transmission distance was increased, as in the case of the optical two tone. Figure 5c shows the maximum RF gain and the transmission distance where the RF gain was maximized as functions of P_0 . The RF gain was maximized at a transmission distance of between 3.8 km and 9.2 km, where P_0 was < 30 dBm. The maximum RF gain increased up to 8.0 dB when P_0 was 29.5 dBm at a transmission distance of 4.0 km. As will be described in Section 3.1, the P_{RF} obtained by the Mach-Zehnder modulator pulse without fiber transmission was 2.6 dB lower than that of the optical two tone. The RF power obtained at this point was therefore 5.4 dB higher than that obtained by an optical two tone with the same average optical power, while the theoretical limit was 6 dB. It should be noted that when P_0 decreased 5 dB, the RF gain decreased only 0.4 dB. It should also be noted that a fair amount of RF gain was obtained even though P_0 was low. For example, when P_0 was 10 dBm, the maximum RF gain of 4.5 dB was obtained with a transmission distance of 9.2 km.

3. Experiment

3.1 RF Output-Power Enhancement with Narrower Optical Pulse

We performed an experiment in order to confirm the RF-power enhancement due to the use of a narrower optical pulse. The measurement principle is shown in Figure 6. First, we illuminated a photodetector with an optical two tone with an average power of P_{ave} , and measured the generated RF power, P_{RF0} , with an RF spectrum analyzer (RFSA). P_{RF0} was used as a reference power. We then illuminated the photodetector with several kinds of optical pulses with the same average power, P_{ave} , and measured the generated RF power, P_{RF} . The amplification factor, F_A , defined by P_{RF}/P_{RF0} , was then obtained. In this experiment, we set the repetition frequency of the optical

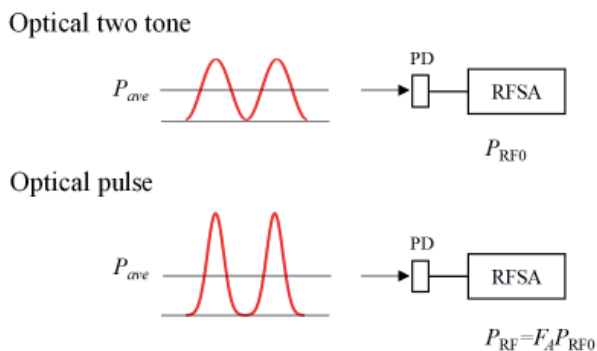


Figure 6. The measurement principle for confirming the RF output-power enhancement with a narrower optical pulse.

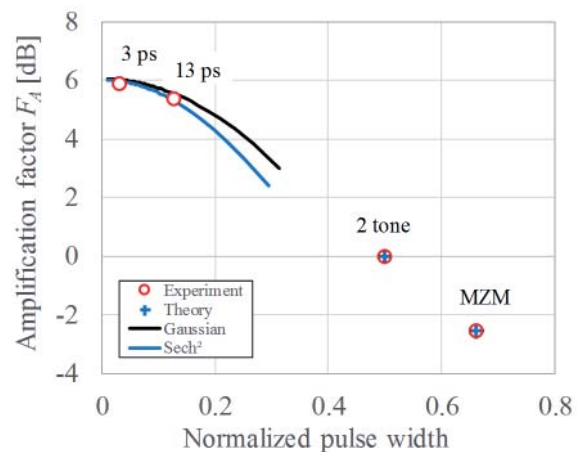
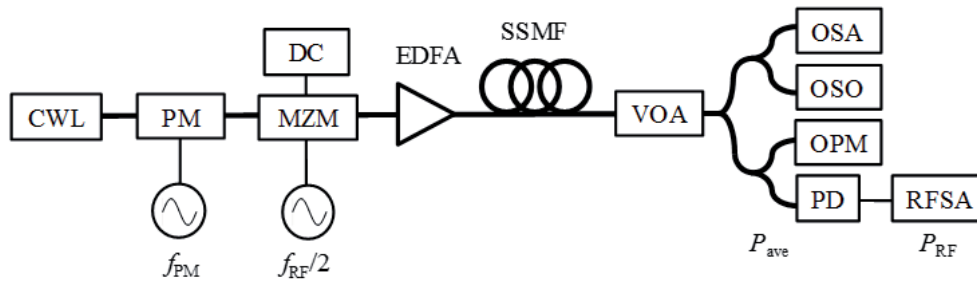


Figure 7. The measured and calculated amplification factors of a 10-GHz RF output as functions of the normalized pulse width.



CWL: CW laser, PM: Phase modulator, MZM: Mach-Zehnder modulator, LO: Local oscillator, FBG: Fiber Bragg grating, EDFA: Erbium doped fiber amplifier, SSMF: Standard single-mode fiber, VOA: Variable optical attenuator, OSA: Optical spectrum analyzer, OSO: Optical sampling oscilloscope, OPM: Optical power meter, PD: Photo detector, RFSA: RF Spectrum analyzer.

Figure 8. The experimental setup for the photonic-based RF generation with output-power enhancement due to the optical-pulse compression.

pulse to be 10 GHz. The bandwidth of the photodetector used in the experiment was 8 GHz. Figure 7 shows the measured and the calculated F_A values of the 10 GHz RF output as functions of the pulse width, normalized by the repetition period. For an optical two tone, the normalized pulse width was 0.5, and F_A was 0 dB. The 3 ps and 13 ps points show the results when 3 ps and 13 ps optical pulses, generated from an actively mode-locked fiber ring laser, were illuminated onto the photodetector. The MZM point shows the result when the optical pulse was generated with a Mach-Zehnder modulator with the same operating conditions described in the previous session, except for $f_{RF} = 10$ GHz. The normalized pulse width was 0.33, and F_A was -2.6 dB. The Gaussian and sech² curves show the calculated values when the optical pulse was a Gaussian pulse and a hyperbolic-secant pulse, respectively. The measured results were well consistent with the calculated results. It was clearly seen that when the pulse width was narrower, the amplification factor, F_A – i.e., the RF output power – was increased [11].

3.2 RF Output Power Enhancement by Optical Pulse Compression

We next performed an experiment in order to confirm the RF power enhancement due to optical-pulse compression. Figure 8 shows the experimental setup. A CW laser output with a wavelength of 1550 nm was phase modulated with a phase modulator (PM) in order to reduce the influence of stimulated Brillouin scattering (SBS) [16]. The modulation frequency, f_{PM} , was 300 MHz. The phase modulator's output was intensity modulated with a Mach-Zehnder modulator. A dc bias voltage was set to the minimum transmission point of the Mach-Zehnder modulator. The driving RF voltage to the Mach-Zehnder modulator was adjusted in such a way that the first-order sideband power to the third-order sideband power was 18.7 dB, using the optical spectrum analyzer (OSA). The driving condition of the Mach-Zehnder modulator then became the same as that used in the simulation. We set $f_{RF}/2 = 10$ GHz. In the

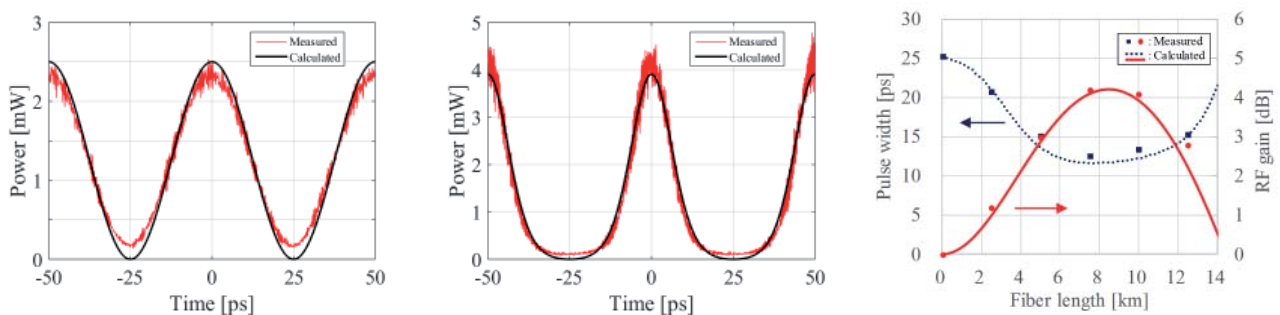


Figure 9. The measured and calculated results in the case of an optical two tone. (a) and (b) show the observed and simulated optical waveforms at fiber lengths of 0 km and 7.5 km, respectively. (c) shows the measured and calculated RF gains and pulse widths as functions of the fiber length.

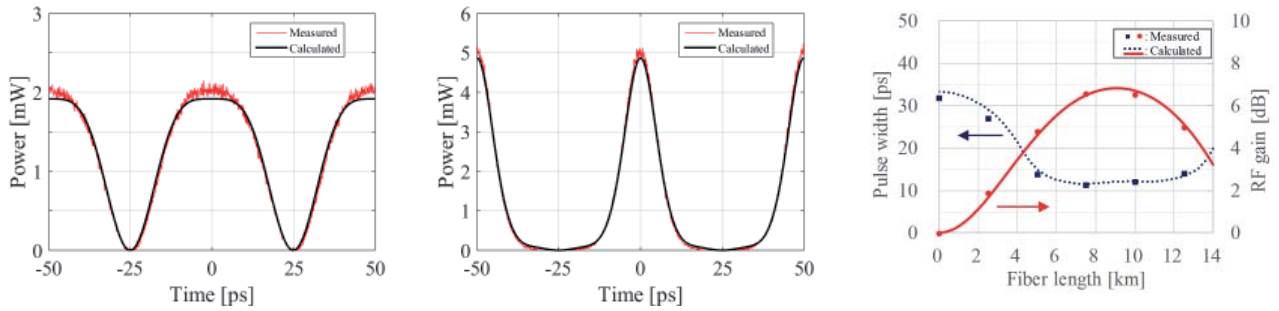


Figure 10. The measured and calculated results in the case of a Mach-Zehnder modulator pulse. (a) and (b) show the observed and simulated optical waveforms at fiber lengths of 0 km and 7.5 km, respectively. (c) shows the measured and calculated RF gains and pulse widths as functions of the fiber length.

case of the optical two tone, the Mach-Zehnder modulator output was filtered by a fiber Bragg grating (FBG) with a bandwidth of 0.15 nm in order to suppress higher-order sidebands. The output was amplified with an erbium-doped fiber amplifier (EDFA) to an average power of 20.0 dBm, corresponding to a peak power for the Mach-Zehnder modulator pulse and the optical two tone of 21.8 dBm and 23.0 dBm, respectively. The amplified optical pulses were transmitted in a standard single-mode fiber, and were attenuated with a variable optical attenuator for setting the average optical power, P_{ave} , to the photodetector to be 1.0 dBm. In a practical case, the variable optical attenuator is useful in order to prevent damage to the photodetector. The bandwidth of the photodetector used in the experiment was 20 GHz. The photodetector output RF power, P_{RF} , was measured by an RF spectrum analyzer (RFSa). The optical intensity waveform to the photodetector was also observed with an optical sampling oscilloscope (OSO). We changed the fiber length to values of 0 km, 2.5 km, 5.0 km, 7.5 km, 10.0 km, and 12.5 km.

Figure 9 shows the measured and calculated results for the case of an optical two tone. Figures 9a and 9b show the observed and simulated optical waveforms at fiber lengths of 0 km and 7.5 km, respectively. Figure 9c shows the measured and calculated RF gains and pulse widths as functions of the fiber's length. The measured results showed good agreement with the calculated results. When the fiber length was 7.5 km, the measured and calculated pulse widths were 12.5 ps and 11.7 ps, respectively, and the measured and calculated RF gains were 4.2 dB and 4.1 dB, respectively. Figure 10 shows the measured and calculated results for the case of a Mach-Zehnder modulator pulse. Figures 10a and 10b show the observed and simulated optical waveforms at fiber lengths of 0 km and 7.5 km, respectively. Figure 10c shows the measured and calculated RF gains and pulse widths as functions of the fiber's length. The measured results showed good agreement with the calculated results. When the fiber length was 7.5 km, the measured and calculated pulse widths were 11.4 ps and 11.5 ps, respectively, and the RF gains were 6.6 dB and 6.4 dB, respectively.

From the results described above, we confirmed the RF output-power enhancement due to optical-pulse compression with a standard single-mode fiber.

4. Toward High-Frequency Generation

According to the scaling law of the generalized nonlinear Schrödinger equation [17], it turns out that when the variables t , \hat{a}_2 , γ , z , \hat{a}_3 , \hat{a} , and A are converted to $T = \kappa_1 t$, $B_2 = \kappa_2 \beta_2$, $\Gamma = \kappa_3 \gamma$, $Z = (\kappa_1^2 / \kappa_2) z$, $B_3 = \kappa_1 \kappa_2 \beta_3$, $A_1 = (\kappa_2 / \kappa_1^2) \alpha$, and $U = \sqrt{\kappa_2 / \kappa_1^2} \kappa_3 A$, the differential equation of U with respect to Z and T exactly takes the same form as Equation (1). This means that if parameters such as the RF frequency ($\propto t^{-1}$), fiber length, and dispersion, and optical power are changed in accordance with the above relationships, the RF gain exactly becomes the same. This gives us a design guideline towards high-frequency RF generation.

Let us suppose that the optical pulse is the Mach-Zehnder modulator pulse, f_{RF} is 50 GHz ($\kappa_1 = 0.4$) and nonzero dispersion-shifted fiber (NZ-DSF) is used as the transmission fiber, where $D = 2$ ps/nm/km ($\kappa_2 = 0.12$) and $A_{eff} = 50 \mu\text{m}^2$ ($\kappa_3 = 1.6$). In this case, the same RF gain of 8.0 dB is expected when the initial peak power, P_0 is 26.1 dBm and the transmission distance is 5.5 km. In this argument, we neglected the loss and the third-order dispersion terms, since those parameters are difficult to control and the transmission distance is not so long. If f_{RF} becomes very high and low-dispersion fiber, such as DSF, is used – in other words, higher-order dispersion lengths become comparable to the second-order dispersion length – the higher-order dispersions need to be considered. In order to check the validity of the expected RF gain, we calculated the RF gain by solving the generalized nonlinear Schrödinger equation with loss and third-order dispersion (0.2 dB/km and 0.6 ps/nm²/km). The RF gain obtained was 8.0 dB, which was the same as that obtained by the scaling law. When f_{RF} was 75 GHz ($\kappa_1 = 0.27$) and the same nonzero dispersion-shifted fiber was used, an RF gain

Table 1. The design parameters for high-frequency RF generation. z and P_0 were obtained from the scaling law, and the RF gain was obtained by solving the generalized nonlinear Schrödinger equation. See the text for details of the fiber's specifications.

Pulse Source	f_{RF} [GHz]	Fiber Type	z [km]	P_0 [dBm]	RF Gain [dB]	F_A [dB]
MMZ	20	SSMF	4.0	29.5	8.0	5.4
	50	NZ-DSF	5.5	26.1	8.0	5.4
	75	NZ-DSF	2.4	29.6	8.0	5.4
Optical 2 tone	20	SSMF	5.9	26.4	5.1	
	50	NZ-DSF	8.0	23.0	5.1	
	75	NZ-DSF	3.6	26.5	5.2	
	100	NZ-DSF	2.0	29.0	5.2	
		HNLF	4.0	18.1	4.8	
	300	HNLF	0.4	27.6	5.1	

of 8.0 dB was expected when P_0 was 29.6 dBm and the transmission distance was 2.4 km. The RF gain obtained by solving the generalized nonlinear Schrödinger equation was also 8.0 dB. As described in Sections 2 and 3.1, the RF gain due to optical-pulse compression of the Mach-Zehnder modulator pulse corresponded to an F_A of 5.4 dB.

We next made the same calculation for the optical two tone. When f_{RF} was 50 GHz and the same nonzero dispersion-shifted fiber was used as the transmission fiber, the same RF gain of 5.1 dB was expected by the scaling law when P_0 was 23.0 dBm and the transmission distance was 8.0 km. The same RF gain was obtained by solving the generalized nonlinear Schrödinger equation with loss and third-order dispersion. When f_{RF} was 75 GHz and the nonzero dispersion-shifted fiber was used, the same RF gain was expected when P_0 was 26.5 dBm and the transmission distance was 3.6 km. An RF gain of 5.2 dB was obtained by solving the generalized nonlinear Schrödinger equation. When f_{RF} was 100 GHz ($\kappa_1 = 0.2$), the same RF gain was expected when P_0 was 29.0 dBm and the transmission distance was 2.0 km. An RF gain of 5.2 dB was obtained by solving the generalized nonlinear Schrödinger equation. These results are summarized in Table 1.

As could be seen in the scaling law, P_0 is proportional to f_{RF}^2 and inversely proportional to D . The use of nonzero dispersion-shifted fiber is effective in reducing P_0 for high-frequency generation as described above. However, P_0 exceeded 30 dBm when $f_{RF} > 100$ GHz. In that case, highly nonlinear fiber (HNLF) is necessary as the transmission fiber. When f_{RF} was 100 GHz and a highly nonlinear fiber where $D = 1$ ps/nm/km ($\kappa_2 = 0.06$) and $\gamma = 12\text{W}^{-1}/\text{km}$ ($\kappa_3 = 10.7$) is used, an RF gain of 5.1 dB was expected when P_0 was 18.1 dBm and the transmission distance was 4.0 km. The RF gain from solving the generalized nonlinear Schrödinger equation with loss and third-order dispersion (1 dB/km and 0.02 ps/nm²/km) was 4.8 dB. The small discrepancy in the RF gain came from the attenuation due to the loss of the highly nonlinear

fiber. When f_{RF} was 300 GHz, the same RF gain was expected when P_0 was 27.6 dBm and the transmission distance was 0.4 km. The same RF gain of 5.1 dB was obtained by solving the generalized nonlinear Schrödinger equation, since the attenuation was negligible.

5. Conclusion

We proposed to use optical-pulse compression in a standard optical fiber in order to enhance the output power in photonic-based RF generation with a Mach-Zehnder modulator and an optical two tone. We numerically analyzed optical-pulse propagation using the generalized nonlinear Schrödinger equation, and obtained the RF gain due to optical-pulse compression. We experimentally confirmed that the RF output power was enhanced by the use of a narrower optical pulse and optical-pulse compression. In the 20-GHz RF generation experiment using a standard single-mode fiber and a Mach-Zehnder modulator pulse, an RF gain of 6.6 dB due to optical-pulse compression was obtained at a fiber length of 7.5 km and a launched average power to the fiber of 20.0 dBm. With an optical two tone, an RF gain of 4.2 dB was obtained with the same fiber length and launched average power to the fiber. Using the scaling law of the generalized nonlinear Schrödinger equation, we found that 50-GHz, 75-GHz, and 100-GHz generation with RF gain was possible with realistic optical power if nonzero dispersion-shifted fiber was used as the transmission fiber, whereas highly nonlinear fiber was necessary for 300-GHz RF generation.

6. Acknowledgement

This research was supported by "Radio technologies for 5G using Advanced Photonic Infrastructure for Dense user environments (RAPID)," the Commissioned Research of NICT, Japan, and SCOPE #165003010, The Ministry of Internal Affairs and Communications, Japan, to which the authors would like to express their gratitude.

7. Reference

1. J. Yao, "Microwave Photonics," *Journal of Lightwave Technology*, **27**, 3, February 2009, pp. 314-335.
2. J. A. Nanzer, P. T. Callahan, M. L. Dennis, and T. R. Clark, Jr., "Photonic Signal Generation for Millimeter-Wave Communications," *Johns Hopkins APL Technical Digest*, **30**, 4, January 2012, pp. 299-308.
3. K. Jung and J. Kim, "All-Fibre Photonic Signal Generator for Attosecond Timing and Ultralow-Noise Microwave," *Scientific Reports*, **5**, 16250, November 2015, pp. 1-7.
4. X. S. Yao and L. Maleki, "Optoelectronic Microwave Oscillator," *Journal of the Optical Society of America B*, **13**, 8, August 1996, pp. 1725-1735.
5. Y. Li, A. Rashidinejad, J. -M. Wun, D. E. Leaird, J.-W. Shi, and A. M. Weiner, "Photonic Generation of W-Band Arbitrary Waveforms with High Time-Bandwidth Products Enabling 3.9 mm Range Resolution," *Optica*, **1**, 6, December 2014, pp. 446-454.
6. T. Nagatsuma, S. Horiguchi, Y. Minamikata, Y. Yoshimizu, S. Hisatake, S. Kuwano, N. Yoshimoto, J. Terada, and H. Takahashi, "Terahertz Wireless Communications Based on Photonics Technologies," *Optics Express*, **21**, 20, October 2013, pp. 23736-23747.
7. D. A. Tulchinsky, J. B. Boos, D. Park, P. G. Goetz, W. S. Rabinovich, K. J. Williams, "High-Current Photodetectors as Efficient, Linear, and High-Power RF Output Stages," *Journal of Lightwave Technology*, **26**, 4, February 2008, pp. 408-416.
8. X. Xie, Q. Zhou, K. Li, Y. Shen, Q. Li, Z. Yang, A. Beling, J. C. Campbell, "Improved Power Conversion Efficiency in High-Performance Photodiodes by Flip-Chip Bonding on Diamond," *Optica*, **1**, 6, 2014, pp. 429-435.
9. E. Rouvalis, F. N. Baynes, X. Xie, K. Li, Q. Zhou, F. Quinlan, T. M. Fortier, S. A. Diddams, A. G. Steffan, A. Beling, and J. C. Campbell, "High-Power and High-Linearity Photodetector Modules for Microwave Photonic Applications," *Journal of Lightwave Technology*, **32**, 20, 2014, pp. 3810-3816.
10. M. N. Hutchinson, V. J. Urick, and N. J. Frigo, "Power Photodiodes for High Dynamic Range Photonic Links," *Applied Optics*, **54**, 31, November 2015, pp. F17-F24.
11. A. Hirata, M. Harada, and T. Nagatsuma, "120-GHz Wireless Link Using Photonic Techniques for Generation, Modulation, and Emission of Millimeter-Wave Signals," *Journal of Lightwave Technology*, **20**, 10, October 2003, pp. 2145-2153.
12. F.-M. Kuo, J.-W. Shi, H.-C. Chiang, H.-P. Chuang, H.-K. Chiou, C.-L. Pan, N.-W. Chen, H.-J. Tsai, and C.-B. Huang, "Spectral Power Enhancement in a 100 GHz Photonic Millimeter-Wave Generator Enabled by Spectral Line-by-Line Pulse Shaping," *IEEE Photonics Journal*, **2**, 5, 2010, pp. 719-727.
13. J. -M. Wun, H. -Y. Liu, C. -H. Lai, Y. -S. Chen, S. -D. Yang, C. -L. Pan, J. E. Bowers, C. -B. Huang, and J. -W. Shi, "Photonic High-Power 160-GHz Signal Generation by Using Ultrafast Photodiode and a High-Repetition-Rate Femtosecond Optical Pulse Train Generator," *IEEE Journal of Selected Topics in Quantum Electronics*, **20**, 6, November 2014, p. 3803507.
14. T. Yamaguchi, H. Morimoto, H. Toda, "Output Power Enhancement by Optical Pulse Compression in Photonic-Based RF Generation," in Proceedings of URSI AP-RASC, August 2016, pp. 1528-1530.
15. G. P. Agrawal, *Nonlinear Fiber Optics, Fifth Edition*, New York, Academic Press, 2013, Chapter 2.
16. A. Kobaykov, M. Sauer, and D. Chowdhury, "Stimulated Brillouin Scattering in Optical Fibers," *Advances in Optics and Photonics*, **2**, 1, March 2010, pp. 1-59.
17. D. Marcuse and C. R. Menyuk, "Simulation of Single-Channel Optical Systems at 100 Gb/s," *Journal of Lightwave Technology*, **17**, 4, April 1999, pp. 564-569.

Survey of Emerging Information Teleportation Networks and Protocols

*Ronald E. Meyers¹, Arnold D. Tunick¹, Keith S. Deacon¹,
and Philip R. Hemmer²*

¹US Army Research Laboratory
2800 Powder Mill Road
Adelphi, MD 20873 USA

²Texas A&M University
College Station, TX 77843, USA

Tel: +1 (301) 394-2111
E-mail: ronald.e.meyers6.civ@mail.mil

Abstract

Quantum-communications technologies, especially involving teleportation, will play an increasingly important role in both the domestic and defense sectors because of the promise for improved security, distributed quantum computing, and quantum sensing. This paper presents a review of this emerging field, summarizing key protocols as well as some representative quantum teleportation experiments conducted both in the laboratory and in the field. Briefly, in recent years, quantum teleportation has been demonstrated in both optical-fiber networks and in long-distance free-space channels, using entanglement on photonic chips as well as between photonic and atom/ion or solid-state qubits.

1. Introduction

The development of emerging information teleportation networks, involving new non-classical technologies such as quantum teleportation, is critically important for the future US Army because it will allow operations and applications that are not feasible using classical techniques. Quantum teleportation relates to the non-local transfer of quantum information between two or more nodes by entanglement of quantum particles [1-5]. Quantum teleportation uses entanglement in a non-local and non-classical way to transfer information between a sender and a receiver, without actually sending the photons that carry the information through the physical space in between. Classical communication techniques do not allow teleportation because they rely on inadequate measurements of and local approximations to the underlying physics. Short-

range teleportation can be performed using just photons. However, long-distance communication and network applications require long-time storage and entanglement purification that can only be accomplished with matter qubits such as atoms, ions, or solid-state emitters.

In recent years, the field of quantum-communication technology has been growing in importance as cybersecurity concerns rise. Future advances in fundamental quantum protocols and experimental demonstrations of teleportation are needed to enable development of the much-needed quantum-network capabilities. Initially, quantum communications such as teleportation may not have the communication speeds of classical networks. However, it must be kept in mind that quantum communications can exploit a richer set of physics and are qualitatively different from classical communications methods, which are fundamentally limited in their applications. Quantum physics needs to be further exploited to advance and apply teleportation for practical benefit. Research is underway on the process of manipulating photons, or photons in combination with matter such as atoms and ions, to efficiently perform teleportation by quantum means. The field of quantum-communication technology is growing in importance. Advances in fundamental quantum protocols and teleportation experiments will enable development of needed information teleportation-network capabilities [6-8]. By reviewing the past and current state-of-the-art, we expedite this process by avoiding duplication and identifying critical areas that need additional research in the near future.

This paper presents a summary of key quantum protocols in Table 1, and recently developed quantum-inspired classical protocols in Table 2. Fundamental

protocols include those related to various aspects of teleportation, including entanglement verification, non-locality, non-classicality, and privacy. Representative quantum-teleportation experiments performed in the laboratory and in the field are highlighted in Table 3. Experimental demonstrations include those using: (a) polarization-entangled photons, (b) time-bin-entangled photons, (c) hyper-entangled (polarization and angular momentum) photons and hybrid (spin and orbital momentum) entangled states, (d) teleportation on a photonic and/or solid-state chip, (e) establishing quantum information transfer from a propagating photonic qubit to a stationary solid-state-spin qubit, (f) teleportation between two macroscopic atomic ensembles, and (g) teleportation between two single trapped atoms/ions. Table 3 also summarizes recent free-space quantum-teleportation experiments with multi-photon entanglement, and includes several recent experiments related to emerging teleportation-network technologies.

2. Quantum Protocols

In this section, we discuss quantum protocols for quantum applications, technologies, and analysis. Quantum protocols can be broadly classified to include not only quantum communications, but also non-locality tests, non-classicality tests, quantum memories, quantum repeaters, and quantum networks.

2.1 Non-Locality, Non-Classicality and Bell-State Protocols (Table 1a)

Table 1a presents protocols for determining the degree to which the quantum nature of the physical process is expressed (i.e., defining metrics to measure the degree to which a process is non-classical). The earliest indication of the consequences of quantum science relating to non-classical communication was described by Einstein, Podolsky, and Rosen [9] in 1935. They showed that if correct, quantum theory must have correlations between particles that classical physics could not predict. Einstein referred to this as “spooky action at a distance,” and it is now known as the EPR effect. This important paper was the foundation for quantum communications and teleportation. Later, John Bell devised a test for the EPR effect that could be implemented in an experiment [10], thereby making Einstein’s predictions accessible to experimentalists. Clauser, Horne, Shimony, and Holt (CHSH) followed Bell, and devised a test that could be implemented with optics and the polarization of photons [11]. The CHSH test was one of the first to be used by experimentalists to show violations of Bell inequalities and thus the validity of quantum theory. Certain measurement-related loopholes of the original CHSH test were closed by Clauser and Shimony in the C-S protocol [12].

Table 1a. A summary of key quantum protocols: non-locality, non-classicality, and Bell state protocols.

Year	Protocol	Investigator(s)	Application	Description	Country	Reference
2015	Dist.-based analysis	Christensen, Nam Kwiat, Knill ...	Non-Locality	Bell inequality test	USA, CA USA, CA	Christensen [29] Knill et al. [30]
2015 2012	CPM	Sheng, Zhou	Bell state analysis	Complete Parity Check Measur.	CN JP, UK	Munro et al. [21] Sheng & Zhou [22]
2014	Multi-party Q comm	Erven, Meyer-Scott Jennewein, Resch	Non-Locality	3 photons entangled	CA, UK, AT USA, AU	Erven et al. [18]
1978	C-S	Clauser, Shimony	Non-Locality	Bell inequality	USA	Clauser & Shimony [12]
1969	CHSH	Clauser, Horne, Shimony, Holt	Non-Locality	Bell inequality test	USA	Clauser et al. [11]
1964	Bell violation	Bell	Non-Locality	Bell inequality	USA, CH	Bell [10]
1963 2015	Multi-boson correlation	Glauber Tamma, Laibacher	Multi-boson measurement	Multi-bosonic interference	USA GER	Glauber [23-25] Tamma & Laibacher [26]
1935	EPR	Einstein, Podolsky, Rosen	Non-Locality	Entanglement	USA	Einstein et al. [9]
2012	CSI	Cauchy, Schwarz	Non-Classicality	Cauchy-Schwarz inequality	AU, FR PL	Kheruntsyan et al. [17]
2000 1999	MDS/MSS	An, Tinh	Non-Classicality	Multimode sum/differ. squeezing	KR, VN VN	An & Tinh [16] An & Tinh [15]
1989	SDS	Hillery	Non-Classicality	Sum/difference squeezing	USA	Hillery [14]
1987	QS	Loudon, Knight	Non-Classicality	Quadrature squeezing	UK	Loudon & Knight [13]

Table 1b. A summary of key quantum protocols: quantum communication network protocols

Year	Protocol	Investigator(s)	Application	Description	Country	Reference
2016	Degraded state swap	Kirby	Q comm networks	Degraded state swapping	USA	Kirby et al. [19]
2016	Switching for entanglement	Drost	Q comm networks	Entanglement distribution	USA	Drost et al. [20]
2014	Loss based error correct.	Munro, Nemoto...	Q comm networks	Qcomm w/out Q memories	JP JP, UK	Munro et al. [21] Munro et al. [27]
2014	Quantum relay	Khalique, Sanders	Q comm networks	Concatenated entangle. swap	PK, CN, CA	Khalique & Sanders [28]

In 1987, Loudon and Knight provided an overview of the physics, generation, measurement, and possible application of squeezed light [13]. Squeezed light takes advantage of the properties of the Heisenberg uncertainty principle by reducing uncertainty in one variable while increasing the uncertainty in the conjugate variable. This squeezing can provide advantages to low-power (i.e., quantum-optical) communication, increased sensitivity in interferometric sensing, and spectroscopy. Hillery [14] introduced the idea of sum and difference squeezing of single-mode fields to expand the classes of non-classical squeezed states. This was followed by An and Tinh [15, 16], who extended the work to the more-general multimode case. In 2012, Kheruntsyan reported a violation of a Cauchy-Schwarz inequality (CSI) in matter waves as an indicator of non-classicality [17]. They recognized that a CSI violation implies but does not assure that the system may be in an EPR state or a Bell state.

In 2014, Erven et al. [18] provided an experimental demonstration of non-locality for a three-photon state. This experiment was important because entanglement between even greater numbers of particles is crucial to some quantum information processing and quantum communications protocol efficiency. Both Munro [21] and Sheng [22] theoretically investigated the use of “logical qubits” for application to quantum communications. A logical qubit is a qubit that is made up of one or more physical qubits, i.e., polarization states of a photon to hold and carry information from a sender to a receiver. They found that with small overhead in terms of physical qubits, quantum communication and measurements could be made more efficient than configurations that employed only the physical qubit. It must be mentioned that the notion of multi-photon interference introduced by Glauber [23-25] forms the basis for much of the theoretical work about entanglement and associated quantum information processing. This includes work on interferometry between n-photon states and single photons in an arbitrary state [26].

2.2 Quantum-Communication Network Protocols (Table 1b)

Quantum communications in a networked environment are currently an active area of research. The media through

which quantum communication propagates may degrade the quality of the state of the quantum system, for example, through scattering and absorption. To overcome a significant bottleneck in networked quantum communications, Nemoto and Munro developed the idea of quantum communications without quantum memories [21, 27]. This concept overcomes the need for nodes to notify their neighbor that an entanglement swap was successful by instead transmitting between nodes a logical qubit consisting of many quantum states. Here, local operations on the logical qubit can recover from losses through quantum-error correction, and a new logical qubit with additional photons can be sent to the next node. Similarly, Khalique and Sanders [28] introduced the notion of concatenated-entanglement swapping between intermediate nodes in a quantum network as a type of quantum relay to entangle remote memory nodes. An analysis by Kirby et al. [19] analytically derived the error bounds when entanglement swapping is performed with degraded states. Another quantum-communications concern in a networked environment is the distribution of the entanglement to distant nodes for use in teleportation or other quantum-communications processes. Adapting typical configurations for scalable, reconfigurable optical-communications networks, Drost et al. [20] derived efficient entanglement distribution-routing protocols for N-node networks.

2.3 Quantum-Communication Protocols (Table 1c)

The earliest quantum-communications protocols were developed for quantum-key distributions (QKD). The first by Bennett and Brassard [38] in 1984 – the so-called BB84 protocol – employed two polarization states in two bases between a sender (Alice) and a receiver (Bob). Later, in 1992, a simplified quantum-key distributions protocol was developed by Bennett [36] (B92) that only used two bases and polarization orientations, and was not as secure as the BB84 protocol. Entangled photons are also able to be used for quantum-key distributions, as shown by Ekert [37] in 1991. Ekert’s protocol is as secure as BB84, but due to the use of entangled photons, it is somewhat more complex to implement. One of the most important non-quantum-key distributions quantum-communications protocols was proposed by Bennett. It described a means

Table 1c. A summary of key quantum protocols: quantum communications protocols

Year	Protocol	Investigator(s)	Application	Description	Country	Reference
2015	SDT	Graham, Bernstein, Wei, Junge, Kwiat	Q comm	SuperDense Teleportation	USA	Graham et al. [31]
2015	DSQC/QSDC	Banerjee, Pathak	Q comm	Direct Secure Qcomm	IN, CZ	Banerjee & Pathak [32]
2006	QSDC	Zhu, Xia, Fan, Zhang	Q comm	Q secure direct comm	CN	Zhu et al. [33]
2005	DSQC w/out entangle	Lucamarini & Mancini	Q comm	Deterministic Secure Qcomm	IT	Lucamarini & Mancini [34]
2002	DSQC with entangle	Bostrom & Felbinger	Q comm	Deterministic Secure Qcomm	GER	Bostrom & Felbinger [35]
1993	Teleportation	Bennett, Brassard, Peres, Wootters..	Q comm	EPR correlated particle pair	USA, CA, FR, IL	Bennett et al. [1]
1992	B92	Bennett	Q comm	QKD	USA	Bennett [36]
1991	E91	Ekert	Q comm	Entangled QKD	UK	Ekert [37]
1984	BB84	Bennett, Brassard	Q comm	QKD	USA, CA	Bennett & Brassard [38]

for quantum teleportation [1] by which the quantum state of a particle could be sent to a receiver with an overhead of only two classical bits. Many advanced quantum-communications and quantum-networking protocols are based on teleportation.

A deterministic quantum-communications protocol was proposed in 2002 by Bostrom and Felbinger [35]. Their protocol requires Bob to retain one photon of an entangled pair of photons and to transmit the other photon to Alice. Alice encodes a message by performing a local operation on her photon to change the Bell state. After the operation, Alice sends the photon back to Bob, who makes a Bell-state measurement. The outcome of the Bell measurement is the encoded message sent by Alice. It was shown that protocols of this type can be developed using non-orthogonal-polarization states, and do not rely on entanglement properties [34].

Other methods, such as secure direct quantum communication using entangled particles, have been proposed. This was first reported in 2006 by Zhu et al. [33], and was followed by a similar protocol in 2015 by Banerjee and Pathak [32]. Neither of these protocols uses teleportation, and they are forms of direct quantum

communications. Lastly, a new and promising protocol using hyper-entanglement [31] has been demonstrated that can encode more information per entangled pair than the usual teleportation protocols. This increases the amount of information teleported per entangled pair.

Tables 1d through 1f present summaries of quantum information transfer, privacy, quantum repeater, and quantum memory protocols.

2.4 Quantum Information Transfer and Privacy Protocols (Table 1d)

In 2013 and 2015, Chiribella and Dur investigated protocols to replicate quantum states and unitary operations. Chiribella et al. [39] found that by relaxing the requirement of a perfect copy it is possible to make imperfect copies of a quantum state within certain error bounds based on probability. The research by Dur et al. [40] found that it is possible to deterministically replicate unitary operations that act on a quantum state multiple times at the expense of success probability. Concerning the goal of privacy, in 2014 Ekert and Renner [41] showed that while research is still needed on the ultimate physical bounds to privacy,

Table 1d. A summary of key quantum protocols: quantum information transfer and privacy protocols

Year	Protocol	Investigator(s)	Application	Description	Country	Reference
2015	Super-replicate	Dur, Sekatski, Skotiniotis	Quant. info. transfer	Deterministic Q cloning	AT	Dur et al. [40]
2013	Super-replicate	Chiribella, Yang, Yao	Quant. info. transfer	Probabilistic Q cloning	CN	Chiribella et al. [39]
2014	Privacy	Ekert, Renner	Privacy	Phys. limits of privacy	UK, SG, CH	Ekert & Renner [41]

Table 1e. A summary of key quantum protocols: quantum repeater protocols.

Year	Protocol	Investigator(s)	Application	Description	Country	Reference
2016	Rydberg	Solmeyer, Li, Quraishi	Q repeater	Entanglement	USA	Solmeyer et al. [42]
2010	Rydberg	Zhao, Zoller,...	Q repeater	Entanglement	AT	Zhao, et al. [43]
2010	Rydberg	Han, Simon,...	Q repeater	Entanglement	CN, CA	Han et al. [44]
2015	M–M S-R, M–S	Jones, Kim, Rakhker, Kwiat, Ladd	Q repeater networks	Entanglement distribution	USA	Jones et al. [45]
2015	Time reversal; Cluster state	Azuma, Tamaki, Lo	Q repeaters	All photonic repeaters	JP, CA	Azuma et al. [46]
2011	SPS	Sangouard, Simon, deRiedmatten, Gisin	Q repeaters	Entangle distant memories	CH, FR, CA, ES	Sangouard et al. [47]
2001	DLCZ	Duan, Lukin, Cirac, Zoller	Q repeaters	Entangle distant memories	AT, CN USA	Duan et al. [49]
1998	BDCZ	Briegel, Dur, Cirac, Zoller	Q repeaters	Entangle distant memories	AT, ES	Briegel et al. [48]

under rather weak assumptions it is possible to keep information private.

3. Quantum-Repeater Protocols (Table 1e)

Quantum repeaters and the distribution of entanglement are vital components for an information-teleportation network. In the following, several important and promising quantum-repeater protocols are discussed. The BDCZ and DLCZ protocols that actually entangle atomic quantum memories were developed by Briegel et al. [48] and Duan et al. [49], respectively. The BDCZ and DLCZ protocols use one-photon interaction with a quantum memory, or interactions between one photon each from two different quantum memories to entangle the memories, and are the focus of intense experimental research. Sangouard et al. [47] described a quantum network comprising nodes of atomic-based quantum memories and entanglement swapping to distribute entanglement to remote nodes. One protocol for entanglement distribution, developed by Jones et al. [45], highlighted that the node-to-node protocol has a large impact on network performance. They found that a mid-point-source-protocol configuration could yield orders-of-magnitude increased performance. A protocol was also suggested in which quantum memories at intermediate nodes could be eliminated in an all-photonic configuration [46]. Proposed by Azuma, this protocol avoids the complexity of interactions with matter-based qubits at nodes in favor of large-photon-number states and efficient photon routing. A recently proposed protocol involves using Rydberg states and Rydberg blockades in atomic ensembles to potentially increase bit rates in neutral-atom-ensemble repeaters by orders of magnitude [42-44].

3.1 Quantum-Memory Protocols (Table 1f)

Quantum-memory protocols use physical interactions between light (photons) and matter (atoms) to store quantum information. One low-noise and efficient scheme is controlled reversible inhomogeneous broadening (CRIB) [50-52], and has been typically used with solid-state rare-earth-doped crystal or fiber quantum memory. Atomic-frequency-comb-based quantum memories also show good results, and have been demonstrated to store multimode quantum information [53]. An early use of the CRIB protocols were the quantum memories that demonstrated the use of gradient echo to store quantum information [54, 55], and are usually fairly easy to implement. Electromagnetically induced transparency (EIT) protocols that can have long storage times with high efficiency and low noise have been shown to be optimal for storage in optically dense media [56, 57].

Table 2 presents a summary of quantum-inspired protocols. In particular, the paper by Qian et al. [58] highlighted the difficulty in determining what is and what is not quantum, and how the quantum features of a phenomenon are determined. As they demonstrated with a particular experimental setup using a diode light source, many of the “standard” tests of entanglement can be met. Similarly, the paper by Rafsanjani et al. [59] experimentally demonstrated that particular states of light encoded into alternate degrees of freedom, such as orbital angular momentum (OAM) or polarization, can be used to transfer information from a sender to a receiver in a manner similar to teleportation but without the benefits of non-locality. Investigations by Banaszek on low-power optical communication showed that even using known

Table 1f. A summary of key quantum protocols: quantum memory protocols.

Year	Protocol	Investigator(s)	Application	Description	Country	Reference
2010	CRIB	Longdell,	Memory	Controll. Revers.	AU, NZ, CN	Hedges et al. [51]
2010	CRIB	Sellers.		Inhomogeneous	CH, ES	Lauritzen et al.
2006	CRIB	Sangouard, Gisin. Tittel, Nilsson.		Broadening	CH, SE, GER	[52] Kraus et al. [50]
2009	AFC	Afzelius, Simon deRiedmatten, Gisin	Memory	Atomic Freq. Comb	CH	Afzelius et al. [53]
2008	GEM	Sellers,	Memory	Gradient Echo	AU, NZ	Hetet et al. [55]
2006	GEM	Longdell... Alexander, Hetet		Memory	Memory	AU
2007	EIT	Gorshkov,	Memory	Electromagnet.	USA, GER	Gorshkov et al.
1991	EIT	Lukin... Boller, Imamoglu...		Induced Trans.	DK, USA	[57] Boller et al. [56]

classical-communications encodings, such as pulse-phase modulation and on-off keying, that the information content per photon in the low-mean-photon-number limit can exceed that of bright optical channels [60]. These bounds are useful for the design and development of low-power mobile ad-hoc networks.

4. Teleportation and Related Quantum Information Science Experiments

This section discusses recent laboratory and field teleportation experiments (see Tables 3a-3g).

4.1 Teleportation Using Polarization, Time-Bin and Hybrid Entangled Photon States (Table 3a)

Quantum teleportation experiments have been conducted in the laboratory using different forms of entanglement, e.g., polarization, time-bin, as well as hyperentangled (polarization and angular orbital

momentum) and hybrid (spin and orbital angular momentum) entangled states [31, 61-64]. These expand the variety of entanglements researchers can use to teleport quantum information between distant locations.

Laboratory and field demonstrations of entanglement swapping and teleportation at telecom wavelengths have been reported using single-photon detectors to perform multi-photon coincidence measurements and Bell-state measurements [65-70]. In particular, exploratory teleportation field demonstrations were achieved by the Pan [67] and Tittel [68] research groups. Entanglement swapping at telecom wavelengths is a major step for developing networked quantum storage and teleportation between remote quantum memories. Interfacing of telecom wavelength photons with atomic memories generally requires frequency conversion from telecom to atomic wavelengths and back. Frequency-conversion research and experiments have demonstrated promising results [71-73].

In addition, there have been demonstrations of continuous-variable teleportation of photonic time-bin qubits [74-76]. Interestingly, quantum storage of time-bin-entangled photons at 795 nm and 1532 nm was experimentally demonstrated in cryogenically cooled rare-earth-ion erbium-doped optical fiber [77, 78], which

Table 2. Summary of quantum inspired classical protocols.

Year	Protocol name	Investigator(s)	Application	Description	Country	Reference
2015	Stat. optical entanglement	Qian, Little, Howell, Eberly	Classical Bell-analysis	Stat. classical optical fields	USA	Qian et al. [58]
2015	PPM encode	Banaszek	Low power Class. Comm.	Quantum measurement	PL	Banaszek [60]
2015	DoF state transfer	Rafsanjani, Mirhosseini Magana-Loaiza, Boyd	Classical teleportation	Classical nonseparability	USA CA	Rafsanjani et al. [59]

Table 3a. Summary of quantum teleportation experiments: Teleportation experiments using different types of entanglement.

Year	Dist.	Lasers	Description	Fidelity	Country	Reference
2016	2 m	FWM 1550nm	Polarization EPS teleportation	- -	USA	Meyers et al. [138]
2016	12.5 km	FWM 1549.36nm & 1555.73nm	Polarization urban network teleportation.	$91 \pm 0.02\%$	CN, CA JP	Sun et al. [67]
2016	8.2 km	PPLN 795nm & 1532nm	Time-bin network teleportation.	$78 \pm 1\%$	CA, USA	Valivarathi et al. [68]
2015	102 km	PPLN 1546.2nm & 1555.8nm	Time-bin entangled photons	$82.9 \pm 1.7\%$	JP, USA	Takesue et al. [69]
2015	- -	792nm \rightarrow 1584nm PPKTP	Entang. swap & teleportation	76.3%	JP	Jin et al. [70]
2015	20 m	1047 nm \rightarrow PPLN 795nm, 1532nm	Quantum storage: telecom photons	$80.8 \pm 4.8\%$	CA, USA	Saglamyurek et al. [77, 78]
2015	- -	394nm pump BBO type-I	Spin-orbit hybrid entangled states	63%	CN	Wang et al. [64]
2014	2 km	795nm, 1621nm 1560nm	Polarization EPS; InGaAs SPD	- -	FR	Kaiser et al. [65, 66]
2014	- -	405nm pump BBO type-I	Teleportation & local noise	- -	AR	Knoll et al. [85]
2014		351nm AR + BBO	Hyperentangled photons	$87 \pm 0.1\%$	USA	Graham et al. [31, 61, 62]
2014	- -	355nm pump BBO type-I	Spin-orbit hybrid entangled states	99.4%	CA USA	Erhard et al. [63]
2013	- -	860nm	Time-bin entangled qubits	79-82%	JP, GER	Takeda et al. [74-76]
2013	- -	ELED: QD InAs/GaAs	Entangled light emitting diode	77%	UK	Nilsson et al. [81, 82]
2012	104 m	404nm pump BBO type-II	Delayed-choice entanglement swap	$68.1 \pm 3.4\%$	AT	Ma et al. [80]
2011	- -	- -	Schrodinger's cat state	$75 \pm 0.5\%$ input $46 \pm 1.0\%$ output	JP, AU	Lee et al. [86]

is relevant for future realization of fiber-based quantum networks. The wavelengths selected for this experiment were wavelengths that are useful for storage not only in doped fibers, but also in atomic (Rubidium) quantum memories. In fiber, there was also an experimental realization of the Peres [79] delayed-choice entanglement-swapping Gedanken experiment [80].

It was recently demonstrated that polarization-entangled photon pairs, generated by an entangled-light-emitting diode (ELED) [81, 82], can be used in quantum teleportation. The ELED light source was comprised of InAs/GaAs quantum dots. More recently, Varnava et al. [83] reported on a quantum relay over 1 km in optical fiber to teleport photonic qubits to a receiver, using their entangled-LED light source. Note that an earlier paper by Jacobs et al. [84] discussed some of the basic differences between a quantum relay and a quantum repeater, e.g., a

quantum-relay system does not require the ability to store photons.

Finally, Knoll et al. [85] conducted an experiment testing how a new quantum-teleportation scheme was affected by local noise, since entangled photon pairs may suffer from de-coherence by interactions with the outdoor environment, producing mixed entangled states. According to Knoll et al. [85], testing on particular teleportation protocols can lead to the design of more-robust, noise-insensitive implementations of quantum information processes. As an example of progress in fielding quantum networks, first explored in the laboratory, it is noteworthy that in 2016, Pan et al. reported a fielded multi-node quantum network test bed to explore teleportation over a 12.5 km range [67]. In 2016, Tittel et al. [68] also fielded a teleportation network with time-bin encoded Teleportation of highly non-classical states of light (i.e., Schrödinger-cat

Table 3b. Summary of quantum teleportation experiments: teleportation experiments implemented on photonic and/or solid-state chips.

Year	Dist.	Lasers	Description	Fidelity	Country	Reference
2015	--	244 nm	Reconfigurable photonic chip	81%	UK, IT	Walmsley et al [87]
2014	--	244 nm	Reconfigurable photonic chip	81%	UK, IT, CN NL	Metcalf et al. [88]
2013	6 mm	Microwave gate lines	Solid-state superconducting circuit	62-80%	CH	Steffen et al. [89]

states) has been demonstrated in the laboratory [86]. These types of non-classical states are useful for fault-tolerant quantum information processing and distributed quantum computing.

In summary, representative demonstrations of teleportation show that differing types of entanglement are feasible. These may be selectively chosen for operation in particular environments, i.e., free space, or to transfer entanglement between different wavelengths for long-distance propagation and storage in quantum memories.

4.2 Teleportation on Photonic and Solid-State Chips (Table 3b)

Quantum teleportation experiments in the laboratory have been implemented on photonic and/or solid-state chips [87-89]. Walmsley et al. reported teleportation and quantum-interference experiments involving three single photons on a reconfigurable integrated photonic chip. The integrated photonic chip was coupled with superconducting-transition edge detectors [87]. Metcalf et al. [88] described a fully integrated implementation of quantum teleportation, such that all the parts of the circuit – i.e., entangled-state preparation, Bell-state analysis, and tomographic-state measurements – were performed on a reconfigurable photonic chip. Here, the individual waveguides were written with a computer-controlled continuous-wave 244 nm laser onto a germanium-doped silica photosensitive waveguide

core. Steffen et al. [89] described a laboratory realization of deterministic quantum teleportation in a solid-state chip-based superconducting circuit architecture. The quantum states (transmon qubits) were teleported between two macroscopic systems separated by 6 mm at a rate of 10,000/s.

Note that Masada et al. [98] reported on the generation and characterization of entangled photon beams in an integrated photonic chip. Entangled photons generated on-chip can greatly increase stability and simplify alignment difficulties, which can be problematic for complex systems. These chip-based photonic and solid-state teleportation experiments demonstrated a means by which quantum information processing and quantum communications can be integrated on a component level with existing computing and communications technologies. For a recent review of the current state-of-the-art for on-chip entangled-photon generation and manipulation, see Matsuda and Takesue [99].

4.3 Quantum Information Transfer from a Propagating Photonic Qubit to a Stationary Solid-State Spin Qubit (Table 3c)

Quantum information transfer was also achieved experimentally from a propagating photonic qubit to a stationary solid-state spin qubit [91-97]. As an example, Hanson's group [91, 92] discussed the teleportation of arbitrary quantum states between diamond spin qubits on

Table 3c. Summary of quantum teleportation experiments: teleportation experiments between two stationary solid-state qubits,

Year	Dist.	Lasers	Description	Fidelity	Country	Reference
2016	--	780nm, 645nm Diamond	Teleportation photon to vibrational	$90.6 \pm 1\%$	CN, USA	Hou et al. [90]
2014	3 m	532 nm, 575 nm, 637 nm	Diamond spin qubits	86%	NL, UK CA	Pfaff et al. [91, 92]
2014	25 km	532 nm, 883 nm & 1338 nm	Teleport polarization state to rare earth ion state	$81 \pm 4\%$	CH, AT, GER FR, USA	Bussieres et al. [93-95]
2013	5 m	--	Teleport QD spin states	$78 \pm 3\%$	CH	Gao et al. [96, 97]

Table 3d. Summary of quantum teleportation experiments: teleportation experiments implemented between two atomic ensembles.

Year	Dist.	Lasers	Description	Fidelity	Country	Reference
2013	0.5 m	--	C-V teleportation: cesium atoms	60-75%	DK, ES, UK	Krauter et al. [102]
2012	150 m (0.6 m)	Memory storage time: $\sim 129 \mu\text{s}$	Heralded teleport: cold ^{87}Rb atoms	88%	CN, GER, TW	Bao et al. [103]
2008	300 m	Memory storage time: 500 ns	Entanglement swap: cold ^{87}Rb atoms	$83 \pm 2\%$	GER, CN, AT	Yuan et al. [104]

separate setups in laboratories separated by 3 m. Here, a photonic channel was used to generate heralded remote entanglement between two nitrogen-vacancy (NV) center electronic spins. In 2016, an experiment by Hou et al. [90] demonstrated the teleportation of a photonic state of light to the mechanical vibrational phonon modes of a diamond crystal memory. This experiment suggested promising applications of macroscopic diamonds to quantum control and quantum information science.

In a step towards teleportation between distant quantum memories, Bussieres et al. [93] reported on quantum teleportation through 25 km of optical fiber. The polarization state of a telecom-wavelength photon was transferred to the state of hyperentangled energy-time and polarization photons at 883 nm and 1338 nm in a solid-state quantum memory comprised of a rare-earth-ion crystal. Bussieres' group [94, 95] experimentally demonstrated quantum storage and retrieval in a solid-state quantum memory (i.e., $\text{Nd}^{3+}:\text{Y}_2\text{SiO}_5$ rare-earth-ion crystals). Similarly, de Riedmatten's group [100] experimentally showed quantum storage (126 4.5 μs) of heralded single photons in a rare-earth Praseodymium-doped crystal ($\text{Pr}^{3+}:\text{Y}_2\text{SiO}_5$)m where the signal photons were 606 nm and the idler photons were 1436 nm. Later, de Riedmatten's group [101] demonstrated an example of a spin-wave solid-state quantum memory using the same rare-earth Praseodymium-doped crystal for time-bin qubits that enabled on-demand readout of the stored qubits.

Alternately, Gao et al. [96] described teleportation of the quantum state of a single photon generated by one quantum dot (QD) in a superposition of two frequency components to the spin-state of another quantum dot located in a different cryostat. To generate a photonic qubit in this

experiment, a neutral self-assembled InGaAs quantum dot was used. Gao et al. [96] reported that the photon-correlation measurements performed on the emitted light from the two dots showed strong anti-bunching, proving that the experimental scheme generated nearly ideal single-photon pulses.

In summary, these representative experiments demonstrated solid-state quantum memory nodes comprised of different materials. They indicated that a solid-state quantum memory can achieve high entanglement rates and be used to make quality quantum networking nodes.

4.4 Teleportation Between Two Macroscopic Atomic Ensembles (Table 3d)

Quantum teleportation experiments in the laboratory were also implemented between two atomic ensembles. Atomic ensembles are generally well-understood physical systems, and have been shown to have long coherence times (memory time). As such, atomic ensembles are often used to test ideas and implementations of teleportation. For example, Krauter et al. [102] reported on an experimental demonstration of deterministic continuous-variable (CV) teleportation between distant (0.5 m separated) macroscopic atomic ensembles (cesium atoms) at room temperature. Interestingly, the continuous-variable teleportation was able to teleport a sequence of time-evolving spin states, which may find other applications for quantum networks. Similarly, Bao et al. [103] reported on heralded, high-fidelity quantum teleportation between two atomic ensembles (rubidium atoms) linked by a 150 m optical fiber using narrow-band single photons to establish the entanglement

Table 3e. Summary of quantum teleportation experiments: teleportation experiments implemented between two single atoms/ions.

Year	Dist.	Lasers	Description	Fidelity	Country	Reference
2013	21 m	Coherence time: $>0.1 \text{ s}$	Teleport: two single ^{87}Rb atoms	$88 \pm 1.5\%$	GER	Nolleke et al. [105]
2012	60 m	Coherence time: $>100 \mu\text{s}$	Entanglement: two single ^{87}Rb atoms	$84 \pm 1.0\%$	GER	Ritter et al. [106]
2009	1 m	Coherence time: $>2.5 \text{ s}$	Teleport: Yb^+ ions	--	USA	Olmschenk et al. [107]

Table 3f. Summary of quantum teleportation experiments: free-space quantum teleportation experiments.

Year	Dist.	Lasers	Description	Fidelity	Country	Reference
2017	500-1200 km	Sagnac SPDC	Entanglement	In Progress	CN	Pan et al. [108, 109]
2015	143 km	808 nm, type-I BBO 404 nm, type-II BBO	Entanglement swapping	- -	AT	Herbst et al. [111]
2014	772 m 686 m	3-photon GHZ entangled states	Non-locality exp.: 3 qcomm nodes	- -	CA, UK, USA, AT, AU	Erven et al. [18]
2012	97 km	788 nm, LiB3O5 394 nm, type-II BBO	Teleport: multi-photon entangled	$80.4 \pm 0.9\%$	CN	Yin et al. [112]
2012	143 km	808 nm, type-I BBO 404 nm, type-II BBO	Quantum teleport independent qubits	$86.3 \pm 3.8\%$	AT, GER CA	Ma et al. [113]
2012	10 m	808 nm, type-I BBO 404 nm, type-II BBO	Quantum teleport: high loss channel	$82 \pm 1.0\%$	AT GER	Ma et al. [114]
2010	16 km	405 nm, type-II BBO SPDC: 810nm	Free-space teleportation	89%	CN	Jin et al. [115]
1997		394 nm, type-II SPDC: 788nm	Free-space teleportation	70% visibility	AT	Bouwmeester, Pan, Mattle, Eibl, Weinfurter, Zeilinger [2]

(physical separation of 0.6 m). The fidelities of the teleported quantum states in this experiment exceeded 90% for the six input states tested.

Alternately, Yuan et al. [104] reported on a laboratory experiment to demonstrate entanglement swapping with storage and retrieval of light using the BDCZ quantum-repeater protocol [48]. The experiment consisted of (1) two sources of atom-photon entanglement, (2) sending the entangled photons to an intermediate station for a Bell-state measurement, and (3) verifying the entanglement between the stationary qubits (i.e., the two remote atomic ensembles). In this case, the atomic memory storage time was 500 ns.

These kinds of teleportation experiments between atomic ensembles showed that atomic ensembles may have use as a long-time storage media for quantum states. Research still needs to be performed to determine the scalability of atomic-ensemble networks.

4.5 Teleportation Between Two Single Trapped Atoms/Ions (Table 3e)

Teleportation between single atoms/ions is an important step in efficient quantum networks. Quantum memories that consist of many atoms in an ensemble or rare-earth-doped crystals must contend with internal atom-atom interactions and motional degrees of freedom that make entanglement purification problematic. An example of quantum teleportation implemented between two single atoms/ions was reported by Nolleke et al. [105], who demonstrated teleportation of quantum bits between two single ^{87}Rb atoms in distant (21 m separated) laboratories.

This experiment, while only attaining teleportation fidelities of 72% to 90%, nevertheless was an important step towards quantum networks with many nodes. Similarly, Ritter et al. [106] used single rubidium atoms trapped in optical cavities to demonstrate the transfer of an atomic quantum state, and the creation of entanglement between two identical nodes in separate laboratories, which resulted in the experimental realization of an elementary quantum network.

Earlier, Olmschenk et al. [107] reported on the teleportation of quantum information between atomic (ion) quantum memories separated by about 1 m. A quantum bit stored in a single trapped ytterbium ion (Yb^+) was teleported to a second Yb^+ ion using a teleportation protocol based on the heralded entanglement of the atoms through interference and detection of photons emitted from each ion and guided through optical fibers. More recently, Casabone et al. [125] described the heralded entanglement of two Ca^+ ions in an optical cavity. Slodicka et al. [126] reported on an experiment where the detection of a single scattered photon generated entanglement between two $^{138}\text{Ba}^+$ ions. Similarly, Kurtsiefer's group reported on Hong-Ou-Mandel interference experiments with single photons generated from (1) scattering by a single rubidium (^{87}Rb) atom, and (2) parametric generation through a four-wave-mixing process in a cloud of cold rubidium atoms [127]. Here, the observed interference between photons emitted by a single atom and those generated from an atom ensemble demonstrated the entanglement between distant nodes made up of different physical systems. Note also that Reiserer and Rempe [128] recently provided a detailed discussion of optical-cavity-based quantum networks with single atoms and photons. As an example, Rempe's group experimentally demonstrated the high-efficiency transfer of a photonic-polarization qubit onto a single rubidium atom within an optical cavity [129].

The recent teleportation experiments between single trapped atoms/ions have demonstrated that these systems, having very long storage times, can teleport quantum states with high fidelity. It is an active area of research to implement these types of single atom/ion memories on a chip, which can improve scalability and simplify their integration into a network of information teleportation nodes.

4.6 Free-Space Quantum Teleportation Experiments (Table 3f)

While implementations of quantum teleportation technologies in fiber have been demonstrated in the laboratory, it is important to also consider free-space quantum communications, which will play an important role in applications such as Earth-to-satellite quantum networking [130-132]. It was recently reported that China has launched a satellite to conduct teleportation and entanglement experiments, such as Bell-inequality measurements over distances from 500 km to 1200 km [108-110]. They reported that the satellite will attempt to teleport a state from a ground station while orbiting at 500 km.

Several free-space quantum teleportation experiments have accomplished transmission and detection of photons over long distances. For example Herbst et al. [111] and Ma et al. [113] reported on the free-space implementation of quantum teleportation and entanglement swapping

over a 143 km path in the Canary Islands. This very-long-distance entanglement-swapping experiment was important as a fundamental benchmark for global entanglement distribution and Earth-to-satellite entanglement distribution. Ma et al. [114] reported on a free-space teleportation experiment in the laboratory (10 m) using a high-loss channel (36 dB attenuation), similar to a ground-to-satellite link, that was simulated using neutral-density filters to show that quantum teleportation is experimentally feasible in adverse conditions.

Alternately, Yin et al. [112] and Jin et al. [115] reported on free-space quantum teleportation with multi-photon entanglement in China over distances of 97 km in 2012 and 16 km in 2010, respectively. In contrast, Erven et al. [18] discussed a quantum non-locality experiment that connected three quantum communications nodes. The nodes shared entanglement that was distributed from one node to two distant nodes through free-space links that were 772 m and 686 m apart. This was a proof-of-principle experiment that may lead to multi-party quantum secret sharing and multi-party teleportation.

Finally, we note that a helpful review of the physics of free-space and atmospheric quantum communications, including discussions on teleportation and quantum measurement processes, can be found in the book chapter by Meyers et al. [7]. Figure 1, updated from the book chapter, illustrates the quantitative relationship between the propagation distance and the year the free-space quantum-communication experiment was conducted. In summary,

Table 3g. Summary of quantum teleportation experiments: related quantum information science experiments.

Year	Dist.	Lasers	Description	Fidelity	Country	Reference
2017	--	--	NV centers diamond entanglement distillation	--	NL, UK	Kalb et al. [116]
2016	300 m	SPDC 850 nm 755 nm	OAM QKD	--	CA, USA IR, GER	Sit et al. [142]
2016	26 km	FWM 1550 nm	Entanglement distribution over installed fiber	USA	Meyers et al. [138]	
2016	--	860 nm CW	CV entanglement & EPR on a chip	--	JP	Masada, Furusawa [117]
2015	--	Nonclassical HOM effect for QIP	Synchronized HOM 2-photon interference	--	JP, GER	Makino et al. [118]
2015	1.3 km	NV centers, diamond; red & yellow lasers	Loophole free Bell inequality violation	$92 \pm 3\%$	NL, ES, UK	Hensen et al. [119]
2015	3 km	Sagnac-type EPS	Entanglement in turbulence	--	AT	Krenn et al. [120]
2015	3.7 km	403 nm → type II PPKTP → 806 nm	Loophole free Bell test in fiber	--	CL, ES, SE, IT	Carvacho et al. [121]
2014	--	CW 860 nm Ti:sapphire:	Nonlocal wave-function collapse	JP, PL, AU	Fuwa et al. [123]	
2014	35.5 km	405 nm → type-I BBO: 760 nm & 867 nm	Test flight: corr. photon system	SG, CH	Tang et al. [124]	

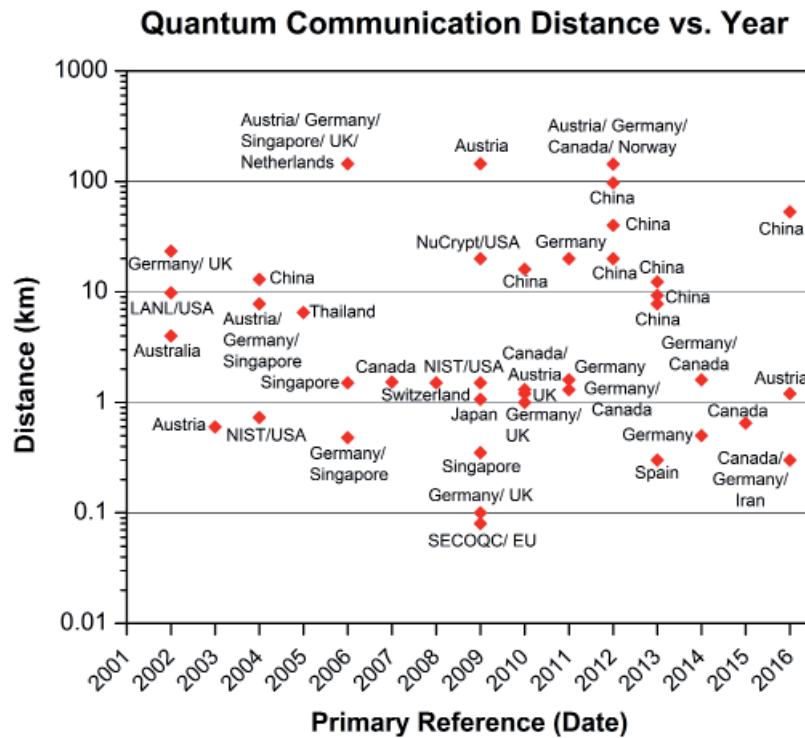


Figure 1. The quantitative relationship between the propagation distance and the year the cited free-space quantum communication experiment was executed (updated from Meyers et al. [7], *Free-Space and Atmospheric Quantum Communications*, New York, Springer, 2014).

the free-space teleportation experiments highlighted above show that long-distance teleportation, such as from ground to satellite, is an achievable goal. Such ground-to-satellite and satellite-to-ground entanglement distribution is a needed technology for a teleportation network with global reach.

4.7 Related Quantum Information Science Experiments (Table 3g)

An example of a related quantum information science experiment that facilitated the development of a quantum network was reported in 2017 by Kalb et al. [116], on distilling entanglement on a cluster of nitrogen-vacancy diamond nodes. In 2016, Furusawa’s group experimentally demonstrated generation of continuous-variable entangled photon beams and EPR beams using an integrated photonic waveguide [117]. They also demonstrated the synchronization of optical photons from independent quantum memories to bring about non-classical HOM two-photon interference [118], which may be scalable for quantum information processing. Another example is from Hanson’s group in the Netherlands [119], which presented the results of an experiment where they used entangled electron spins from nitrogen-vacancy diamond centers to achieve a loophole-free CHSH Bell-inequality violation over a distance of 1.3 km. Krenn et al. [120] reported the results of an outdoor, long-distance (3 km) entanglement-distribution experiment that used orbital-

angular-momentum photons generated from a high-fidelity Sagnac-type polarization-entanglement source. The benefit of this type of experiment is that orbital-angular-momentum entanglement allows for larger alphabets and an increased number of quantum channels to exploit for increased data rates. Other experiments have explored using orbital angular momentum in quantum-key-distribution atmospheric applications, but did not use entanglement or teleportation [142]. To show that entanglement is a practical resource for quantum communications, in 2016, Meyers et al. [138] demonstrated two-photon polarization-entanglement distribution over an installed 27 km fiber network loop from ARL to JQI and back. The ambient environment experiment verified the survival of entanglement over the intercity optical-fiber network that ran under the Washington DC beltway.

Two related quantum information science experiments included examination of loopholes in Bell-inequality tests. Carvacho et al. [121] experimentally demonstrated Bell-inequality tests over 3.7 km of optical fiber, which mitigated post-selection process loopholes that can lead to communications security vulnerabilities. This work suggested that their energy-time entanglement setup could be used to implement practical secure communications over existing telecommunication infrastructure. Similarly, Christensen et al. [29] presented an analysis of coincidence-time loopholes in experimental Bell tests. They applied the distance-based Bell-test analysis method of Knill et

al. [30] to three experimental data sets where conventional analyses had failed or required additional assumptions. As a result of this analysis, Christensen et al. [29] reported an improved protocol for Bell tests.

For a global quantum network, various environmental and relativistic effects must be examined. For example, Lin et al. [122] conducted experiments to explore relativistic effects and environmental influences in quantum teleportation. Here, relativistic effects included those related to reference-frame dependence on quantum entanglement, time dilation, and relativistic Doppler shift. The environmental influences studied were related to quantum de-coherence and the Unruh effect. In this paper, Lin et al. [122] discussed the fidelity of quantum teleportation results from four representative teleportation cases where Alice was at rest and (1) Bob was also at rest, (2) Bob was uniformly accelerated, (3) Bob was the traveling twin in the twin problem, and (4) Bob experienced alternating uniform acceleration. Understanding of these effects is important when considering teleportation of quantum information between ground-to-satellite, air-to-satellite, air-to-air, moving platforms, and ground-to-air stations. In another example, Furusawa's group [123] experimentally demonstrated the non-local wavefunction collapse of a single photon, which in essence was a proof of Einstein's EPR [9] concept of "spooky action at a distance." They argued that a single photon split between two spatially distant modes is an important entanglement resource for quantum information applications, and that their experiment was a verification of this type of entanglement.

Finally, Tang et al. [124] presented the results of a high-altitude balloon test flight of a rugged, compact, and power-efficient device for generating and monitoring polarization correlations between photon pairs at 760 nm and 867 nm under adverse ascent and descent conditions to 35.5 km. The Center for Quantum Technologies (CQT) group aims to deploy the compact device on a platform such as a nanosatellite operating at a low-Earth-orbiting altitude of 400 km [133]. CQT's recent test results demonstrated that an entangled photon source and detector package could be designed and manufactured to withstand mechanical vibrations, accelerations, changes in internal and external temperature, relative humidity and pressure, i.e., environmental conditions that most setups in the laboratory cannot endure.

Entanglement has been shown to be a phenomenon vital to modern quantum information processing. Scientific experiments are investigating both such fundamentals as non-classicality, the relation of quantum and relativistic physics, and also such practical applications as high-order entanglement for increased quantum-channel capacity. It was also shown that entanglement sources and measurements can be engineered to be robust to harsh, non-laboratory challenges.

5. Summary

The *quantum Internet*, with fixed, free-space, and atmospheric quantum network channels, is becoming a reality [134, 135]. Quantum information will be teleported through *information teleportation networks* that necessarily will include satellites. This paper has presented a review and discussion of key quantum protocols and recent developments in quantum teleportation experiments. These all contribute to the development of future quantum networks with increased security, bandwidth, and speed beyond classical capabilities. Achieving a quantum information teleportation network will require further advances in research involving both theory and experiments. For this purpose, the US Army Research Laboratory (ARL) has been developing quantum communication technologies [136-141], and is performing additional experiments to advance the state-of-the-art. Advancement in fundamental quantum protocols and teleportation technology, both involving experimental exploration, are necessary to implement future information teleportation networks.

6. Acknowledgements

Ronald E. Meyers, Keith S. Deacon, and Arnold Tunick thank the US Army Research Laboratory (ARL) for support. Philip R. Hemmer acknowledges the support of the Army Research Laboratory cooperative agreement W911NF-16-2-0094.

7. References

1. C. H. Bennett, G. Brassard, C. Crepeau, R. Jozsa, A. Peres and W. K. Wootters, "Teleporting an Unknown Quantum State via Dual Classical and Einstein-Podolsky-Rosen Channels," *Physical Review Letters*, **70**, 13, 1993, pp. 1895-1899.
2. D. Bouwmeester, J.-W. Pan, K. Mattle, M. Eibl, H. Weinfurter and A. Zeilinger, "Experimental Quantum Teleportation," *Nature*, 390, 1997, pp. 575-579.
3. N. Gisin, S. Tanzilli and W. Tittel, "Quantum Teleportation and Nonlocality: The Puzzling Predictions of Entanglement Are Coming of Age," arXiv: 1508.05962v1, 24 August 2015.
4. T. E. Northup and R. Blatt, "Quantum Information Transfer Using Photons," *Nature Photonics*, **8**, 2014, pp. 356-363.
5. R. Van Meter, "Teleportation," in *Quantum Networking*, Chichester, UK, John Wiley & Sons, Ltd., 2014.

6. A. Tunick, T. Moore, K. S. Deacon, R. E. Meyers, "Review of Representative Free-Space Quantum Communications Field Experiments," *Proc. SPIE*, **7815**, "Quantum Communications and Quantum Imaging VIII," 2010.
7. R. E. Meyers, K. S. Deacon, A. D. Tunick, "Free-Space and Atmospheric Quantum Communications," in A. Majumdar (ed.), *Advanced Free Space Optics: A System Approach*, New York, Springer, 2014.
8. S. Pirandola, J. Eisert, C. Weedbrook, A. Furusawa, S. L. Braunstein, "Advances in Quantum Teleportation," arXiv:1505.07831v1, 28 May 2015.
9. A. Einstein, B. Podolsky, and N. Rosen, "Can Quantum-Mechanical Description of Physical Reality Really be Considered Complete?" *Physical Review*, **47**, 1935, p. 777.
10. J. Bell, "On the Einstein Podolsky Rosen Paradox," *Physics* **1**, 3, 1964, pp. 195-200.
11. J. F. Clauser, M. A. Horne, A. Shimony and R. A. Holt, "Proposed Experiment to Test Local Hidden-Variable Theories," *Physical Review Letters*, **23**, 1969, pp. 880-884.
12. J. F. Clauser and A Shimony, "Bell's Theorem. Experimental Tests and Implications," *Reports on Progress in Physics*, **41**, 12, 1978, pp. 1881-1927.
13. R. Loudon and P. L. Knight, "Squeezed Light," *Journal of Modern Optics*, **34**, 6-7, 1987, pp. 709-759.
14. M. Hillery, "Sum and Difference Squeezing of the Electromagnetic Field," *Physical Review A*, **40**, 1989, p. 3147.
15. N .B. An and V. Tinh, "General Multimode Sum-Squeezing," *Physics Letters A*, **261**, 1-2, 1999, pp. 34-39.
16. N. B. An and V. Tinh, "General Multimode Difference-Squeezing," *Physics Letters A* **270**, 1-2, 2000, pp. 27-40.
17. K. V. Kheruntsyan, J.-C. Jaskula, P. Deuar, M. Bonneau, G. B. Partridge, J. Ruaudel, R. Lopes, D. Boiron and C. I. Westbrook, "Violation of the Cauchy-Schwarz Inequality with Matter Waves," *Physical Review Letters* **108**, 2012, p. 260401.
18. C. Erven, E. Meyer-Scott, K. Fisher, J. Lavoie, B. Higgins, Z. Yan, C. Pugh, J. Bourgoïn, R. Prevedel, L. Shalm, L. Richards, N. Gigov, R. LaFlamme, G. Weighs, T. Jennewein, K. Resch, "Experimental Three-Photon Quantum Non-Locality Under Strict Locality Conditions," *Nature Photonics* **8**, 2014, pp. 292-296.
19. B. T. Kirby, S. Santra, V. S. Malinovsky, and M. Brodsky, "Entanglement Swapping of Two Arbitrarily Degraded Entangled States," arXiv:1512.06093v2 [quant-ph], 25 July 2016.
20. R. J. Drost, T. J. Moore, and M. Brodsky, "Switching Networks for Pairwise-Entanglement Distribution," *Journal of Optical Communications and Networking*, **8**, 5, 2016, pp. 331-341.
21. W. J. Munro, A. M. Stephens, S. J. Devitt, K. A. Harrison and K. Nemoto, "Quantum Communication Without the Necessity of Quantum Memories," *Nature Photonics*, **6**, 2012, pp. 777-781.
22. Y.-B Sheng and L. Zhou, "Two-Step Complete Polarization Logic Bell-State Analysis," *Scientific Reports*, **5**, 2015, p. 13453.
23. R. J. Glauber, "Photon correlations," *Physical Review Letters* **10**, 3, 1963, pp. 84-86.
24. R. J. Glauber, "The Quantum Theory of Optical Coherence," *Physical Review* **130**, 6, 1963, pp. 2529-2539.
25. R. J. Glauber, "Coherent and Incoherent States of the Radiation Field," *Physical Review* **131**, 6, 1963, pp. 2766-2788.
26. V. Tamma and S. Laibacher, "Multiboson Correlation Interferometry with Arbitrary Single-Photon Pure States," *Physical Review Letters*, **114**, June 2015, p. 243601.
27. W. J. Munro and K. Nemoto, "High Performance Quantum Communication Without Quantum Memories," *Proc. SPIE*, **9225**, "Quantum Communications and Quantum Imaging XII," 2014.
28. A. Khalique and B. C. Sanders, "Long-Distance Quantum Communication Through Any Number of Entanglement-Swapping Operations," *Physical Review A* **90**, 2014, p. 032304.
29. B. G. Christensen, A. Hill, P. G. Kwiat, E. Knill, S. W. Nam, K. Coakley, S. Glancy, L. K. Shalm, and Y. Zhang, "Analysis of Coincidence-Time Loopholes in Experimental Bell Tests," arXiv:1503.07573v1, 25 March 2015.
30. E. Knill, S. Glancy, S. W. Nam, K. Coakley and Y. Zhang, "Bell Inequalities for Continuously Emitting Sources," *Physical Review A* **91**, 2015, p. 032105.
31. T. M. Graham, H. J. Bernstein, T.-C Wei, M. Junge and P. G. Kwiat, "Superdense Teleportation Using Hyperentangled Photons," *Nature Communications* **6**, 2015, p. 7185.
32. A. Banerjee and A. Pathak, "Maximally Efficient Protocols for Direct Secure Quantum Communication," *Physics Letters A* **376**, 45, 2012, pp. 2944-2950.

33. A.-D Zhu, Y. Xia, Q.-B Fan and S. Zhang, "Secure Direct Communication Based on Secret Transmitting Order of Particles," *Physical Review A*, **73**, 2006, p. 022338.
34. M. Lucamarini and S. Mancini, "Secure Deterministic Communication Without Entanglement," *Physical Review Letters* **94**, 2005, p. 140501.
35. K. Bostrom and T. Felbinger, "Deterministic Secure Direct Communication Using Entanglement," *Physical Review Letters*, **89**, 2002, p. 187902.
36. C. Bennett, "Quantum Cryptography Using Any Two Nonorthogonal States," *Physical Review Letters* **68**, 1992, pp. 3121-3124.
37. A. Ekert, "Quantum Cryptography Based on Bell's Theorem," *Physical Review Letters*, **67**, 1991, pp. 661-663.
38. C. Bennett and G. Brassard, "Quantum Cryptography: Public Key Distribution and Coin Tossing," Proc. IEEE Intl. Conf. on Computers, Systems and Signal Processing, Bangalore, 1984, pp. 175.
39. G. Chiribella, Y. Yang and A. C.-C Yao, "Quantum Replication at the Heisenberg Limit," *Nature Communications*, **4**, 2013, p. 2915.
40. W. Dur, P. Sekatski and M. Skotiniotis, "Deterministic Superreplication of One-Parameter Unitary Transformations," *Physical Review Letters*, **114**, 2015, p. 120503.
41. A. Ekert and R. Renner, "The Ultimate Physical Limits of Privacy," *Nature*, **507**, 2014, pp. 443-447.
42. N. Solmeyer, X. Li, and Q. Quraishi, "High Teleportation Rates Using Cold-Atom-Ensemble-Based Quantum Repeaters with Rydberg Blockade," *Physical Review A*, **93**, 2016, p. 042301.
43. B. Zhao, M. Muller, K. Hammerer, and P. Zoller, "Efficient Quantum Repeater Based on Deterministic Rydberg Gates," *Physical Review A*, **81**, 2010, p. 052329.
44. Y. Han, B. He, K. Heshami, C.-Z. Li, and C. Simon, "Quantum Repeaters Based on Rydberg-Blockade-Coupled Atomic Ensembles," *Physical Review A*, **81**, 2010, p. 052311.
45. C. Jones, D. Kim, M. T. Rakher, P. G. Kwiat and T. D. Ladd, "Design and Analysis of Communication Protocols for Quantum Repeater Networks," arXiv:1505.01536, 06 May 2015.
46. K. Azuma, K. Tamaki and H.-K Lo, "All-Photonic Quantum Repeaters," *Nature Communications*, **6**, 2015, p. 6787.
47. N. Sangouard, C. Simon, H. de Riedmatten and N. Gisin, "Quantum Repeaters Based on Atomic Ensembles and Linear Optics," *Review of Modern Physics*, **83**, 2011, pp. 33-80.
48. H. J. Briegel, W. Dur, J. I. Cirac and P. Zoller, "Quantum Repeaters: The Role of Imperfect Local Operations in Quantum Communication," *Physical Review Letters*, **81**, 1998, pp. 5932-5935.
49. L.-M Duan, M. D. Lukin, J. I. Cirac and P. Zoller, "Long-Distance Quantum Communication with Atomic Ensembles and Linear Optics," *Nature*, **414**, November 2001, pp. 413-418.
50. B. Kraus, W. Tittel, N. Gisin, M. Nilsson, S. Kroll and J. I. Cirac, "Quantum Memory for Nonstationary Light Fields Based on Controlled Reversible Inhomogeneous Broadening," *Physical Review A*, **73**, 2006, p. 020302.
51. M. P. Hedges, J. J. Longdell, Y. Li and M. J. Sellars, "Efficient Quantum Memory for Light," *Nature*, **465**, 2010, pp. 1052-1056.
52. B. Lauritzen, J. Minar, H. de Riedmatten, M. Afzelius, N. Sangouard, C. Simon and N. Gisin, "Tele-Communication Wavelength Solid-State Memory at the Single Photon Level," *Physical Review Letters*, **104**, 2010, p. 080502.
53. M. Afzelius, C. Simon, H. de Riedmatten and N. Gisin, "Multimode Quantum Memory Based on Atomic Frequency Combs," *Physical Review A*, **79**, 2009, p. 052329.
54. A. L. Alexander, J. J. Longdell, M. J. Sellars and N. B. Manson, "Photon Echoes Produced by Switching Electric Fields," *Physical Review Letters*, **96**, 2006, p. 043602.
55. G. Hetet, J. J. Longdell, A. L. Alexander, P. K. Lam and M. J. Sellars, "Electro-Optic Quantum Memory for Light Using Two-Level Atoms," *Physical Review Letters*, **100**, 2, 2008, p. 023601.
56. K. J. Boller, A. Imamoglu and S. E. Harris, "Observation of Electromagnetically Induced Transparency," *Physical Review Letters*, **66**, 1991, pp. 2593-2596.
57. A. V. Gorshkov, A. Andre, M. Fleischhauer, A. S. Sorensen and M. D. Lukin, "Optimal Storage of Photon States in Optically Dense Atomic Media," *Physical Review Letters*, **98**, 2007, p. 123601.
58. X.-F Qian, B. Little, J. C. Howell and J. H. Eberly, "Shifting the Quantum-Classical Boundary: Theory and Experiment for Statistically Classical Optical Fields," *Optica*, **2**, 2015, pp. 611-615.

59. S. M. H. Rafsanjani, M. Mirhosseini, O. S. Magana-Loaiza and R. W. Boyd, "State Transfer Based on Classical Nonseparability," *Physical Review A*, **92**, 2015, p. 023827.
60. K. Banaszek, "Low-Power Optical Communication: Approaching the Quantum Limit," *Proc. SPIE* **9615**, "Quantum Communications and Quantum Imaging XIII," 2015.
61. T. M. Graham, H. J. Bernstein, T. Wei, and P. Kwiat, "SuperDense Teleportation using Hyperentangled Photons," OSA Research in Optical Sciences, paper QTh3A.3, 2014.
62. T. M. Graham, H. J. Bernstein, H. Javadi, B. J. Geldzahler and P. Kwiat, "Superdense Teleportation for Space Applications," *Proc. SPIE*, **9123**, "Quantum Information and Computation XII," 2014, p. 912302.
63. M. Erhard, H. Qassim, H. Mand, E. Karimi and R. W. Boyd, "Real-Time Imaging of Spin-to-Orbital Angular Momentum Quantum State Teleportation," arXiv:1404.7573v1, 2014.
64. X.-L. Wang, X.-D. Cai, Z.-E. Su, M.-C. Chen, D. Wu, L. Li, N.-L. Liu, C.-Y. Lu and J.-W. Pan, "Quantum Teleportation of Multiple Degrees of Freedom of a Single Photon," *Nature*, **518**, 2015, pp. 516-519.
65. F. Kaiser, A. Issautier, L.A. Ngh, D. Aktas, T. Delord and S. Tanzilli, "Towards Continuous-Wave Regime Teleportation for Light Matter Quantum Relay Stations," arXiv:1412.7648v1, 2014.
66. F. Kaiser, T. Delord and S. Tanzilli, "Continuous Regime Quantum Teleportation Experiment for Hybrid Quantum Nodes," OSA Research in Optical Sciences, paper QTu3A.4, Quantum Information and Measurement Conference, Berlin, Germany, 18-20 March 2014.
67. Q.-C. Sun, Y.-L. Mao, S.-J. Chen, W. Zhang, Y.-F. Jiang, Y.-B. Zhang, W.-J. Zhang, S. Miki, T. Yamashita, H. Terai, X. Jiang, T.-Y. Chen, L.-X. You, X.-F. Chen, Z. Wang, J.-Y. Fan, Q. Zhang and J.-W. Pan, "Quantum Teleportation with Independent Sources and Prior Entanglement Distribution Over a Network," *Nature Photonics*, **10**, 2016, pp. 671-676.
68. R. Valivarthi, M. G. Puigibert, Q. Zhou, G. H. Aguilar, V. B. Verma, F. Marsili, M. D. Shaw, S. W. Nam, D. Oblak. and W. Tittel, "Quantum Teleportation Across a Metropolitan Fibre Network," *Nature Photonics*, **10**, 2016, pp. 676-680.
69. H. Takesue, S. D. Dyer, M. J. Stevens, V. Verma, R. P. Mirin and S. W. Nam, "Quantum Teleportation Over 100 km of Fiber Using Highly Efficient Superconducting Nanowire Single-Photon Detectors," *Optica*, **2**, 10, 2015, pp. 832-835.
70. R.-B. Jin, M. Takeoka, U. Takagi, R. Shimizu and M. Sasaki, "Highly Efficient Entanglement Swapping and Teleportation at Telecom Wavelength," Scientific Reports, **5**, 2015, p. 9333.
71. N. Maring, K. Kutluer, J. Cohen, M. Cristiani, M. Mazzer, P. Ledingham. and H. de Riedmatten, "Storage of Up-Converted Telecom Photons in a Doped Crystal," *New Journal of Physics*, **16**, 2014, p. 113021.
72. H. Rütz, K.-H. Luo, H. Suche and C. Silberhorn, "Quantum Frequency Conversion Between Infrared and Ultraviolet," *Physical Review Applied*, **7**, 2017, p. 024021.
73. M. Schleier-Smith, "Editorial: Hybridizing Quantum Physics and Engineering," *Physical Review Letters*, **117**, 2016, p. 100001.
74. S. Takeda, T. Mizuta, M. Fuwa, P. van Loock and A. Furusawa, "Deterministic Quantum Teleportation of Photonic Quantum Bits by a Hybrid Technique," *Nature*, **500**, 2013, pp. 315-318.
75. S. Takeda, M. Fuwa, P. van Loock and A. Furusawa, "Entanglement Swapping Between Discrete and Continuous Variables," *Physical Review Letters*, **114**, 2015, p. 100501.
76. M. Fuwa, S. Toba, S. Takeda, P. Marek, L. Mista, R. Filip, P. van Loock, J. Yoshikawa and A. Furusawa, "Noiseless Conditional Teleportation of a Single Photon," *Physical Review Letters*, **113**, 2014, p. 223602.
77. E. Saglamyurek, J. Jin, V. B. Verma, M. D. Shaw, F. Marsili, S. W. Nam, D. Oblak and W. Tittel, "Quantum Storage of Entangled Telecom-Wavelength Photons in an Erbium-Doped Optical Fibre," *Nature Photonics*, **9**, 2015, pp. 83-87.
78. E. Saglamyurek, T. Lutz, L. Veissier, M. P. Hedges, C. W. Thiel, R. L. Cone and W. Tittel, "Efficient and Long-Lived Zeeman-Sublevel Atomic Population Storage in an Erbium-Doped Glass Fiber," arXiv:1507.03012v1, 2015.
79. A. Peres, "Delayed Choice for Entanglement Swapping," *Journal of Modern Optics* **47**, 2000, pp. 139-143.
80. X.-S. Ma, S. Zotter, J. Kofler, R. Ursin, T. Jennewein, C. Brukner and A. Zeilinger, "Experimental Delayed-Choice Entanglement Swapping," *Nature Physics*, **8**, 2012, pp. 479-484.
81. J. Nilsson, R. M. Stevenson, K. H. A. Chan, J. Skiba-Szymanska, M. Lucamarini, M. B. Ward, A. J. Bennett, C. L. Salter, I. Farrer, D. A. Ritchie and A. J. Shields, "Quantum Teleportation Using a Light-Emitting Diode," *Nature Photonics*, **7**, 2013, pp. 3110-315.
82. R. M. Stevenson, J. Nilsson, A. J. Bennett, J. Skiba-Szymanska, I. Farrer, D. A. Ritchie and A. J. Shields,

- “Quantum Teleportation of Laser-Generated Photons with an Entangled-Light-Emitting Diode,” *Nature Communications* **4**, 2013, p. 2859.
83. C. Varnava, R. M. Stevenson, J. Nilsson, J. Skiba-Szymanska, B. Dzurinak, M. Lucamarini, R. V. Penty, I. Farrer, D. A. Ritchie and A. J. Shields, “An Entangled-LED Driven Quantum Relay Over 1 km,” arXiv: 1506.00518v1, 2015.
 84. B. C. Jacobs, T. B. Pittman and J. D. Franson, “Quantum Relays and Noise Suppression Using Linear Optics,” *Physical Review A*, **66**, 2002, p. 052307.
 85. L. T. Knoll, C. T. Schmiegelow and M. A. Larotonda, “Noisy Quantum Teleportation: An Experimental Study on the Influence of Local Environments,” *Physical Review A*, **90**, 2014, p. 042332.
 86. N. Lee, H. Benichi, Y. Takeno, S. Takeda, J. Webb, E. Huntington, A. Furusawa, “Teleportation of Nonclassical Wave Packets of Light,” *Science* **332**, 2011, pp. 220-222.
 87. I. A. Walmsley, B. J. Metcalf, J. B. Spring, P. C. Humphreys, M. Barbieri, W. S. Kolthammer, J. C. Gates, P. G. R. Smith, “Multiphoton Quantum Interference in Multiport Integrated Optical Circuits: From Teleportation to Boson Sampling,” European Quantum Electronics Conference 2015, Munich, Germany, 2015.
 88. B. J. Metcalf, J. B. Spring, P. C. Humphreys, N. Thomas-Peter, M. Barbieri, W. S. Kolthammer, X.-M. Jin, N. K. Langford, D. Kundys, J. C. Gates, B. J. Smith, P. G. R. Smith and I. A. Walmsley, “Quantum Teleportation on a Photonic Chip,” *Nature Photonics*, **8**, 2014, pp. 770-774.
 89. L. Steffen, Y. Salathe, M. Oppliger, P. Kurpiers, M. Baur, C. Lang, C. Eichler, G. Puebla-Hellmann, A. Fedorov and A. Wallraff, “Deterministic Quantum Teleportation with Feed-Forward in a Solid State System,” *Nature*, **500**, 2013, pp. 319-322.
 90. P.-Y. Hou, Y.-Y. Huang, X.-X. Yuan, X.-Y. Chang, C. Zu, L. He and L.-M. Duan, “Quantum Teleportation from Light Beams to Vibrational States of a Macroscopic Diamond,” *Nature Communications*, **7**, 2016, p. 11736.
 91. H. Bernien, B. Hensen, W. Pfaff, G. Koolstra, M.S. Blok, L. Robledo, T. H. Taminiau, M. Markham, D. J. Twitchen, L. Childress and R. Hanson, “Heralded Entanglement Between Solid-State Qubits Separated by Three Metres,” *Nature*, **497**, 2013, pp. 86-90.
 92. W. Pfaff, B. J. Hensen, H. Bernien, S. B. van Dam, M. S. Blok, T. H. Taminiau, M. J. Tiggelman, R. N. Schouten, M. Markham, D. J. Twitchen and R. Hanson, “Unconditional Quantum Teleportation Between Distant Solid-State Qubits,” *Science* **345**, 2014, pp. 532-535.
 93. F. Bussieres, C. Clausen, A. Tiranov, B. Korzh, V. B. Verma, S. W. Nam, F. Marsili, A. Ferrier, P. Goldner, H. Herrmann, C. Silberhorn, W. Sohler, M. Afzelius and N. Gisin, “Quantum Teleportation from a Telecom-Wavelength Photon to a Solid-State Quantum Memory,” *Nature Photonics*, **8**, 2014, pp. 775-778.
 94. A. Tiranov, J. Lavoie, A. Ferrier, P. Goldner, V. B. Verma, S. W. Nam, R. P. Mirin, A. E. Lita, F. Marsili, H. Herrmann, C. Silberhorn, N. Gisin, M. Afzelius and F. Bussieres, “Storage of Hyperentanglement in a Solid-State Quantum Memory,” arXiv:1412.6488v1, 2014.
 95. A. Tiranov, “Exploring Storage Capability of a Solid-State Quantum Memory for Light,” Thèse de doctorat, Univ. Genève, 2016, no. Sc. 4993.
 96. W. B. Gao, P. Fallahi, E. Togan, A. Delteil, Y. S. Chin, J. Miguel-Sanchez, A. Imamoglu, “Quantum Teleportation from a Propagating Photon to a Solid-State Spin Qubit,” *Nature Communications* **4**, 2013, p. 2744.
 97. W. B. Gao, A. Imamoglu, H. Bernien and R. Hanson, “Coherent Manipulation, Measurement and Entanglement of Individual Solid-State Spins Using Optical Fields,” *Nature Photonics*, **9**, 2015, pp. 363-373.
 98. G. Masada, K. Miyata, A. Politi, T. Hashimoto, J. L. O’Brien and A. Furusawa, “Continuous-Variable Entanglement on a Chip,” *Nature Photonics*, **9**, 2015, pp. 316-319.
 99. N. Matsuda and H. Takesue, “Generation and Manipulation of Entangled Photons on Silicon Chips,” *Nanophotonics* **5**, 3, 2016, pp. 440-455.
 100. D. Rielander, K. Kutluer, P. M. Ledingham, M. Gundogan, J. Fekete, M. Mazzera and H. de Riedmatten, “Quantum Storage of Heralded Single Photons in a Praseodymium-Doped Crystal,” *Physical Review Letters*, **112**, 2014, p. 040504.
 101. M. Gundogan, P. M. Ledingham, K. Kutluer, M. Mazzera and H. de Riedmatten, “A Solid State Spin-Wave Quantum Memory for Time-Bin Qubits,” arXiv:1501.03980v1, 2015.
 102. H. Krauter, D. Salart, C. A. Muschik, J. M. Petersen, H. Shen, T. Fernholz and E. S. Polzik, “Deterministic Quantum Teleportation Between Distant Atomic Objects,” *Nature Physics*, **9**, 2013, pp. 400-404.
 103. X.-H. Bao, X.-F. Xu, C.-M. Li, Z.-S. Yuan, C.-Y. Lu and J.-W. Pan, “Quantum Teleportation Between Remote Atomic-Ensemble Quantum Memories,” *Proceedings of the National Academy of Sciences (PNAS)*, **109**, 50, 2012, pp. 20347-20351.

104. Z.-S. Yuan, Y.-A. Chen, B. Zhao, S. Chen, J. Schmiedmayer and J.-W. Pan, "Experimental Demonstration of a BDCZ Quantum Repeater Node," *Nature*, **454**, 2008, pp. 1098-1101.
105. C. Nolleke, A. Neuzner, A. Reiserer, C. Hahn, G. Rempe and S. Ritter, "Efficient Teleportation Between Remote Single-Atom Quantum Memories," *Physical Review Letters*, **110**, 2013, p. 140403.
106. S. Ritter, C. Nolleke, C. Hahn, A. Reiserer, A. Neuzner, M. Uphoff, M. Mucke, E. Figueroa, J. Bochmann and G. Rempe, "An Elementary Quantum Network of Single Atoms in Optical Cavities," *Nature*, **484**, 2012, pp. 195-200.
107. S. Olmschenk, D. N. Matsukevich, P. Maunz, D. Hayes, L. M. Duan and C. Monroe, "Quantum Teleportation Between Distant Matter Qubits," *Science* **323**, 2009, pp. 486-489.
108. J. Aron, "Quantum Experiments at Space Scale (QUESS)," *New Scientist*, August 2016.
109. Y. Cao, Q. Zhang, C.-Z. Peng, J.-W. Pan, "Quantum Information Experiments with Free-Space Channels," in R. Bertlmann, A. Zeilinger (eds.), *Quantum [Un]Speakables II: Half a Century of Bell's Theorem*, New York, Springer, 2017.
110. E. Gibney, *Nature*, **535**, 28 July 2016, pp. 478-479.
111. T. Herbst, T. Scheidl, M. Fink, J. Handsteiner, B. Wittmann, R. Ursin and A. Zeilinger, "Teleportation of Entanglement Over 143 km," arXiv:1403.0009v4, 2015.
112. J. Yin, J.-G. Ren, H. Lu, Y. Cao, H.-L. Yong, Y.-P. Wu, C. Liu, S.-K. Liao, F. Zhou, Y. Jiang, X.-D. Cai, P. Xu, G.-S. Pan, J.-J. Jia, Y.-M. Huang, H. Yin, J.-Y. Wang, Y.-A. Chen, C.-Z. Peng and J.-W. Pan, "Quantum Teleportation and Entanglement Distribution Over 100-Kilometre Free-Space Channels," *Nature*, **488**, 2012, pp. 185-188.
113. X.-S. Ma, T. Herbst, T. Scheidl, D. Wang, S. Kropatschek, W. Naylor, B. Wittmann, A. Mech, J. Kofler, E. Anisimova, V. Makarov, T. Jennewein, R. Ursin and A. Zeilinger, "Quantum Teleportation Over 143 Kilometres Using Active Feed-Forward," *Nature*, **489**, 2012, pp. 269-273.
114. X.-S. Ma, S. Kropatschek, W. Naylor, T. Scheidl, J. Kofler, T. Herbst, A. Zeilinger and R. Ursin, "Experimental Quantum Teleportation Over a High-Loss Free-Space Channel," *Optics Express* **20**, 21, 2012, p. 23126.
115. X.-M. Jin, J.-G. Ren, B. Yang, Z.-H. Yi, F. Zhou, X.-F. Xu, S.-K. Wang, D. Yang, Y.-F. Hu, S. Jiang, T. Yang, H. Yin, K. Chen, C.-Z. Peng, and J.-W. Pan, "Experimental Free-Space Quantum Teleportation," *Nature Photonics*, **4**, 2010, pp. 376-381.
116. N. Kalb, A. A. Reiserer, P. C. Humphreys, J. J. W. Bakermans, S. J. Kamerling, N. H. Nickerson, S. C. Benjamin, D. J. Twitchen, M. Markham, and R. Hanson, "Entanglement Distillation Between Solid-State Quantum Network Nodes," arXiv:1703.03244v1 [quant-ph], 9 March 2017.
117. G. Masada and A. Furusawa, "On-Chip Continuous-Variable Quantum Entanglement," *Nanophotonics*, **5**, 3, 2016, pp. 469-482.
118. K. Makino, Y. Hashimoto, J.-i. Yoshikawa, H. Ohdan, T. Toyama, P. van Loock and A. Furusawa, "Synchronization of Optical Photons for Quantum Information Processing," arXiv:1509.04409v1, 15 September 2015.
119. B. Hensen, H. Bernien, A. E. Dreau, A. Reiserer, N. Kalb, M. S. Blok, J. Ruitenbergh, R. F. L. Vermeulen, R. N. Schouten, C. Abellan, W. Amaya, V. Pruneri, M. W. Mitchell, M. Markham, D. J. Twitchen, D. Elkouss, S. Wehner, T. H. Taminiau and R. Hanson, "Experimental Loophole-Free Violation of a Bell Inequality Using Entangled Electron Spins Separated by 1.3 km," *Nature*, **526**, 21 October 2015, pp. 682-686.
120. M. Krenn, J. Handsteiner, M. Fink, R. Fickler and A. Zeilinger, "Twisted Photon Entanglement Through Turbulent Air Across Vienna," arXiv:1507.06551v1, 2015.
121. G. Carvacho, J. Carine, G. Saavedra, A. Cuevas, J. Fuenzalida, F. Toledo, M. Figueroa, A. Cabello, J.-A. Larsson, P. Mataloni, G. Lima and G. B. Xavier, "Post-Selection Loophole-Free Bell Test Over an Installed Optical Fiber Network," arXiv:1503.07535v1, March 2015.
122. S.-Y. Lin, C.-H. Chou and B. L. Hu, "Quantum Teleportation Between Moving Detectors," arXiv:1502.03539v1, 12 February 2015.
123. M. Fuwa, S. Takeda, M. Zwierz, H. M. Wiseman and A. Furusawa, "Experimental Proof of Nonlocal Wavefunction Collapse for a Single Particle Using Homodyne Measurement," arXiv:1412.7790v1, 2014.
124. Z. Tang, R. Chandrasekara, Y. Y. Sean, C. Cheng, C. Wildfeuer and A. Ling, "Near-Space Flight of a Correlated Photon System," *Scientific Reports*, **4**, 2014, p. 6366.
125. B. Casabone, A. Stute, K. Friebe, B. Brandstatter, K. Schuppert, R. Blatt and T. E. Northup, "Heralded Entanglement of Two Ions in an Optical Cavity," *Physical Review Letters*, **111**, 2013, p. 100505.

126. L. Slodicka, G. Hetet, M. Hennrich and R. Blatt, "Free Space Interference Experiments with Single Photons and Single Ions," arXiv:1502.04302v2, 17 February 2015.
127. V. Leong, S. Kosen, B. Srivathsan, G. K. Gulati, A. Cere and C. Kurtsiefer, "Hong-Ou-Mandel Interference Between Triggered and Heralded Single Photons from Separate Atomic Systems," arXiv:1504.00818v1, 2015.
128. A. Reiserer and G. Rempe, "Cavity-Based Quantum Networks with Single Atoms and Optical Photons," arXiv:1412.2889v1, 2014.
129. N. Kalb, A. Reiserer, S. Ritter and G. Rempe, "Heralded Storage of a Photonic Quantum Bit in a Single Atom," arXiv:1503.06709v1, 23 March 2015.
130. Z. Merali, "Data Teleportation: The Quantum Space Race," *Nature*, **492**, 2012, pp. 22-25.
131. T. Jennewein, C. Grant, E. Choi, C. Pugh, C. Holloway, J. P. Bourgoin, H. Hakima, B. Higgins and R. Zee, "The NanoQEY Mission: Ground to Space Quantum Key and Entanglement Distribution Using a Nanosatellite," *Proc. SPIE*, **9254**, 2014, p. 925402.
132. P. Komar, E. M. Kessler, M. Bishof, L. Jiang, A. S. Sorensen, J. Ye and M. D. Lukin, "A Quantum Network of Clocks," *Nature, Physics*, **10**, 2014, pp. 582-587.
133. C. Cheng, R. Chandrasekara, Y. C. Tan and A. Ling, "Space Qualified Nanosatellite Electronics Platform for Photon Pair Experiments," arXiv:1505.06523v1, 2015.
134. P. Hemmer, "Closer to a Quantum Internet," *Physics*, **6**, 2013, p. 62.
135. H. J. Kimble, "The Quantum Internet," *Nature*, **453**, 2008, pp. 1023-1030.
136. R. E. Meyers and K. S. Deacon, "Entangled Quantum Communications and Quantum Imaging," *Proc. SPIE*, **5161**, 2004, p. 280.
137. R. E. Meyers, P. Lee, K. S. Deacon, A. Tunick, Q. Quraishi and D. Stack, "A Quantum Network with Atoms and Photons," *Proc. SPIE*, **8518**, 2012, pp. 8518-14.
138. R. E. Meyers, K. S. Deacon, A. Tunick, Q. Quraishi, and P. Lee, "A Quantum Network with Atoms and Photons," Technical Report No. ARL-TR-7786, US Army Research Laboratory, September 2016.
139. R. E. Meyers, K. S. Deacon and D. L. Rosen, "Entangled Quantum Communications and Quantum Imaging," US Patent 7,536,012, 19 May 2009.
140. R. E. Meyers and K. S. Deacon, "Quantum Fourier Transform Based Information Transmission System and Method," US Patent 7,660,553, 9 February 2010.
141. R. E. Meyers and K. S. Deacon, "Quantum Based Information Transmission System and Method," US Patent 8,503,885, 6 August 2013.
142. A. Sit, F. Bouchard, R. Fickler, J. Gagnon-Bischo, H. Larocque, K. Heshami, D. Elser, C. Peuntinger, K. Gunthner, B. Heim, C. Marquardt, G. Leuchs, R. W. Boyd, and E. Karimi, "High-Dimensional Intra-City Quantum Cryptography with Structured Photons," arXiv:1612.05195v1, 2016.

Appendix

Table 4. List of symbols, abbreviations, and acronyms.

ARL	US Army Research Laboratory
AR+	Argon ion
AFC	Atomic frequency comb
B92	A simplified QKD protocol developed by Bennett in 1992
BB84	First protocol for QKD developed by Bennett and Brassard in 1994
BBO	Beta Barium Borate
BDCZ	Briegel, Dur, Cirac, and Zoller
BPSK	Binary phase shift keying
CHSH	Clauser, Horne, Shimony, and Holt
CPM	Complete parity check measurement
CQT	Center for Quantum Technologies
CRIB	Controlled reversible inhomogeneous broadening
C-S	Clauser and Shimony
CSI	Cauchy-Schwarz inequality
CV	Continuous variable
DLCZ	Duan, Lukin, Cirac and Zoller
DoF	Degree(s) of freedom
DSQC	Direct secure quantum communications
E91	QKD protocol for entangled photons developed by Ekert in 1991
EIT	Electromagnetically induced transparency
ELED: QD	Entangled light emitting diode: Quantum dot
EPR	Einstein, Podolsky, and Rosen
EPS	Entangled photon source
FWM	Four wave mixing
GEM	Gradient echo memory
GHZ	Three-photon Greenberger-Horne-Zeilinger state
HOM	Hong-Ou-Mandel
InGaAs	Indium gallium arsenide
JQI	Joint Quantum Institute
LBO	Lithium borate
M-M, S-R, M-S	Protocols for distributing entanglement between two neighboring repeaters using single photons labeled as MeetInTheMiddle, SenderReceiver, and MidpointSource
MDS	Multimode difference squeezing
MSS	Multimode sum squeezing
NV	Nitrogen vacancy
OAM	Optical orbital angular momentum
PPKTP	Periodically poled potassium titanyl phosphate
PPLN	Periodically poled lithium niobate
PPM	Pulse position modulation
Qcomm	Quantum communications
QIP	Quantum information processing
QKD	Quantum key distribution
QS	Quadrature squeezing
QSDC	Quantum secure direct communications
SDS	Sum/difference squeezing
SDT	Super dense teleportation
SPDC	Spontaneous parametric down conversion
SPD	Single photon detector
SPS	Single-photon source based protocol

Table 5. Country abbreviation list.

AR	Argentina
AT	Austria
AU	Australia
CA	Canada
CH	Switzerland
CL	Chile
CN	China
CZ	Czech Republic
DK	Denmark
ES	Spain
FR	France
GER	Germany
IL	Israel
IN	India
IR	Iran
IT	Italy
JP	Japan
KR	South Korea
NL	Netherlands
NZ	New Zealand
PK	Pakistan
PL	Poland
SE	Sweden
SG	Singapore
TW	Taiwan
UK	United Kingdom
USA	United States of America
VN	Vietnam

URSI France 2017 Workshop on Radio Science for Humanity

Journées scientifiques URSI-France 2017

Radiosciences au service de l'humanité (Part 2)

Copernicus, A Major European Cooperation Program: From the Early Concept to Operational Services

Guy Duchossois

Former ESA Earth observation Mission Manager
Expert/consultant attached to the European Commission for Copernicus
E-mail: guy.duchossois@libertysurf.fr

Abstract

The Copernicus program (previously known as GMES: Global Monitoring for Environment and Security) is a major European undertaking for the continuous monitoring of the Earth system. Copernicus is one of the two pillars – together with the Galileo program – of the cooperation between the European Union (EU), the European Space Agency (ESA), and their Member States. This paper describes the implementation evolution of Copernicus, from the initial proposal elaborated in May 1998 until 2017, including the operational services available, the space component, and the agreed governance for the management of this ambitious program. This paper is based on [1].

1. The Background of Copernicus

GMES (which turned into Copernicus in 2013) was proposed on May 19, 1998, by a European group of space-community leaders (ESA, Eumetsat, CNES, DLR, ASI, BNSC...). They were invited at the initiative of the European Commission to participate in a meeting held in Baveno, Italy. The European Association of Remote Sensing

Companies (EARSC) was also invited as a representative of the downstream value-added sector. The purpose of this meeting was to envisage the development of space-based environmental services in Europe, with a view to move from a research/application demonstration status to the provision of fully operational and sustainable information services to policymakers and public authorities. These indeed needed reliable and timely information to support the development of environmental legislation and policies, or to take critical decisions in the event of an emergency, such as a natural disaster or a humanitarian crisis. The private sector would also benefit from GMES/Copernicus via the development of innovative value-added products, resulting in new business opportunities.

The outcome of this meeting, known as the “Baveno Manifesto,” defined four main high-level objectives for GMES, namely:

- To provide Europe with an autonomous and sustainable capacity for observation and monitoring of the Earth;
- To provide reliable information and services to support EU environment and security policies based on satellite data and in situ observations;

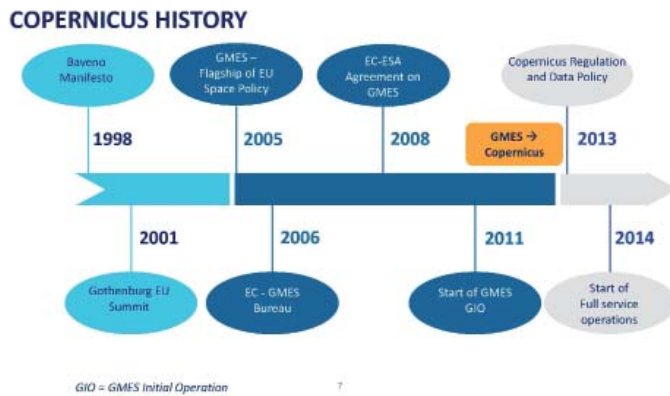


Figure 1. Milestones in the history of Copernicus.

- To develop downstream applications and services, stimulate innovation and SMEs (small and medium enterprises), to encourage the creation of start-ups, and to increase the demand for skilled jobs;
- To stimulate scientific research and international cooperation.

A short anecdote: GMES initially stood for “Global Monitoring of Environmental Security.” However, after Baveno (in 1999), it quickly became “Global Monitoring of Environment and Security,” because environmental monitoring covers more than just security.

The Baveno meeting was the outcome of a long process of joint activities in the 1990s between the European Union/ European Commission and the European Space community, as demonstrated by:

- The involvement and participation of the European Union in all international conferences related to climate change in the 1990s (Rio Summit in 1992, adoption of Kyoto Protocol on 11 December 1997 and ratification by EU countries...);
- The priority for Europe to reduce emission of greenhouse gases (GHGs) and to develop evaluation/control tools using Earth observation techniques as essential tools;
- The participation of the European Commission (EC) in CEOS (Committee on Earth Observation Satellites – “Club of Space agencies” created in 1984) meetings where the concept of an IGOS (Integrated Global Observation System) was proposed in 1995-1996 to better coordinate space assets for monitoring of the Earth;
- The participation of the EC in the IGOS-P (IGOS-Partnership) with associated international organizations in charge of major environmental/climate programs (IGBP, WCRP, WOCE...). IGOS-P was set up in 1998 with the objective to derive key climate variables from space observations, and to contribute to advanced climate models and to better understand/forecast climate change.

2. The History of Copernicus

The detailed definition of the content of Copernicus spanned almost 10 years. This included a number of major political steps, large consultations of European users’ communities performed by the EC and ESA to define their requirements, and preliminary definition of possible GMES candidate services. Some of these milestones are recalled hereafter, and are illustrated in Figure 1:

- The elaboration, in 2000, of a European Earth observation strategy with all European partners, involving a downstream industry sector represented by EARSC.
- The adoption of several EC communications on GMES by the European Council and Parliament.
- The approval of ESA resolutions on GMES by successive ESA Council meetings at the ministerial level, to initiate the implementation and provide funding for the program.
- The organization of a series of GMES colloquia by successive EU presidencies in the early 2000 (Lille in October 2000, Stockholm in March 2001, Brussels in October 2001,...) to further promote the program at the highest political level.
- The creation in 2002 of a GMES steering committee, co-chaired by the EC (DG environment/ Catherine Day) and ESA (José Achache/Director of EO programs).
- The creation of two GMES bureaus in 2006, one located at ESA/ESRIN in Frascati, and one at EC DG ENTR in Brussels.
- The preliminary definition of candidate GMES services with funding allocated for a five-year period (2002-2007). This funding came from the EC/6th Framework Programme for Research and Technological Development (FP6) and from the ESA GMES Service Element program (GSE).

Copernicus architecture concept/ « perimeter »

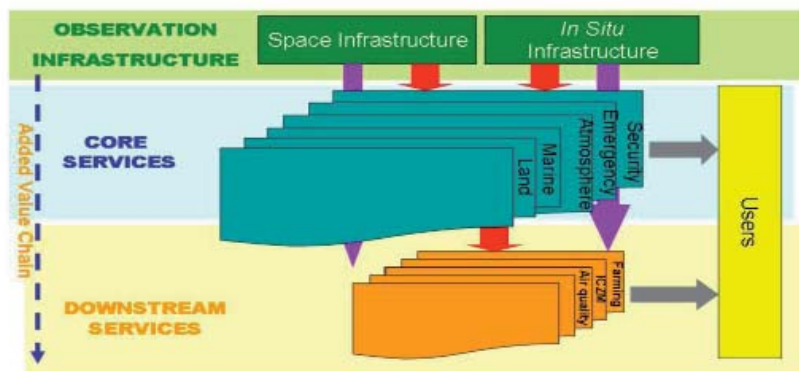


Figure 2. The three main components of Copernicus.

- The decision to develop GMES in steps through the introduction of “pilot services,” starting with three “fast-track services” (land, marine, emergency) by the end of 2008.
- The start of GMES Initial Operations (GIO) in 2011, and full service in 2014.

3. The Copernicus Concept

Copernicus is composed of three main components. There is a space Earth observation component. There is an in-situ (non-space) Earth observation component. There is a service component, delivering products that result from the processing/assimilation of these space and non-space data into models of varying complexity, as illustrated in Figure 2.

Copernicus delivers core products in a number of selected thematic domains. These core products can be directly used for some applications, or can be further processed to generate tailored downstream products/services by value-added companies. The Copernicus “perimeter” is strictly limited to the generation and delivery of the core products, thus avoiding any competition with the value-added SMEs (small and medium enterprises) sector.

4. The Copernicus Development Approach

The implementation of Copernicus was carried out according to four successive phases/steps over the period between 2000 and 2017+, including the following:

- *Initial Exploratory Phase (2000-2003)*: focusing on the definition of user needs in terms of product and service portfolios by expert advisory groups, international consultations, high-level EU presidency forums, economic benefit studies,....

- *Development Phase (2004-2008)*: thematic projects with EC FP 6 and ESA funding, a top priority being given to the three selected for “fast track.” During that period, the development of the space “Sentinels” satellite component was started in industry under ESA management. A detailed inventory and evaluation of existing in-situ observation facilities in Europe was carried out.

- *Pre-operational phase (2009-2014)*: the continuation of Sentinels development in industry (with Airbus Defence & Space, Thales Alenia Space, ...) and the implementation of major projects for five of the six selected priority thematic areas, namely: oceanography/marine environment (“MyOcean” project); land and soil management (“GEOLAND” project); atmosphere for air quality/air pollution (“MACC” project); risk management (“SAFER” project); civil security and humanitarian aid (“MOSAIC” project). These projects were performed by European consortia (50-60 partners) composed of a mix of research institutions and operational agencies/companies. The sixth thematic service (for climate) relies on the ESA Climate Change Initiative program, plus contributions from other priority services.

- *Operational phase (2015-2020)*: the procurement, launch, and operations of the Copernicus dedicated “Sentinels” satellites, and the delivery of operational products and services for the six priority thematic areas via European consortia selected and financed by the EC for the provision of these services.

5. Copernicus Services

Copernicus services are illustrated in Figure 3. They include (summary only):

- The land service, divided into three main components:

Copernicus priority services

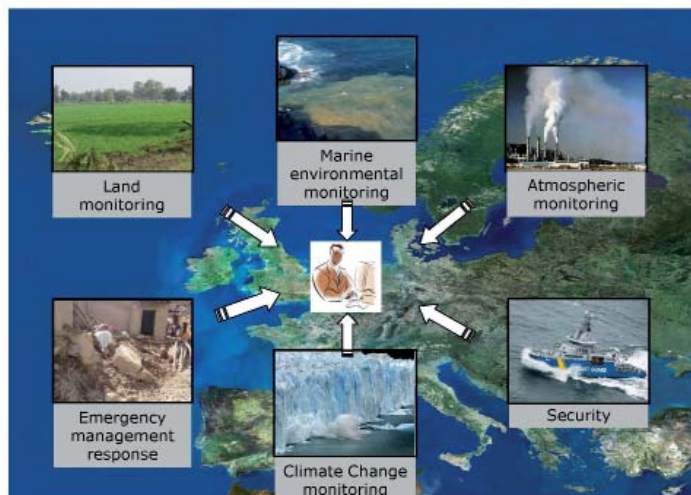


Figure 3. Copernicus priority services.

1. The global component, providing bio-geophysical products of global land surface at mid- and low-spatial resolution, and used to monitor the vegetation, the water cycle, and the energy budget.
 2. The pan-European component, providing information about the land cover and land use (LC/LU), land-cover and land-use changes, and land-cover characteristics.
 3. The local component, focusing on different hotspots, i.e., areas that are prone to specific environmental challenges and problems. This includes detailed LC/LU information for the larger EU cities (urban atlas), riparian zones along European river networks, and NATURA 2000 sites.
- The marine service, providing core information related to four benefit areas:
 1. Maritime safety: support to any safe activities at sea, including ship routing services, offshore operations, or search and rescue operations, including oil-spill response and remediation.
 2. Marine resources: contributions to the protection and the sustainable management of living marine resources, in particular for aquaculture, fishery research, or regional fishery organizations.
 3. Coastal monitoring service at European and national levels for water-quality monitoring and pollution control, coastal erosion, marine ecosystems in European seas
 4. Weather and marine meteorological forecasting services and climate-change indicators.
 - The atmosphere service, addressing five main themes:
 1. Air quality, with the production of daily five-day forecasts of the state of the atmosphere, as well as four-day forecasts of air quality.
 2. Climate forcing, with the monitoring of the global CO₂ and CH₄ surface fluxes.
 3. Ozone layer and UV, with the provision of forecasts of stratospheric ozone concentrations up to five days ahead, and five-day forecasts of UV radiation.
 4. Solar radiation, providing global and direct irradiances for Europe, Africa, the Middle East, and Asia for the solar-energy industry, the electricity sector, governments, and renewable-energy organizations and institutions.
 5. Emissions and surface fluxes providing emission inventories that serve as inputs to the atmospheric chemistry-transport models.
 - The emergency management service (EMS), including two main components, early warning and rapid mapping, as well as a dedicated component for risk and recovery mapping tailored to user needs.
 - The security service, to support crisis prevention, preparedness and response in three key areas:
 1. Border surveillance, to reduce the number of illegal immigrants entering the EU undetected, and to reduce the death toll of illegal immigrants by rescuing more lives at sea.
 2. Maritime surveillance, to support Europe's maritime security objectives and related activities in the maritime domain (safety of navigation, support to fisheries control, combating marine pollution, and law enforcement).
 3. Support to EU external action to assist third countries in a situation of crisis or emerging crisis and to prevent global and trans-regional threats having a destabilizing effect.
 - The climate change service, providing access to information for monitoring and predicting climate change and help to support adaptation and mitigation. This also provides access to several climate indicators (ECVs) and climate indices.

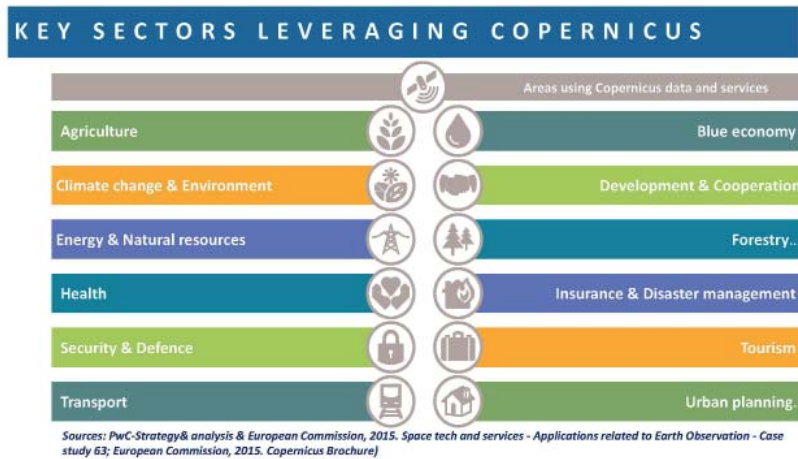


Figure 4. Key application sectors that benefit from Copernicus.

Numerous examples of Copernicus thematic products are provided at www.copernicus.eu. Figure 4 illustrates key application sectors benefiting from Copernicus.

6. Copernicus Space Component








The Copernicus space component includes a set of dedicated satellites (the “Sentinel” series) and contributing missions (based on existing commercial and public Earth-observation satellites). The Sentinel satellites are specifically designed to meet the needs of the Copernicus services and their users.

There are five series of Sentinel missions, each composed of four units: A, B, C, and D. Each unit is designed for a minimum lifetime of seven years. The data continuity of these series is therefore guaranteed until

2025-2030. Sentinel 5P is a one-off mission to prepare the Sentinel 5 series. Five Sentinel satellites are currently fully operational in orbit, namely Sentinel 1-A and 1-B, Sentinel 2-A and 2-B, and Sentinel 3-A.

Additional missions are contributing and/or will contribute to Copernicus, such as:

- ESA Earth Explorer missions (SMOS, Cryosat, GOCE...)
- European Meteorological missions (ESA/Eumetsat) and non-European meteorological missions (NOAA...)
- European national contributing missions: France, Germany, Italy...
- Non-European contributing missions: Canada, USA, Japan, China, India...

THE SENTINELS			Key Features
Sentinel Mission and Status			
	SENTINEL-1: 4-40m resolution, 3 day revisit at equator	2 sats in orbit	Polar-orbiting, all-weather, day-and-night radar imaging
	SENTINEL-2: 10-60m resolution, 5 days revisit time	1 Sat in Orbit	Polar-orbiting, multispectral optical, high-res imaging
	SENTINEL-3: 300-1200m resolution, <2 days revisit	1 Sat in Orbit	Optical and altimeter mission monitoring sea and land parameters
	SENTINEL-4: 8km resolution, 60 min revisit time	1st Launch in 2020	Payload for atmosphere chemistry monitoring on MTG-S
	SENTINEL-5p: 7-68km resolution, 1 day revisit	Launch by in 2017	Mission to reduce data gaps between Envisat, and S-5
	SENTINEL-5: 7.5-50km resolution, 1 day revisit	1st Launch in 2021	Payload for atmosphere chemistry monitoring on MetOp 2 nd Gen
	SENTINEL-6: 10 day revisit time	1st Launch in 2020	Radar altimeter to measure sea-surface height globally

FULL, FREE AND OPEN

Figure 5. The Copernicus Sentinel satellites.

Potential Contributing Missions to Copernicus – Some examples

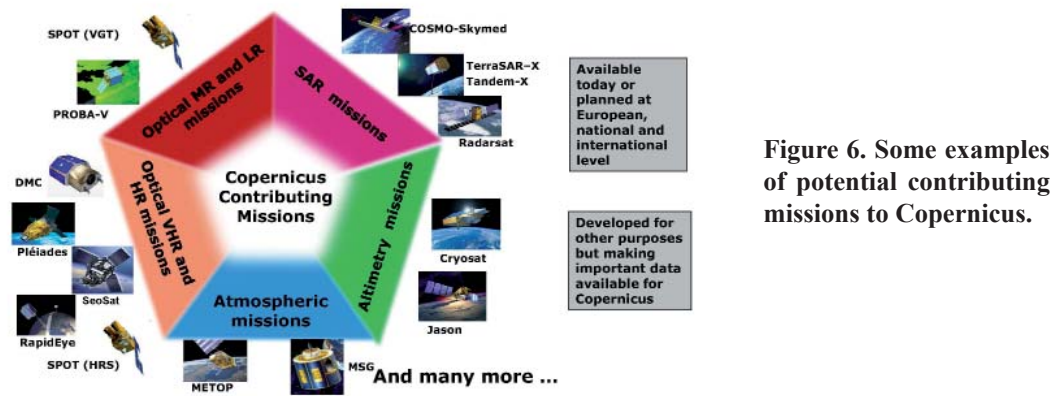


Figure 6. Some examples of potential contributing missions to Copernicus.

Figures 5 and 6 provide illustrations of the overall Copernicus space component.

Copernicus also collects information from in-situ systems that deliver data acquired by a multitude of sensors on land, at sea, or in the atmosphere. Copernicus services transform this wealth of satellite and in-situ data into value-added information.

7. Copernicus Governance and Organization

The Copernicus program is coordinated and managed by the European Commission. The development of the observation infrastructure is performed under the aegis of the European Space Agency for the space component, and under the European Environment Agency and the Member States for the in-situ component. Specific responsibilities are as follows (see Figure 7):

- The Commission has the overall responsibility for the program, including the coordination of the

various components, supervision of implementation, definition of priorities, user participation, costs, timing, results, contracting, relations with third countries and international agencies.

- ESA, by delegation of the Commission, is responsible for the technical coordination of the space component, the overall architecture of the space component and its evolution, and supplying the Sentinels. The ESA-European Commission framework agreement was signed in October 2014.
- Eumetsat, by delegation of the Commission, is responsible for the operations of dedicated Sentinel missions (Sentinel-3 and Sentinel-6 for the oceans, Sentinel-4, 5-Precursor, and 5 for the atmosphere). The ESA-Eumetsat framework agreement was signed in June 2009.
- The EEA (European Environment Agency) is responsible for the coordination of in-situ observations provided by the Member States.

COPERNICUS GOVERNANCE

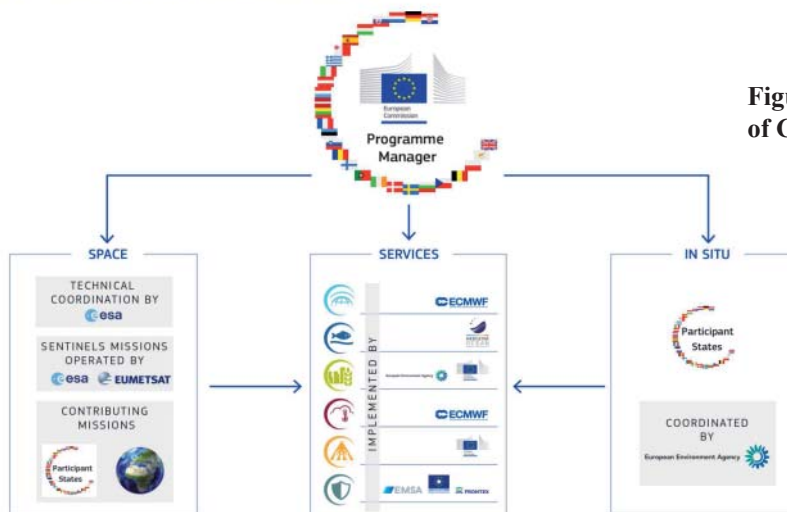


Figure 7. The organization of Copernicus governance.

COPERNICUS FUNDING (EU contribution)



Figure 8. The EU contribution to the Copernicus funding.

By delegation of the Commission, services are awarded to European entities (EEA, ECMWF, EMSA, FRONTEX, and SatCen) and to one private company (Mercator Ocean).

Data policy: The free, full, and open data policy adopted for the Copernicus program foresees access available to all users for the Sentinel data products via a simple pre-registration.

8. The Funding of the Copernicus Program

Copernicus is jointly financed by ESA and the European Union, as follows:

2001-2006: ~200 M€ (83 M € by ESA and 103 M € by EU FP 6)

2007-2013: A total of 3.5 B€, including 2.3 B € by ESA for the development of the first units of the Sentinel missions, and 1.2 B€ by EU FP 7 (550 M€ for the development of services, and 650 M€ as a contribution for the development of the Sentinel missions)

2014-2020: 4.3 B€ by EUH2020 for the supply of the C and D recurring units of the Sentinel missions (to be launched after 2020), and the provision of operational services for all selected priority areas

The total cost of the program is ~7.5 B€ until 2020. Figure 8 provides the EU contribution.

9. Copernicus Evolution

On October 26, 2016, the European Commission released the “Space Strategy for Europe.” The communication referred to Copernicus in calling for the strengthening of “...the dissemination of Earth observation data generated by Copernicus....” It also stated

Additional services will be considered to meet emerging needs in specific priority areas, including:

- (i) climate change and sustainable development, to monitor CO₂ and other greenhouse gas emissions, land use and forestry, and changes in the Arctic with Copernicus; and
- (ii) security and defence to improve the EU’s capacity to respond to evolving challenges related to border controls and maritime surveillance with Copernicus and Galileo/EGNOS

Currently, several groups of experts have been set up and are working on the definition of candidate missions as per (i). At the 11th Copernicus Committee and the 12th User Forum, Greenhouse-gas monitoring was confirmed as priority one for Copernicus evolution activities.

10. Conclusions: The Way Forward

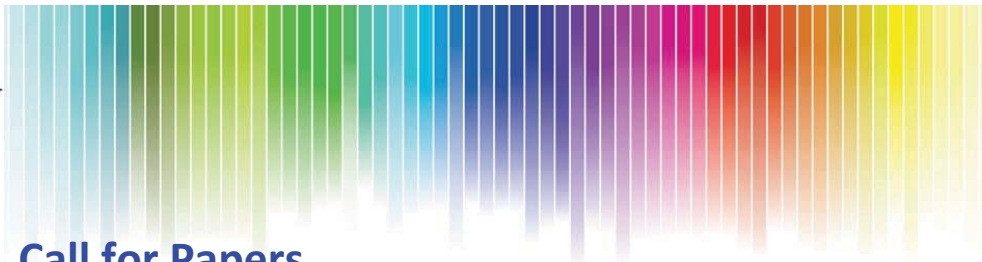
Copernicus is one of the successful pillars of the European cooperation among the EU, ESA, Eumetsat, and their Member States. It mobilizes Europe’s technological, scientific, industrial, and human skills and capabilities. It strengthens Europe’s strategic position on the world stage, and its autonomy in the field of environmental information. Copernicus is stimulating exports by European industry of Earth observation satellites and services. It contributes to growth and creation of qualified jobs.

11. Acknowledgements

Special thanks are addressed to Dr. Josef Aschbacher (ESA), Dr. Virginia Puzzolo (REA), and Dr. Peter Breger (EC DG Grow) for their support in preparing this paper.

12. Reference

1. Guy Duchossois, “Copernicus, A Major European Cooperation Program: From the Early Concept to Operational Services,” URSI-France 2017 Workshop “Radio Science for Humanity,” Sophia Antipolis, February 2, 2017.



Important deadlines

Paper submission
January 10, 2018
Notification
February 21, 2018
Early bird
registration
March 24, 2018
Conference start
May 28, 2018

Call for Papers

2nd URSI Atlantic Radio Science Conference (URSI AT-RASC)

May 28 - June 1, 2018

ExpoMeloneras Convention Centre, Gran Canaria

The triennial URSI Atlantic Radio Science Conference (URSI AT-RASC) is one of the URSI flagship conferences besides the URSI General Assembly and Scientific Symposium and the AP-RASC conference (Asia-Pacific Radio Science Conference).



This 2nd URSI AT-RASC will have a series of convened and open sessions within the domains covered by all ten Commissions of URSI:

- | | |
|----------------------------------------------------------------|--------------------------------------------------------|
| Commission A: Electromagnetic Metrology | Commission F: Wave Propagation and Remote Sensing |
| Commission B: Fields and Waves | Commission G: Ionospheric Radio and Propagation |
| Commission C: Radiocommunication and Signal Processing Systems | Commission H: Waves in Plasmas |
| Commission D: Electronics and Photonics | Commission J: Radio Astronomy |
| Commission E: Electromagnetic Environment | Commission K: Electromagnetics in Biology and Medicine |

Please consult www.at-rasc.org for the latest information

Paper submission deadline: January 10, 2018

Detailed information on paper submission as well as travel information will become available through the website: www.at-rasc.org. Papers presented at this 2nd URSI AT-RASC will be submitted for posting to IEEE Xplore. In addition, there will be special programs for young scientists, a student paper competition and programs for accompanying persons.

Technical Programme Committee

- | | |
|--------------------|-----------------------------------------------------|
| Chair: | Prof. P.L.E. Uslenghi |
| European Liaison : | Prof. O. Santolik, Prof. A. Sihvola, Prof. J. Wiart |
| AP-RASC Liaison : | Prof. K. Kobayashi |

Publication Chair: Dr. W.R. Stone

Organizing Committee:

- | | |
|-------------|--------------------|
| Chair: | Prof. P. Van Daele |
| Vice-Chair: | Prof. P. Lagasse |



In Memoriam: Michael C. Sexton

Prof. (emeritus) Michael C. Sexton, University College Cork, Cork, Ireland, died peacefully July 18, 2016. He was bereaved by his beloved wife Leonore; their dear children Angela-Mary, Tom, Leo and Michael; grandchildren Conor, Tomás, Moira, and Aisling; his brother, Jerry; daughters-in-law Kathleen and Margaret; extended family, relatives, and a wide circle of friends in Ireland, Italy (Padua), and internationally.



Michael was very active in URSI, especially in Commissions F and G, and had articles published in *Radio Science*. In the 1980s and 1990s, he chaired the organizing and technical program committees of the URSI All-Ireland biennial research colloquia and joint URSI All-Ireland-UK research colloquia, under the auspices of the Royal Irish Academy, of which he was a

member. He also represented Ireland at the URSI General Assemblies on several occasions. While Michael had a wide range of research interests, his main focus was in the field of plasma physics and fusion engineering. He inspired and directed many young engineers and physicists along their research careers. One of those, Carlo G. Someda, in the preface of his book on *Electromagnetic Waves*, acknowledged his inspiration and recommendation to him to write the book. Michael was always a delight to be with, a very entertaining host and guest. URSI offers their condolences to his wife and family. May he rest in peace.

Mairtin S. O'Droma
Ireland
E-mail: Mairtin.ODroma@ul.ie

14th International Workshop on Finite Elements for Microwave Engineering FEM2018



The International Workshop on Finite Elements for Microwave Engineering is a highly-focused biannual event. It provides an ideal meeting place for researchers and practitioners active in the theory and application of the Finite-Element Method in RF and microwave engineering.

September 10-14, 2018 Cartagena De Indias, Colombia
Jointly held with 20th ICEAA

Jointly organized by
the Colorado State University and the University of Florence.

Scope Topics will include, but are not limited to: • Advanced FEM Techniques • Optimization Techniques, Model Order Reduction • Multigrid and Domain Decomposition Methods • Discontinuous Galerkin Methods • FEM for Multiphysics Problems • FEM for Metamaterials and Nanophotonics • Time Domain FEM • Adaptive methods • Hybrid Methods • FEM Modeling and Applications • CAD / Meshing Advances and Tools • Parallel Computation on Multi- and Many-Core Computers • Adaptive methods • Integral Equation Methods • Hybrid Methods.

Publication Workshop abstracts will appear on IEEE Xplore. Selected workshop contributions will be published in a Special Issue of journal Electromagnetics.

General Chairs

Branislav Notaros, Colorado State University (USA)
Stefano Selleri, University of Florence (IT)

Scientific Committee

A. Boag, Tel Aviv University, (IL); • A. C. Cangellaris, University of Illinois Urbana-Champaign (USA); • D. B. Davidson, University of Stellenbosch, (ZA); • R. Dyczij-Edlinger, Universität des Saarlandes (DE); • T. Eibert, Technische Universität München (DE); • G. Ghione, Politecnico di Torino, (IT); • R. D. Graglia, Politecnico di Torino, (IT); • J. Jin, University of Illinois, Urbana-Champaign (USA); • L. Kempel, Michigan State University (USA); • J.-F. Lee, Ohio State University (USA); • R. Lee, Ohio State University (USA); • Z. Nie, University of Electronic Science and Technology of China (CN); • B. M. Notaros, Colorado State University (USA); • G. Pelosi, University of Florence (IT); • A. F. Peterson, Georgia Institute of Technology (USA); • M. Salazar-Palma, Universidad Carlos III de Madrid (ES); • C.J. Reddy, EMSS (USA); • S. Selleri, University of Florence (IT); • B. Shanker, Michigan State University (USA) • A. Toscano, University of Roma Tre (IT); • J. L. Volakis, Ohio State University (USA); • M. N. Vouvakis, University of Massachusetts (USA); • J. P. Webb, McGill University (CA); • A. Yilmaz, University of Texas at Austin (USA); • J. Zapata, Universidad Politécnica de Madrid (ES).



Young Researcher Award Starting with 14th edition a solid gold "Fiorino" coin will be awarded by the Department of Information Engineering of the University of Florence to the Best Paper by a Young Researcher.

Important Dates

Abstract submission: March 9, 2018
Notification of acceptance: April 9, 2018
Registration: June 8, 2018

notaros@colostate.edu
stefano.selleri@unifi.it

www.FEM2018.unifi.it



UNIVERSITÀ
DEGLI STUDI
FIRENZE
DINFO
DIPARTIMENTO DI
INGEGNERIA
DELL'INFORMAZIONE

Book Review



George Trichopoulos

Electrical, Computer & Energy Engineering ISTB4
555D

Arizona State University

781 E Terrace Road, Tempe, AZ, 85287 USA

Tel: +1 614 364 2090

E-mail: gtrichop@asu.edu

Interferometry and Synthesis in Radio Astronomy, Third Edition, by A. Richard Thompson, James M. Moran, and George W. Swenson Jr., Springer International Publishing, 2017, 872 pages; ISBN 978-3-319-44429-1 (hardcover) € 55.00; ISBN 978-3-319-44431-4 (eBook) free.

When we look at the sky with the unaided eye, the eye's angular resolving power of about one arc minute allows us to see many hundreds of separate stars. We can also see structure in the brightness distribution of the full moon. A telescope of only 10 cm diameter already provides us with a resolution of about one arc second at optical wavelengths. In the early 1940s, Grote Reber made the first systematic radio observations of the sky with a parabolic dish of 10 m diameter at a wavelength of about 1.9 m. This resulted in an intensity map of the "radio sky" with an angular resolution of about 12 degrees! Although some regions of higher intensity protruded from the smooth radiation from the Galactic Plane, it was out of the question to learn about their character, such as determining the celestial position and angular size. Any comparison with an optical companion was impossible.

In this frustrating situation, the early radio astronomers – many of whom came from wartime radar laboratories, notably in Australia and England – quickly turned to the use of interferometers in order to improve the angular resolution, which would be proportional to the distance between the two elements of the interferometer rather than their individual size. In early experiments in Australia, a "sea-cliff" interferometer was realized with a single antenna located about 100 m above sea level, using the direct and reflected paths from the ocean's surface to create interference fringes. The improved resolution led to the optical identification of the powerful radio sources Cygnus A and Taurus A with a distant galaxy and a supernova in our Galaxy, respectively.

In the early 1950s, several large interferometric radio telescopes were built that operated at relatively long wavelengths, of the order of one meter. Both in Australia and in England, the method of aperture

synthesis was developed, in which data from a number of interferometers with different spacings were combined to *synthesize* a two-dimensional telescope.

With the advent of fully steerable parabolic reflectors operating at shorter cm wavelengths, the method of *Earth-rotation synthesis* was introduced. The object under observation was then tracked for up to 12 hours along its daily path. This caused the projection of the EW-interferometer baseline to rotate with respect to the source, thus providing baselines in all orientations. From these observations, a two-dimensional picture of the brightness distribution of the source could be derived. Major early instruments of this category were the "one mile" and "5 km" arrays in Cambridge, UK (1962, 1968), the Westerbork Synthesis Radio Telescopes (1970), and the Very Large Array in the USA (1980). Parallel to these, the technique of VLBI (very-long-baseline interferometry) was developed in the late 1960s.

In 1986, this all provided sufficient impetus to the authors of the book under review here to present a comprehensive discussion of the principles and applications of "Interferometry and Synthesis in Radio Astronomy." It has been the standard text ever since, not the least due to a greatly updated second edition in 2001. Now, again 15 years later, the authors have added another 200 pages, for a total of almost 900, to cover the developments in the field to the present. I would classify the new edition as the radio astronomy equivalent to "Born & Wolf" for optics. It is complete, almost encyclopedic. However, it is not an encyclopedia! It is a successful combination of a graduate-course textbook and a compendium of answers to any question one might have on the subject. The latter is helped by the systematic reference to original publications and the extensive subject index.

All aspects of the subject are covered in 17 well-structured chapters. The basic concepts are occasionally introduced in a heuristic approach, with the rigorous treatment shifted to a later chapter. There is a parallel here with the structure of Born and Wolf's classic book on

optics. While the pointing to later details may occasionally be somewhat frustrating to the expert, it keeps the general reader on track in gaining understanding without getting immersed in fine details. The first chapter provides a very nice historical introduction, with abundant use of illustrations from original publications. Contemporary students may be surprised to see how much information could be gleaned from a tracing on an analogue chart recorder. The theory of interferometry and synthesis imaging is presented in Chapter 2, and further developed in Chapter 3. The essential role of the Fourier Transform and the concept of convolution are discussed in detail. Chapter 4 covers the aspects of the geometry of the interferometer. It describes the sampling of the spatial-frequency plane that delivers the visibility function. After a discussion of polarization, the chapter concludes with the introduction of the *measurement equation*. This equation includes all instrumental and outside (e.g., atmospheric) parameters that influence the measured visibility, and hence need to be calibrated to obtain intrinsic visibility data on the observed object.

Multi-element interferometer systems are usually called (*aperture*) *synthesis arrays*, and can be geometrically configured in several ways. These are discussed in Chapter 5, with emphasis on practical matters such as selecting the best configuration for a particular observational purpose. The vehicle for this is the *spatial transfer function*, which connects the measured visibility function with the object's brightness distribution via the Fourier transform. Several implementations of actual arrays are described.

Chapter 6 deals with the response of the electronic receiver system. Frequency conversion (mixing) is treated for single- and double-sideband operation, along with the methods of delay correction and fringe rotation. The response to noise and the effects of bandwidth are analyzed in detail. A chapter on system design follows, in which a detailed exposé is presented of receiver and local-oscillator systems, including aspects of noise and delay and gain errors on the sensitivity of the system.

We have now reached the point where normally the signals are digitized. Chapter 8 on digital signal processing has grown from 50 pages in the second edition to 80 pages in the new edition. It reflects the growing application of digital circuits in the steps from signal reception by the receiver front end to the digital data that represent the image of the observed object. This chapter treats in detail the sampling and quantization issues in digital processing. It is followed by a description of digital delay lines and digital correlators, which are now standard in synthesis telescopes. The different types of correlators (XF, FX, hybrid, and digital) are quantitatively compared.

In 1967, a special form of interferometer was introduced. In it, the physical connection of the elements by cable or radio link was replaced by adding very accurate time stamps to the received signal. These were "lined up" in

the offline correlator to create the interference function. This enabled baselines of hundreds to thousands of kilometers, with commensurate extremely high angular resolution. The method is known as very-long-baseline interferometry (VLBI). The special features of this technique are covered in Chapter 9. It covers the transition from magnetic tape to hard disks for the recording medium that occurred in 2001, at about the time that the second edition was published. Apart from an indication in the Preface, this edition does not mention the further step of using the Internet for data and timing transport that essentially renders VLBI into a real-time connected interferometer. First experiments along this line have recently been performed with success. Geodesists and "astrometrists" adopted the VLBI technique with its exquisitely high angular resolution for the precise measurement of continental drift and of the position of celestial objects. The great advances obtained in this field are presented in Chapter 12.

Chapter 10, on "Calibration and Imaging," and Chapter 11, on "Further Imaging Techniques," are more than double their size from the second edition, reflecting the enormous development of these techniques over the last 15 years. In addition to the full Fourier transformation of the visibility data to obtain the source-brightness image, model fitting and closure phase are widely used. These are given extensive attention in this edition. Image-processing algorithms, such as CLEAN, and self-calibration schemes are discussed, and the advances in the field are also striking here.

A serious impediment to interferometry with spatially separated elements is the influence of the fluctuating index of refraction of the propagation medium, such as the Earth's ionosphere and troposphere. The resulting path-length variations cause differential phase errors in the measured complex visibilities that are hard to separate from the true celestial signal, if it can be done at all. Great progress in understanding and new methods of measurement in this area have also been achieved since the publication of the second edition. In the current version, separate chapters have been assigned to the treatment of the neutral atmosphere (troposphere) in Chapter 13, and on ionized media (ionosphere, interplanetary, and interstellar) in Chapter 14. The emergence of large arrays, with baselines up to 10 km or more (for instance, ALMA in the Atacama Desert of Chile), has inspired strong efforts toward measuring the tropospheric path-length variations (mainly caused by water vapor) in real time, to correct the observed visibility phase. Separate small antennas thus measure the water-vapor content along the line of sight, from which the path-length variations can be derived.

Such measurements are routinely made in the evaluation of the suitability of a site for a millimeter- or sub-millimeter-wavelength telescope. Where the troposphere seriously affects observations at short cm and mm wavelengths, long-wavelength observations suffer under the influence of variations in the ionosphere.

The emergence of large arrays at meter wavelengths (for instance, LOFAR) puts the need for corrections on the front burner. These telescopes also have to cope with the generally unavoidable interference from man-made radiation, be it TV transmitters, communication channels, or industrial “noise.” Chapter 16 is devoted to this mundane but important aspect of observational radio astronomy.

In Chapter 15, the authors return to the theoretical basis of synthesis in a full discussion of the van Cittert-Zernike theorem, and aspects of the coherence of the radiation field. This chapter can be considered to be the rigorous treatment of the material presented in Chapters 3 and 4. The book closes with a chapter on “Related Techniques” by shortly discussing the intensity interferometer, lunar-occultation methods, tracking of space debris, and optical interferometry.

Most chapters have appendices with full mathematical derivations and additional material, and an extensive index of names and subjects is added. References to original papers

are given throughout the book, and the resulting reference lists should make the use of Google Scholar superfluous.

Overall, the book delivers a comprehensive treatment of all aspects of interferometry and synthesis in a lucid and flowing tale that is a pleasure to read. The historical notes that are scattered throughout the text add flavor to the reading. My favorite is the discovery, at the Parkes telescope, that some weird intermittent interference was caused by a microwave oven in one of the observatory buildings. For all working in this field, the book is invaluable. So, what does it cost? Here is the best of all: it is published as open access. It can be downloaded for free by anyone who is interested in an 880-page masterpiece. For those, as your reviewer, who prefer to hold this “brick” in their hands, Springer will sell it to you for about 55 Euros, a remarkably small amount, certainly for Springer.

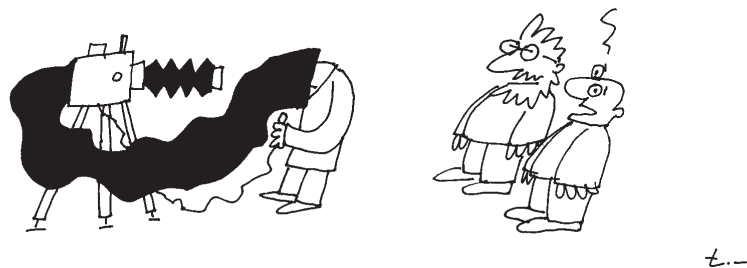
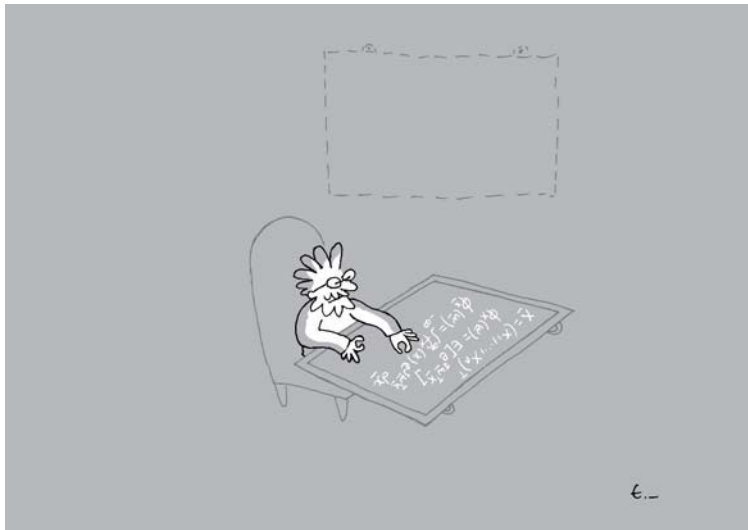
Jacob W. M. Baars
Max-Planck-Institut für Radioastronomie
Bonn, Germany
E-mail: jacobbaars@arcor.de

Et Cetera



Tayfun Akgül

Istanbul Technical University
Dept. of Electronics and Communications Engineering
Telecommunications Division
80626 Maslak Istanbul, Turkey
Tel: +90 212 285 3605; Fax: +90 212 285 3565
E-mail: tayfunakgul@itu.edu.tr.



“It looks like our professor of history is investigating the origin of the selfie again.”



Randy L. Haupt
Colorado School of Mines
Brown Building 249
1510 Illinois Street, Golden,
CO 80401 USA
Tel: +1 (303) 273 3721
E-mail: rhaupt@mines.edu



Amy J. Shockley
E-mail: aj4317@gmail.com

Ethical Boxes

Randy L. Haupt and Amy J. Shockley

I guess you can call me a box collector. I save almost all of the boxes that we get from Amazon and put them in our basement. Whenever we send presents to grandchildren or other relatives, I pick out an appropriately sized box to contain the gifts. We do not buy presents based on the size of the boxes that lie in the basement; however, we have not had to buy any boxes, because I maintain an adequate inventory.

Linear programming optimizes a linear model having linear constraints. The linear constraints are inequalities that form boundaries, or the sides of the solution box. A corner point occurs at the vertex of the box (polygon). If an optimum exists, it occurs at one or more of the corner points, or along a line segment between two corner points. In other words, the best solution pushes the boundary of the box.

The problems we solve in electromagnetics have boundary conditions in the spatial domain, and initial conditions in the time domain. The conditions define the box for our problem. Without them, Maxwell's equations are nice mathematical constructs, but they have no practical use. If we want to design an antenna, we have to define the constraints, or the box, that contains the antenna.

The term "thinking outside the box" originated with the nine-dots puzzle, in which a three by three square of equally spaced dots are to be connected by drawing four straight lines without lifting the pencil (Figure 1). Most people assume that the lines cannot go outside the imaginary box that contains the dots, so they cannot solve

the problem. False assumptions limit potential simple yet innovative solutions.

Some of the problems that we face in life have a clearly defined box, while others are merely dots allowing for innovative thinking and new approaches. Identifying dots and boxes is the first step to finding an optimum solution. Many situations seem to have clearly defined constraints that do not actually exist. For example, Einstein broke out of the Newtonian box, and Tesla broke out of the dc power-transmission box. In order to deal with the problem at hand, it is important to ask the questions:

- 1) What is the end goal?
- 2) Why have we been approaching it in this manner?

In too many scenarios the answer to the second question is, "because that is how we have always done it." Revisiting these types of problems and using creative problem-solving skills leads to superior solutions that lie outside of the presumed constraints.

Ethics defines our problem-solving boundaries. It is much easier to face ethical dilemmas when morals and core values are well-defined. They act as constraints, similar to linear-programming problems. Optimum solutions exist at the vertexes where morals and core values meet. The answer to the second question in these scenarios is, "because this is what is morally and ethically right."

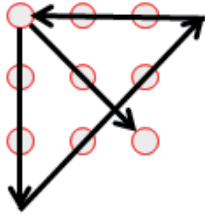


Figure 1. The nine-dots puzzle.

When my daughter was taking a speech class in college, she asked me to listen to her presentation and provide her with feedback. She was very sensitive to criticism at the time, so I knew she would not take any negative comments well. However, I wanted to help her succeed and improve her public-speaking skills. The normal approach was to listen to her, then give her the bad news, which she would not take well and might impact her

confidence in presenting. My morals and values include both developing my children and acting with kindness, creating a conflict in this approach. In order to work within the constraints of my values, the solution that I chose was to suggest she videotape herself giving the speech. This solution actually worked quite well, by allowing her to improve her self-awareness and improve her speaking skills, but kept me out of the backlash from my teenage daughter insulted by negative feedback.

It is important to identify and categorize constraints in solving problems. Sometimes, these are arbitrary, and the constraint is simply fear of change. At other times, these constraints are concrete, and require optimizing within the solution space. Questioning the end goal and how to get there can help define these situations. Engineers and scientists love to solve problems and think up new ideas. These skills are perfect for solving ethical problems as well as technical problems. Our ethics provide us with the appropriate box that fits our situation, much as a proper-size box fits a present for mailing to a granddaughter.



Özgür Ergül

Department of Electrical and Electronics Engineering
Middle East Technical University
TR-06800, Ankara, Turkey
E-mail: ozergul@metu.edu.tr

SOLBOX-07

Şirin Yazar, Barışcan Karaosmanoğlu, and Özgür Ergül

Department of Electrical and Electronics Engineering
Middle East Technical University
TR-06800, Ankara, Turkey

E-mails: sirin.yazar@metu.edu.tr, bariscankaraosmanoglu@gmail.com, ozergul@metu.edu.tr

1. Introduction

Photonic crystals are well-known electronic devices that enable modification, transformation, and selection of light or, more generally, electromagnetic waves [1]. Even though they have a long history of more than 100 years, these structures are becoming increasingly popular, thanks to the rapid developments in nanotechnology and material science, enabling the design and fabrication of very small details [2]. As in all areas of electromagnetics, numerical simulations of photonic crystals are important, since they can provide the analysis and investigation of these structures before their fabrication [3-12]. Three-dimensional simulations, where the photonic crystals are modeled as finite, aperiodic, and possibly inhomogeneous structures, are especially essential to understanding the electromagnetic responses of various designs [8, 11].

In this issue of Solution Box, two different photonic crystals are considered at the higher THz frequencies (SOLBOX-07). While these problems involve homogeneous dielectric objects, the challenges are related to the geometries (three-dimensional and finite structures that host cylindrical holes) and the relatively large sizes in terms of the wavelength (i.e., around eight wavelengths). Fast three-

dimensional solvers are therefore needed for the analysis of these structures. Sample solutions of the problems using a brute-force approach, employing the Multilevel Fast Multipole Algorithm (MLFMA), as well as the reference results obtained are also included in this issue.

Once again, we are looking for alternative solutions of the same problems using other solvers, especially those that are more efficient and/or accurate. Please submit your solutions (not only for SOLBOX-07, but also for the previous problems, SOLBOX01-06) to ozergul@metu.edu.tr.

2. Problems

2.1 Problem SOLBOX-07 (by Ş. Yazar, B. Karaosmanoğlu and Ö. Ergül)

The geometry of the photonic crystal considered in the first problem of SOLBOX-07 is depicted in Figure 1a (a triangular discretization around one of the edges is also shown). A total of 234 cylindrical holes were opened on a dielectric slab of size $3.3 \mu\text{m} \times 0.25 \mu\text{m} \times 12.15 \mu\text{m}$ (the

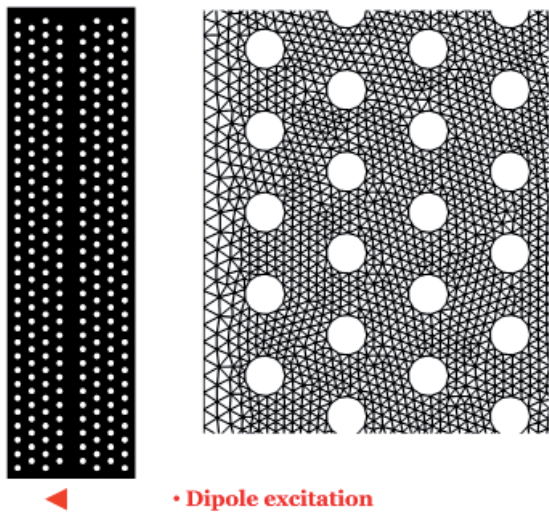


Figure 1a. The geometry of the photonic crystal considered in SOLBOX-07: A waveguide structure that is obtained by removing a row of holes at the center. A typical triangulation in the vicinity of an edge of the first geometry is also shown.



Figure 1b. The geometry of the photonic crystal considered in SOLBOX-07: A modified version that is obtained by removing further holes to form a hole-free cavity.

large surfaces were on the y - z planes, and the thickness was $0.25 \mu\text{m}$). The diameter of the holes was 180 nm , and they were arranged as a triangular grid, as shown in Figure 1. The center-to-center distance between the hole rows was 360 nm in both the y and z directions, except at the center, where a path was created by removing a single row of holes, making the structure behave like a waveguide. The relative permittivity of the slab was 10.0 , while it was not magnetic. The slab was located in free space. It was excited by a Hertzian dipole (or any simple source), which was located as depicted in Figure 1, at 200 THz (or at similar frequencies). The distance between the dipole and the slab was 300 nm . With this geometry and configuration, the photonic crystal was expected to guide the electromagnetic energy along the center hole-free path. It was also expected that some reflections would occur at the air/dielectric and dielectric/air interfaces, as well as escaping waves from the side surfaces. The purpose was to see how the transmission occurs, preferably by considering the electric-field intensity, magnetic-field intensity, and power density inside and outside the slab.

The second problem of SOLBOX-07 involved a modified version of the first geometry. As also shown in Figure 1b, some of the holes were further removed such that a hole-free region (cavity) was formed at the center of the slab. The excitation and other parameters (e.g., the frequency) were the same. In this case, it was required to investigate how the cavity changed the transmission properties, and, especially, if it improved the transmission (or not).

3. Solution to Problem SOLBOX-07

3.1 Solution Summary

Solver type (e.g., noncommercial, commercial): Noncommercial research-based code developed at CEMMETU, Ankara, Turkey.

Solution core algorithm or method: Frequency-domain Multilevel Fast Multipole Algorithm (MLFMA).

Programming language or environment (if applicable): *MATLAB + MEX*

Computer properties and resources used: 2.5 GHz Intel Xeon E5-2680v3 processors (using single core)

Total time required to produce the results shown (categories: $< 1 \text{ sec}$, $< 10 \text{ sec}$, $< 1 \text{ min}$, $< 10 \text{ min}$, $< 1 \text{ hour}$, $< 10 \text{ hours}$, $< 1 \text{ day}$, $< 10 \text{ days}$, $> 10 \text{ days}$): $< 10 \text{ hours}$ (per problem)

3.2 Short Description of the Numerical Solutions

Both of the two problems in SOLBOX-07 were solved by using an in-house implementation of the MLFMA in the frequency domain [13, 14]. The problems were formulated

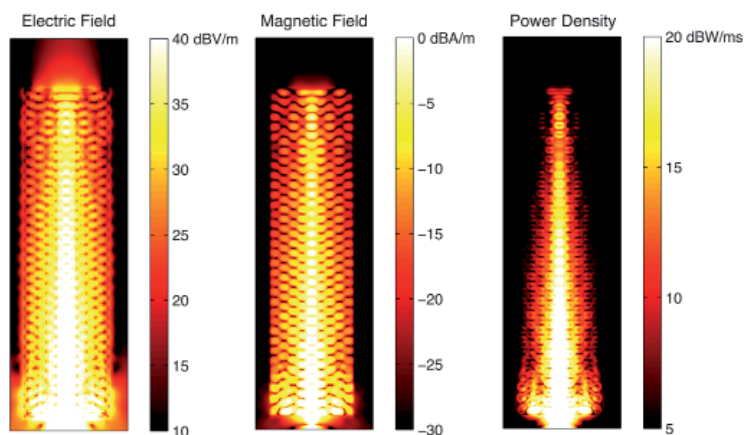


Figure 2. The electric-field intensity, magnetic-field intensity, and power density obtained for the first structure (waveguide) of SOLBOX-07 when it was excited at 200 THz.

with the electric-magnetic current combined-field integral equation (JMCFIE) [15, 16], which was discretized with the Rao-Wilton-Glisson (RWG) functions [17] for numerical solutions. The surfaces were discretized by using small triangles with respect to the wavelength (wavelength/20). Discretizations of the first problem (waveguide) and the second problem (waveguide with cavity) led to matrix equations involving 174,606 and 156,222 unknowns, respectively. The excitation was selected as a Hertzian dipole with unit dipole moment. The problems were solved by using a two-layer iterative mechanism, where FGMRES and GMRES were used in an inner-outer scheme [18]. The required matrix-vector multiplications were performed by using a six-level MLFMA. The maximum relative errors in both near-zone and far-zone interactions were set to 1%. The residual error for the iterative convergence was set to 0.0001. The number of iterations for each solution was around 120. Once the current coefficients were found, they were used to compute the near-zone fields inside and outside the structures.

3.3 Results

Figures 2 and 3 present the results of simulations of two photonic crystal structures excited at 200 THz. In each

case, the electric-field intensity (dBV/m), the magnetic-field intensity (dB A/m), and the power density (dBW/ms) were plotted inside and outside the structure. We noted that the holes were not directly visible, since the fields were also computed inside the holes. For the visualization, the dynamic ranges were selected as 30 dB for the intensities, and 15 dB for the power density.

In the first case (Figure 2), it could be observed that the electromagnetic energy was carried along the path at the center of the photonic crystal. Nevertheless, the intensity and density values tended to decrease from the bottom (source side) to top (transmission side), despite the fact that the dielectric was modeled as lossless. This seemed to be due to the reflections at the air/dielectric and dielectric/air interfaces, which may be improved if matching mechanisms were to be used.

In the second case (Figure 3), large intensity and density values were observed in the hole-free cavity. Specifically, the cavity acted like a mid-point collector, which improved the overall transmission in comparison to the no-cavity case. This was evident when both intensity and density plots in Figures 2 and 3 were compared to each other.

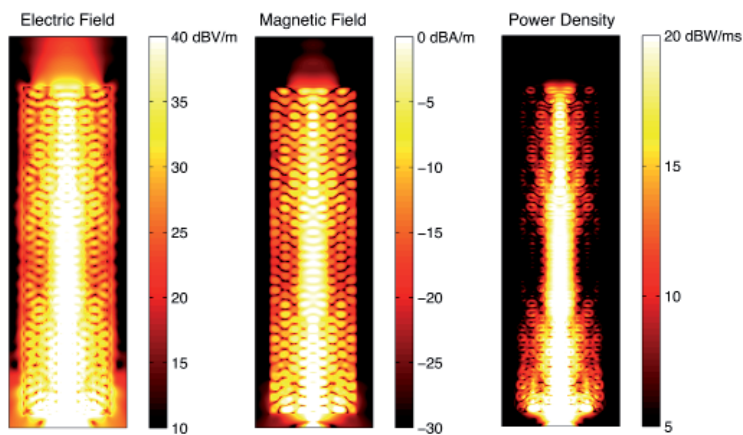


Figure 3. The electric-field intensity, magnetic-field intensity, and power density obtained for the second structure (waveguide with cavity) of SOLBOX-07 when it was excited at 200 THz.

4. References

1. J. D. Joannopoulos, S. G. Johnson, J. N. Winn, and R. D. Meade, *Photonic Crystals, Molding the Flow of Light*, Princeton, NJ, Princeton University Press, 2008.
2. T. Ding, K. Song, K. Clays, C.-H. Tung, "Fabrication of 3D Photonic Crystals of Ellipsoids: Convective Self-Assembly in Magnetic Field," *Adv. Mat.*, **21**, February 2009, pp. 1936-1940.
3. D. Pissort, E. Michielssen, D. V. Ginste, and F. Olyslager, "Fast-Multipole Analysis of Electromagnetic Scattering by Photonic Crystal Slabs," *J. Lightwave Technol.*, **25**, 9, September 2007, pp. 2847-2863.
4. D. Gagnon, J. Dumont, and L. J. Dube, "Beam Shaping Using Genetically Optimized Two-Dimensional Photonic Crystals," *J. Opt. Soc. Am. A*, **29**, 12, December 2012, pp. 2673-2677.
5. R. Stoffer, H. J. W. M. Hoekstra, R. M. De Ridder, E. Van Groesen, and F. P. H. Van Beck Um, "Numerical Studies of 2-D Photonic Crystals: Waveguides, Coupling Between Waveguides and Filters," *Opt. Quantum Electron.*, **32**, August 2000, pp. 947-961.
6. S. Venakides, M. A. Haider, and V. Papanicolaou, "Boundary Integral Calculations of Two-Dimensional Electromagnetic Scattering by Photonic Crystal Fabry-Perot Structures," *J. Appl. Math.*, **60**, 5, May 2000, pp. 1686-1706.
7. T.-L. Wu, J.-S. Chiang, and C.-H. Chao, "A Novel Approach for Calculating the Dispersions of Photonic Crystal Fibers," *IEEE Photon. Technol. Lett.*, **16**, 6, June 2004, pp. 1492-1494.
8. S. Boscolo and M. Midrio, "Three-Dimensional Multiple-Scattering Technique for the Analysis of Photonic-Crystal Slabs," *J. Lightwave Technol.*, **22**, 12, December 2004, pp. 2778-2786.
9. W. Kuang, W. J. Kim, and J. D. O'Brien, "Finite-Difference Time Domain Method for Nonorthogonal Unit-Cell Two-Dimensional Photonic Crystals," *J. Lightwave Technol.*, **25**, 9, September 2007, pp. 2612-2617.
10. J. Yuan, Y. Y. Lu, and X. Antoine, "Modeling Photonic Crystals by Boundary Integral Equations and Dirichlet-to-Neumann Maps," *J. Comput. Phys.*, **227**, 9, April 2008, pp. 4617-4629.
11. Ö. Ergül, T. Malas, and L. Gürel, "Analysis of Dielectric Photonic-Crystal Problems with MLFMA and Schur-Complement Preconditioners," *J. Lightwave Technol.*, **29**, 6, March 2011, pp. 888-897.
12. H. Kettunen, J. Qi, H. Wallen, and A. Sihvola, "Homogenization of Thin Dielectric Composite Slabs: Techniques and Limitations," *ACES J.*, **26**, 3, March 2011, pp. 179-187.
13. Ö. Ergül, "Solutions of Large-Scale Electromagnetics Problems Involving Dielectric Objects with the Parallel Multilevel Fast Multipole Algorithm," *J. Opt. Soc. Am. A.*, **28**, 11, November 2011, pp. 2261-2268.
14. A. Çekinmez, B. Karaosmanoğlu, and Ö. Ergül, "Integral-Equation Formulations of Plasmonic Problems in the Visible Spectrum and Beyond," in M. Reyhanoglu (ed.), *Dynamical Systems – Analytical and Computational Techniques*, Rijeka, Croatia, InTech, 2017, pp. 191-214.
15. P. Yla-Oijala and M. Taskinen, "Application of Combined Field Integral Equation for Electromagnetic Scattering by Dielectric and Composite Objects," *IEEE Trans. Antennas Propagat.*, **53**, 3, March 2005, pp. 1168-1173.
16. Ö. Ergül and L. Gürel, "Comparison of Integral-Equation Formulations for the Fast and Accurate Solution of Scattering Problems Involving Dielectric Objects with the Multilevel Fast Multipole Algorithm," *IEEE Trans. Antennas Propagat.*, **57**, 1, January 2009, pp. 176-187.
17. S. M. Rao, D. R. Wilton, and A. W. Glisson, "Electromagnetic Scattering by Surfaces of Arbitrary Shape," *IEEE Trans. Antennas Propagat.*, **AP-30**, 3, May 1982, pp. 409-418.
18. Ö. Ergül, T. Malas, and L. Gürel, "Solutions of Large-Scale Electromagnetics Problems Using an Iterative Inner-Outer Scheme with Ordinary and Approximate Multilevel Fast Multipole Algorithms," *Prog. Electromagn. Res.*, **106**, 2010, pp. 203-223.



Stefan J. Wijnholds

Netherlands Institute for Radio Astronomy
Oude Hoogeveensedijk 4
7991 PD Dwingeloo, The Netherlands
E-mail: wijnholds@astron.nl

Introduction by the Associate Editor

Presentations at conferences play an essential role in the dissemination of new ideas, and are often triggers for fruitful discussions between scientists. However, giving an effective oral presentation is not easy. We can probably all remember how we felt when we stepped on the stage in front of a room full of people for the first time. Even the early-career researchers reading this column have likely already seen some of the good, the bad, and the ugly of delivering a scientific presentation. A contribution from a

seasoned presenter was therefore high on the wish-list for this column. I am very grateful to Chat Hull for his very nice and lively contribution on this subject. Chat covers many aspects of preparing for and giving a scientific presentation for a range of audiences. Some of these aspects even have value for experienced academics, so I encourage everyone to take a look.

This contribution is an excellent example of an experienced researcher providing tips and tricks on a particular aspect of the trade of academic research. If you have a suggestion for another aspect that you would like to see discussed in this column, please let me know.

How to Give a Great Talk

Chat Hull

National Astronomical Observatory of Japan
Joint ALMA Observatory
E-mail: chat.hull@nao.ac.jp

The art of the scientific presentation – much like the art of the perfect plot, the art of the compelling proposal, and the art of the killer job application – is generally not something we’re taught in school. In classic Millennial style, one of the first things I did when I was asked to write this piece was therefore to ask Google, “how to give a scientific presentation,” to see what the Internet had to say. I’ve attempted to avoid boring you with laundry lists of “do’s” and “don’ts,” as many of the top Google hits did [1]. However, I have incorporated a wide range of tips – and some interesting vignettes – both from the online hive mind, and from my approximately eight years of regularly giving astronomy and radio-science presentations.

1. Practice and Timing

We all know the adage that 10,000 hours of practice makes you an expert. While 10,000 hours of rehearsal for a single colloquium is probably overkill, a few hours go a long way. In short, *practice is critical!* I’ve gotten pretty good at giving talks after nearly a decade of giving over 100 presentations, but some people are still surprised to hear that before every presentation I give, I practice at least once, if not two or three times, depending on the importance (i.e., job interview versus 15-minute lunch seminar) and the amount of new material I’m covering.

Practice is a magical thing: it makes you more familiar with your own material; it gives you a chance to explain concepts out loud instead of in a questionably formatted LaTeX document; it allows you to smooth out the flow and arc of your story telling; and it allows you to calibrate your timing. Speaking of that, in this era of infinite distraction and limited attention span, this is arguably one of the most important pieces of advice I can give: *don't exceed your allotted time!*

For conference talks (e.g., 12 minutes plus three minutes for questions), I plan to stop right at 12 minutes (much to the delight of the session chair), since audiences tend not to ask questions until the end. However, for a 60-minute colloquium, I'm much more generous, usually planning only about 40 minutes of material without questions. (Note that I don't abide by the one-slide-per-minute rule, partially because many of my animations, zoom-ins, and overlays tend to be composed of series of slides.) It's a win-win: if the audience peppers you with questions, you have plenty of time to answer all of them, and still end within the 60 minutes. If the audience is full of question-less zombies, then you end 15 minutes early: nothing wrong with that!

All of us have secretly cringed when the opposite happens: the speaker plans unwisely for 60 minutes of material, but after fielding a few on-the-fly questions, is on track to go 10 minutes over. Toward the end, if the chair is overly permissive, the speaker simply plows forward, and the audience slowly starts to dissipate through the rear exit. However, if the chair is stricter, the outcome is arguably even worse: the speaker arrives at the conclusions – the most important section of the talk – *and completely glosses over them!* This is not wise in the ways of science. Note that even if you do go over time, you can mitigate this problem by stating your conclusions at the very beginning of the talk (and in the middle...and as many other times as possible, because people *will* periodically fall asleep!). Don't be one of those speakers who says, "I'm withholding the conclusion until the end so that you'll pay attention:" that's a recipe for disaster.

A strategic note: one way to maximize the likelihood of timing nirvana is to check in advance with your host, and to find out how interactive the audience tends to be (and, even better, who the usual question-askers are). This can help you adjust both your timing and your preparation of backup slides to address detailed questions that aren't worth covering in your talk.

Here's my general recipe for practicing talks. Once you have a decent draft up and running, go through the talk for the first time. Don't time it. As you're making your way through it, correct small text errors, slide order, animation order, and other things that interrupt your flow. Note that especially if you've added a lot of new material or are presenting work that's less familiar to you, *this first run-through will be terrible!* Don't despair. Press on: go

get a cup of coffee, and once you've recovered from feeling like you don't understand anything about the paper you just wrote, stand up and go through the presentation again. You'll be astounded by how much better it is the second time. This time, time it. If the timing is about right, then you're probably good to go. If you go way over, go back and delete some slides (or hide them, or move them to the "extra slides" section after the talk), and run through it one more time. A final note: even if you have a polished talk that you're going to give several times in quick succession, try to practice at least once within 24 hours of the talk (ideally, right before you go to bed the night before). Within a few hours of the talk, then make sure to find three minutes to sit down and click through all of your slides without speaking, just to pre-load the information into your brain.

At this point, you're totally ready: so ready that you can actually punctuate your slide transitions with words that emphasize the material you're showing. Not only will knowing your slide order make you feel more at ease, but it will impress the audience. When I'm watching a speaker who obviously doesn't know which slide is coming up, I tend to tune out, because it's obvious that they didn't care enough to prepare. It's just like being a journal referee and getting a draft full of typos that a spellchecker could have caught. Don't waste the audience's time.

Under some circumstances – such as faculty interviews – it pays to actually memorize your slide numbers (or to at least have a note card on hand with the few most important slide numbers). In both *PowerPoint* and *Keynote*, you can type a number and then hit Enter, and it will take you right to that slide. The new MacBook Pro's tiny "Touch Bar" makes this even easier. All of these tips will save you from the inglorious few seconds of revealing your desktop – or worse, clicking through 85 animations – while you search for a particular slide.

2. Knowing Your Audience and Tweaking Your Delivery

I did a grand job-talk tour when I was applying for my first postdoc, and before I arrived at each institution I scanned the faculty page to see who was interested in star formation. Most of them I would e-mail in advance: *especially* if they were known for having a penchant for shredding speakers whose ideas conflicted with their own personal views of the field. This has worked wonders for me any number of times: at one point during my tour, I invited a particularly notorious professor to my talk, at the end of which that person merely asked me one or two productive, positively-spun questions. My host was astounded, not only because the professor made a rare appearance at a seminar, but because that person also seemed to have a genuinely positive reaction to my work. Another less-involved version of this tip is the following: before you give a talk (and *especially* before a job interview), look over a few of the most important publications from each faculty

member who is likely to be interested in your work, and then weave in appropriate verbal (or even written) citations to the work in your talk. Never underestimate the power of showing people that their work, presence, experience, and professional opinions are appreciated.

In addition to that, never underestimate the power of telling people things they already know (science is hard: it's good to feel smart every now and then!). I was recently invited to give a colloquium, and the invitation specifically stated:

We encourage you to present a general colloquium with ample introduction to the topic, rather than a specialized talk that would appeal only to experts. Don't underestimate the pleasure physicists and astronomers take in hearing about subjects that are already familiar to them.

People have varying opinions about the ideal breakdown of a talk in terms of expertise level, but I generally try to adhere to the rule of thirds: the first third of the talk should be extremely general (in my case, "stars form out of blobs of dust and gas"), 100% understandable by everyone in the audience. The second 33% can be aimed at experts in star formation, but not necessarily those who work very closely with you. The last bit of the talk might then be aimed at the few people whom you've come to collaborate. In my opinion, it's best if you avoid focusing that sharply at the end, aiming instead to keep as much of the audience as possible engaged for the entire time.

As for actually *giving* your talk, the first vague piece of advice I usually give is, "be yourself!" I'm a total ham, so I make jokes. However, if you're not a ham, then don't! It's okay: crafting a presentation style consistent with your own personality is far easier than forcing yourself to be someone you're not.

However, in that vein, one area where I truly believe many scientists *should* sometimes deviate from their own typical behavior is their appearance: *dress up!* Show the audience that you care! I admit that I was educated for ten years in the state of Virginia, where I wore a coat and tie at least once a week (and a suit or a tux at least once every couple of months). However, I believe that even if you're a wrinkly-T-shirt-and-shorts kind of person, as many scientists are, that doesn't mean that you have to look wrinkly for your talk. Much as knowing your slide transitions shows that you care about the audience's time, wearing decent clothes (even just an ironed shirt and pants/skirt with a pair of non-sneaker shoes) shows that you respect them enough to professionalize your appearance for the hour that they're dedicating to your presentation.

Regarding presentation style, there is an art to striking the right tone. The first presentation I gave in graduate school was in the much-feared Journal Club seminar, where you have to go through the somewhat unnatural process of

presenting a summary of a recently published paper as if you had written it yourself. As a first-year graduate student who didn't even know what an early-type galaxy was, this was quite difficult. After I finished my presentation, the faculty member in charge of Journal Club came up to me and said, "you have to stop saying, 'I don't know!'" That feedback has stuck with me, and forever changed how I set the tone of my talks. I think the faculty member was wrong to tell me that in such a general way. However, there is some truth to the sentiment, because we as scientists need to strike the right balance between being totally unsure of our work, and being so confident that we dismiss constructive comments from our colleagues. My way of dealing with this is generally to request questions before (and sometimes during) the talk, so that as the talk progresses the audience gets comfortable bantering with me about the material. Even more importantly, I truly believe it is appropriate to admit ignorance under the right circumstances. Adding, "I don't know" or "that's a great avenue to pursue, let's talk afterward" to a thoughtful but inconclusive response to a question is a good way to show that you know what you're talking about, but you don't know everything, and you're willing to consider (and you appreciate) the intelligent ideas of your fellow scientists.

A few other things I focus on stray into the realm of oratory technique. First, look people in the eye when you speak: it engages them, and makes it less likely that you'll stand with your back to the audience reading the slides. Second: *slow down*. One of my favorite parts of astronomy is its global nature: we come from everywhere, and as a result, a vast number of astronomers speak English as a second (or third, fourth, fifth) language. It thus pays to speak slowly. Furthermore, while fancy vocabulary can be fun, it should be used sparingly so that as many readers and listeners as possible can understand our work. In addition to speaking slowly, a well-placed pause can be a nice reprieve for the audience after several dense slides. Occasional silence is okay: it gives people a few moments to absorb what you just said (or the plot that you have strategically left up on the projector), and it gives you a second to take a drink of water!

3. Crafting a Great Presentation

We now come to the technical details of how to make an excellent presentation. In some regards, this is the area where opinion matters least (in my opinion[!]), because there are cognitive research studies showing that certain color schemes and slide layouts are objectively better than others. There is no shortage of advice out there. I recommend that you peruse it at your leisure, from Edward Tufte's books on data visualization, to Web sites such as Presentation Zen [2], to presentation style recommendations from the creators of *PowerPoint*, themselves [3].

I personally subscribe to the "less is more" philosophy, and use as little text as possible (approaching, if not quite

achieving, a terse “Lessig-style” presentation [4], with only a few words per slide). A sage colleague of mine once said, “pixels are finite; slides are infinite.” In short: make your images HUGE, annotating them with just the little bit of text you need to make them understandable. That way, the audience will listen more closely to your interpretation of the plot (which they’ll be able to see, because it’s so huge), and you won’t be tempted to stare at the screen and repeat the words on the slide (which the audience will have finished reading long before you’ve finished saying them).

4. Avoiding Technical Problems

It is well known that multivariate calculus is far easier for most scientists than using an overhead projector. Invariably, this leads to a substantial amount of lost time at every conference, and at a non-negligible fraction of colloquia and seminars. While it is impossible to prepare for all technical glitches, there are a few things you can do that will help you avoid a complete technological meltdown, and that will make your presentation flow much more smoothly.

The first thing to do is to figure out what the projection situation will be during your presentation. If you’re presenting at a conference, the Web site will usually have instructions regarding whether transferring your presentation file is necessary, and what sort of laptops (e.g., Mac, PC) and programs (e.g., *Keynote*, *PowerPoint*) will be available. If you can’t easily locate this information (or if you’re giving an informal lunch talk somewhere), then you should send an e-mail to inquire well in advance so you can prepare. In most cases, if you have an up-to-date version of *Keynote* or *PowerPoint*, all will be well, especially if you can use your own laptop. When I used *PowerPoint* on my MacBook Pro, I virtually never had any issues. The only issue I’ve had since switching to *Keynote* about a year ago was one instance where I was required to present using *PowerPoint* on a conference-supplied machine, and the conversion from *Keynote* to *PowerPoint* mangled some of the fonts I was using. A way around that is to use extremely basic fonts; however, in my experience it’s very rare to be forced to convert your presentation file. Note that my generally-problem-free experience has been enabled by being a stereotypical scientist who uses an expensive MacBook with expensive Microsoft and Apple software. Users of *Linux* machines and software such as *OpenOffice* should proceed at their own risk, but should also know that their pursuit of excellence with different software and machinery is appreciated by the open-access community!

My first order of business on the day of my presentation is to load my laptop bag full of all of the possible laptop accoutrements I might need, including all possible VGA, DVI, and HDMI dongles; a USB stick for transferring talk files; and my own clicker/laser pointer (I recommend the Logitech Wireless Presenter with a *green laser pointer*: see below for a discussion of laser color). Having multiple dongles can solve projector issues (e.g., if for some reason

the projector works with a VGA connection but not with HDMI), and also solves the problem created by Apple’s constant modification of their laptop ports (and the fact that, for example, some older MacBook Air models have no HDMI port, whereas the same generation of MacBook Pros do). For talk flow, I find that having my own pointer/clicker is critical, mainly because I know where all the buttons are, so I can easily use the laser pointer and click through my slides without accidentally blanking the screen or mashing a button that causes my presentation to mysteriously skip forward by 13 slides.

Another good thing to do before plugging in the projector is to turn off your wireless connection, quit other running programs, and disable all desktop notifications. This will help avoid both annoyance (when your computer repeatedly complains about not being able to connect to the guest wireless network) and embarrassment (when your calendar automatically reminds you about your upcoming dentist appointment...or perhaps something less benign).

When the moment of truth comes and you plug in the screen, 80% of the time it will work. For the other 20%, it really, really pays to know how your laptop works (easier said than done, I know): again, practice, practice, practice! Over the years, I’ve gotten very good at manipulating the Display preferences under “System Preferences” on my Mac, tweaking everything from display mirroring to output resolution to the physical scaling of the image so that the bottom of my slide doesn’t get cut off. Know your machine.

Finally, if all hell truly breaks loose, you can always resort to exporting your presentation to a PDF and presenting it on someone else’s computer (remember your handy USB stick!). Just remember to avoid overlapping animations: by splitting progressive animations into multiple slides you’ll be able to simulate the animation even in PDF mode, and you won’t confuse audiences with a single slide featuring 14 randomly overlapping plots that faded in and out in your original *PowerPoint* file. Of course, in a PDF you won’t be able to show movies or have your text fly in dramatically from overhead, but you’ll still be able to transmit the crux of your scientific story, which is all that matters.

5. A Few More Suggestions

I will now indulge myself, and outline a few remaining items on my wish list for great talks:

- Equations: don’t show them. Maybe $\theta \sim \lambda/D$ is okay, but nothing more complicated. This is just my seasoned observer’s opinion.
- Citations: cite everything, every image, plot, photo, etc. Many of your talk files will end up on the Internet: the more attribution, the better.
- Animations: use them to your advantage, and use them to guide the eye. If you must use substantial amounts of text (e.g., in the conclusion slide – which, by the

way, should still feature representative plots as visual summaries!), then animate each bullet independently, so that the audience doesn't get distracted by the rest of the text.

- Be colorblind friendly: this is my personal soapbox, as I suffer from mild colorblindness, along with ~10% of the white male population. First, use a green laser pointer. Red laser pointers are invisible (although I admit that it's better to use green lasers that have very low wattage, as the normal stargazing pointers can be exceptionally bright and distracting). Second, when you make plots, use bright colors: red and black dots are indistinguishable, for example. However, if you must use similar colors, use different symbol styles (e.g., red triangles and black squares). Third, use highly contrasting text with respect to your slides' background color. Red on black = bad. Blue on black = bad. Yellow on white = super-bad. I don't know how many times I've seen people try to highlight the critical word in a sentence in red, which was thus rendered unreadable on the black background! When in doubt, consult the outstanding Colorbrewer Web site [5], which brews up the perfect, colorblind-safe color combinations for your plots, complete with hex codes!

Finally, regarding plot complexity, when it comes to showing plots in a talk (versus in a paper), I abide by the KISS method ("Keep it simple, stupid!"). Don't dwell on technicalities. If a detail of a plot is likely to be distracting or is irrelevant, either cover it up, crop it out, or make a new plot for your talk. Axis labels on plots copied from papers are also almost always too small: crop the original axes and replace them with HUGE text, with something intuitive like "Brightness," as opposed to, say, $\text{erg/s/cm}^2/\text{Hz}$.

Note that the above advice is relevant mainly for the default presentation style today, in the late 2010s: *Keynote* or *PowerPoint* slides on a big projector. However, of course, many other presentation styles exist: shared screens on video-cons and *Skype* interviews; chalk talks; posters at conferences; etc. For example, when you're giving an online interview, you'll want to make sure to build in time for the interviewers to flip through your slides, and you'll want to practice saying, "next slide...next slide..." and, "on the bottom of slide 13 you see..."

6. A Few Final Words

That, my fellow scientists, is my current understanding of how to give a great talk. I hope the above stories and tips form a coherent picture of how to craft understandable slides, practice effectively, learn the ins and outs of your audience, avoid technological catastrophe, and execute your talk on time and in an engaging manner. At some level, nearly all of this is subjective, and the breakneck pace of technological development means that we'll all need to revisit this topic regularly throughout our careers. However, for now, onward and upward, practice-practice-practice, and break a leg!

7. References

1. An example of a Google search result that, while very list-like, includes a wealth of good tidbits: biostat.wisc.edu/~kbroman/talks/giving_talks.pdf.
2. Presentation Zen by Garr Reynolds, presentationzen.com.
3. Advice on PowerPoint presentation styles, tinyurl.com/PPTPresentationStyles.
4. The "Lessig Method" of presentation, presentationzen.blogspot.com/presentationzen/2005/10/the_lessig_method.html.
5. Colorbrewer advice on color combinations, colorbrewer2.org.

[Editor's note: For radio scientists from some URSI Commissions, equations are an integral part of the language of their science. The most common problem they encounter in making presentations at conferences is an incompatibility between fonts used in their presentations and fonts available on the computer used for presentations at the conference. For suggestions on methods to avoid such problems, see the section on "How to Avoid Font Problems When Presenting Papers" in the column openly available at <http://ieeexplore.ieee.org/document/7533585/> or <http://ieeexplore.ieee.org/stamp/stamp.jsp?tp=&arnumber=7533585>.]

Introducing the Author

Chat Hull has been giving scientific presentations of various sorts since his days as an undergraduate at the University of Virginia; later, as a summer research student at the University of Rochester; a high school professor in both Virginia and Guatemala; an astronomy graduate student at the University of California, Berkeley; and a Jansky Fellow of the National Radio Astronomy Observatory, based at the Harvard-Smithsonian Center for Astrophysics. He is currently working for the National Astronomical Observatory of Japan as an NAOJ Fellow, based at the ALMA observatory in Santiago de Chile.





Asta Pellinen-Wannberg
Umeå University, Department of Physics and
Swedish Institute of Space Physics
S-90187 Umeå, Sweden
Tel: +46 90 786 7492
E-mail: asta.pellinen-wannberg@umu.se

Introduction by the Associate Editor

In February, I was invited by the Research Organization of Information and Systems (ROIS) Female Research Development Office to spend some time in Japan. The Japanese government has gotten interested in promoting gender equality in science through its research organizations. For example, one of the purposes of my visit was to tell how Sweden is striving towards gender balance in academia.

I had opportunities to discuss gender issues with Prof. Genshiro Kitagawa, at that time the President of the Inter-University Research Institute Corporation, ROIS, as well as with the incoming President, Prof. Ryoichi Fujii, whom I have known since long ago, when we both were members of the EISCAT Council. I also met the ROIS Female Research Development Office leader, Prof. Isao Katsura, and the coordinator, Dr. Yoshiko Nakamura, who was friendly in guiding me through the offices and surroundings.

I had a chance to have discussions with female researchers at the National Institute of Polar Research (NIPR) and the National Institute of Information and Communications Technology (NICT), where I gave scientific talks. I was happy to see that the whole leadership of NIPR – the Director-General, Prof. Kazuyuki Shiraishi, as well as the three Vice Director-Generals, and Profs. Hiroyuki Enomoto, Yoshifumi Nogi, and Takuji Nakamura – were present at the seminar, “Gender Issues in Science,” and they were eager to afterwards discuss the topic. Takuji was my very good host during the whole visit, and we had many interesting discussions.

Through my meetings with female scientists, I had a possibility of recruiting some new people for my Women in Radio Science column. This time, I will present for the first time a Japanese researcher, Yuka Sato, a PhD and project researcher in the Space and Upper Atmospheric Science Group at NIPR. It was especially nice to meet Yuka, together with her (at that time) eight-month-old son, Soshi. She was still on parental leave in February, but is now back in business. Here comes her own story.



Figure 1. Dr. Yuka Sato with her son, Soshi.

Reflections on a Career in Radio Science

Yuka Sato

National Institute of Polar Research
10-3 Midoricho, Tachikawa, Tokyo 190-8518 Japan
Tel: +81-42-512-0760
E-mail: sato.yuka@nipr.ac.jp

Although I had some ambiguous interest in the origins of life and of the universe in my childhood, I naively believed that I would be a teacher for local schools because I had good familiar examples, including my father. However, a happy encounter during high school led me to make up my mind to study geophysics, and auroral physics, in particular. It was a book written by Dr. Kazuyo Sakanoi, who studied “flickering aurora,” and was one of the first Japanese women to join an Antarctic wintering team. I was deeply impressed that she accomplished her scientific mission facing a challenging environment, and moreover, she was married.

I was lucky enough to enter Tohoku University, the same university as she. In my third year of university, in 2003, I joined the Space and Terrestrial Plasma Physics Group, led by Prof. Takayuki Ono. Prof. Ono was my supervisor until my doctoral course, and I undertook analysis working on lightning radio waves using existing datasets from ground-based observations. After a while, I started thinking about engaging in the development of observational instruments, because I wanted to understand any unexplained phenomena with instruments of my own making. In my master’s course, I jumped at a heaven-sent opportunity to develop a new instrument for observing electromagnetic waves spontaneously emitted from the auroral ionosphere. Some of their generation mechanisms are still poorly understood. They are important because they not only offers a tool of great promise for the remote sensing of ionospheric plasma processes and parameters, but they also give the foundation for understanding various radiation mechanisms that arise in planetary magnetospheres and plasma in space.

I visited Iceland to install the instrument for the first time in 2005. This work involved making electronic circuits, and also unscientific, physical tasks such as digging holes for antenna poles. Although one of my seniors said that my work was nothing like what woman liked to do, it was enjoyable and worthwhile for me. The most exciting thing was to find a new observational fact after improving the instrument one year after the initial installation.

In finishing my master’s, I was divided between two choices: to be a teacher for local schools, or to continue my research. I could not imagine myself surviving in academia while my observational instrument had just begun to detect interesting phenomena. After a lot of thinking, and also with strong encouragement from my supervisor, I decided to continue for at least a year, until I could mark the end to my research with any gratifying results. However, the more research was advanced, the more interesting questions came up, which led to now.

After receiving my doctorate from Tohoku University in 2010, I continued my research on auroral radio emissions there for two years. After that, I moved to the National Institute of Polar Research as a project researcher, and I am still there. While continuing research on auroral radio emissions, I worked on the “IUGONET” project. This aims to develop new research platforms for upper atmospheric physics (<http://www.iugonet.org>).

Now I am trying a new research subject: Langmuir turbulence in the auroral ionosphere, observed by the European Incoherent SCATter (EISCAT) radar. I have hope that it gives me a deeper understanding of plasma physics in the auroral ionosphere, which leads to a new perspective on auroral radio emissions.

My first child was born last July (Figure 1). This April, I came back after about 10 months of maternity leave. It was only when I had my own child that I realized that child-raising took up much more time and power than I had imagined. When women continue and advance their research careers, it is highly important to get the understanding and cooperation from supervisors and colleagues. In addition, support from family, especially your partner, is vital. In my case, he is not a researcher, but holds a master’s degree in geophysics. We can easily share the difficulties I have, and his optimistic remark encourages me to take one step further: “Things will work out as long as you believe it.”

Although I am still struggling to survive in academia, I keep in mind what my supervisor used to tell me: Try

to find your research niche of importance and make your own unique contribution.

My former future vision to be a teacher evolved into efforts for science-outreach activities directed to the general public. I sometimes visit my alma mater, local schools, science museums, and other educational facilities to give talks or host public events. When I was a graduate student, I launched a voluntary group for promoting outreach activities, which consist of young researchers or members of a Japanese academic society. Outreach activities by young researchers in some cases are more effective than

activities by senior researchers, especially at offering a sense of affinity. I always feel that there is no big difference in response from participants between boys and girls. Problems that we face with getting girls into science may just start with a gender bias at a young age. We need all kinds of efforts to eliminate gender stereotypes in the classroom and at home that discourage girls from cultivating their seed of curiosity about science. I believe that one of the solutions is to interact with the public in various ways, which can provide specific, practical role models and motivate young people to consider and pursue careers in science.



Madhu Chandra

Microwave Engineering and Electromagnetic Theory
Technische Universität Chemnitz
Reichenhainerstrasse 70
09126 Germany
E-mail: madhu.chandra@etit.tu-chemnitz.de

Welcome to this new column on education. In some capacity or other, all radio scientists are in many ways perpetual learners and teachers. Thanks to the interdisciplinary nature of radio science (which makes it so exciting), and the fast evolving developments in this colorful field, keeping abreast with evolving frontiers of knowledge is not only a challenge, but also a requirement.

Allow me to win your interest for this column on radio science education and to introduce myself. I will, with the help of your feedback and contributions, keep us involved in tracking down current developments in:

- Emerging educational topics in radio science
- Open-source educational tools and knowledge resource, particularly for early stage radio scientists
- Educational opportunities, especially those accompanying URSI conferences and events
- New educational trends in radio science
- Modern educational methods, e.g., the flipped classroom

In a lighter vein, I should also like to provide you with some “intellectual entertainment” under the heading of “Brain Teasers.” In this part of the column, we shall demystify selected radio-science topics using the language of electromagnetic fundamentals.

Clearly, a forum with such a broad spectrum of interests must remain open to all areas of all URSI Commissions! However, the common binding factor always is radio science, itself.

With your participation and contributions, I will maintain this column. We will be glad to hear from you and know about topics and features you think this column should address. My contact coordinates are given above.

In all communications, please mention “Radio Science Education Column” in the subject field of your e-mail.

Before signing off for this time, I will leave you with a simple “back-to-the fundamentals brain teaser” from the colorful field of radio science:

Brain Teaser 1:

1. What is the exact and complete statement of the units of radar backscatter cross section?
2. Talking about dual-polar antennas: in your opinion, what is the difference between co-to-cross-polar isolation (XPI) and co-to-cross-polar discrimination?

Your responses are most welcome. Responses with educational contents will be reported in this column. Naturally, my own answers will be given in the next issue of this column.

You are heartily invited to stay tuned to this column and I also look forward to hearing from you.

Introducing the Associate Editor for the Education Column

Prof. **Madhu Chandra** studied Mathematics and Physics at the universities of Cambridge, London, and Salford, obtaining BSc and PhD degrees from the Universities of London and Salford, respectively, in 1978 and 1981. He joined the academic staff of the Department of Electrical Engineering at the University of Bradford (UK) in 1980. Ever since then, he has been since actively involved in the areas of multi-parameter radars, wave propagation, and remote sensing. In 1984, he joined the DLR (German Aerospace Research Centre) as a research scientist at the Institute of High Frequency Physics and Radar Technology. In 1986, Prof. Chandra was awarded the international best paper award by the IEE for his contribution

in the field of wave propagation in polarimetric-Doppler radar applications. He was also the recipient of the URSI International Young Scientist Award in recognition of his contributions in the field of propagation and weather-radars. During 1990-2002, he was the leader of the DLR group on radar scattering physics and wave propagation. He also represented Germany in the working groups for radar in COST-210 and COST-75 actions on radar remote sensing, sponsored by the European Union. He is one of the designers of the versatile fully polarimetric C-band weather radar of DLR. He developed computational algorithms for dealing with signal processing, propagation correction, EM scattering, and calibration of polarimetric radars.

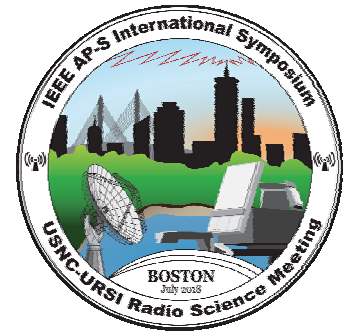
Since April 2002, Prof. Chandra has been the Chair for Microwave Engineering and Electromagnetic Theory at the faculty of Electrical Engineering and Information Technology of Chemnitz University of Technology, Germany. He has also served as the Dean of the faculty, and

is a member of the academic board for PhD studies. Prof. Chandra is the current Chair of the council of all faculties of electrical and electronic engineering of German universities, and held the chair for the accreditation committee on all areas of electrical, electronic, and information engineering.

To date he has published more than 150 papers in refereed conference proceedings and research journals in the field of multi-parameter radar remote sensing. He is the Chair of the German URSI Commission F, and the national group (of ITG Germany) on Wave Propagation. He was Chair of URSI Commission F during 2008-2011/2005-2008. Prof. Chandra is an URSI Fellow. In addition to being on the reviewer's panel for EU project applications, he has served as the principal investigator in several EU-sponsored projects in the field of radar remote sensing. Prof. Chandra grew up in Britain and his nationality is German. He is married and has two daughters.



**2018 IEEE International Symposium
on Antennas and Propagation and
USNC-URSI Radio Science Meeting
Boston, MA
July 8-14, 2018**



The 2018 IEEE AP-S Symposium on Antennas and Propagation and USNC-URSI Radio Science Meeting will be held on July 8-14, 2018, at the Westin Boston Waterfront in Boston, Massachusetts. The combined symposium and meeting are co-sponsored by the IEEE Antennas and Propagation Society (AP-S) and the U.S. National Committee (USNC) of the International Union of Radio Science (URSI). The technical sessions, workshops, and short courses will be coordinated between the two organizations to provide a comprehensive and well-balanced program. This meeting is intended to provide an international forum for the exchange of information on state-of-the-art research in antennas, propagation, electromagnetic engineering, and radio science. The paper submission deadline is **January 15, 2018**.

The symposium Web site, www.2018apsursi.org has instructions for the preparation and submission of papers, the details for the Student Paper Competition and Student Design Contest, as well as the full Call for Papers. Information for potential exhibitors, special session proposals, and the contact person for those wishing to organize a short course or workshop are also included in the Call for Papers.

Questions should be directed to:

Steven Best – Chair
E-mail: Steve.Best@comcast.net

Mike Shields – co-Chair
E-mail: shields@LL.mit.edu

Alan Fenn – TPC Chair
E-mail: AJF@LL.mit.edu

www.2018apsursi.org

D. V. Giri Receives Indian Awards

Dr. D. V. Giri, Chair of URSI Commission E for 2014-2017, received the Hind Rattan award (Figure 1) and the Non-Resident Person of Indian Origin (NRI) of the Year award (Figure 2) during the 36th International Congress of NRIs in New Delhi, held during the January 2017 Indian Republic Day celebrations. The Hind Rattan award is one of the highest awards given by the NRI Welfare Society of India. The award ceremony was attended by senior members of the government of India and of the Supreme Court of India.



Figure 2. The NRI of the Year award.



Figure 1. Dr. D. V. Giri holding the Hind Rattan award.

Clerk Maxwell Foundation Newsletter

The *James Clerk Maxwell Newsletter* is published by the James Clerk Maxwell Foundation. The latest issue is available on the foundation's Web site at http://www.clerkmaxwellfoundation.org/Newsletter_2017_Spring.pdf. It contains an article by Hugh Griffiths on "Some Reflections on the History of Radar from its Invention up to the Second World War."



2018, 35th National Radio Science Conference (NRSC2018)

March 27 - 29, 2018

Misr International University (MIU), Cairo, Egypt

<http://nrsc2018.miu.egypt.edu.eg>

Call for Papers

The National Radio Science Committee (NRSC) of the Academy of Scientific Research and Technology (ASRT) and Misr International University (MIU) are organizing the 35th National Radio Science Conference from the 27th to 29th of March 2018. The conference program will consist of invited sessions on selected topics, tutorials, and contributed sessions. The submitted papers must describe original work and be within the scope of International Union of Radio Science (URSI) commissions A-K, namely:

- A. Electromagnetic metrology
- B. Fields and waves
- C. Wireless communication systems and signal processing
- D. Electronics environment and photonics
- E. Electromagnetic noise and interference
- F. Wave propagation and remote sensing
- G. Ionospheric radio and propagation
- H. Waves in plasmas
- J. Radio astronomy
- K. Electromagnetics in biology and medicine

Review papers describing new trends and state of the art of some of the URSI activities are welcome. Accepted papers will be published in the conference proceedings conditionally upon presentation of the paper at conference venue. Presented papers will be considered for inclusion in IEEE Xplore. A special student session will host a limited number of posters presenting B.Sc. graduation Projects, without registration fees. Best papers and best student papers will be selected by the organizing committee for awards.

Submission Instructions

Prospective authors of papers describing original work are invited to get the standard format and to submit papers electronically through the conference website. The maximum number of pages is 8 per paper.

Important Dates

Paper submission deadline: **November 19, 2017**

Notification of acceptance: **January 14, 2018**

Camera-ready manuscript: **February 11, 2018**

Registration Fees (per paper)

From Egypt, LE750, from outside Egypt; €400. Fees cover attending sessions, proceedings, lunches, and coffee breaks for the period of the conference for one of the authors. Nonrefundable fees, LE300 (from outside Egypt, €200), are paid with paper submission. The remaining registration fees are paid with the camera ready submission. Extra pages will be charged LE100 (from outside Egypt, €50) per page with maximum of two.

Organizers and Technical Sponsors

Academy of Scientific Research and Technology (ASRT)

International Union of Radio Science (URSI)

IEEE - Egypt section

Misr International University (MIU)

NRSC2018 Organizing Committees

Conference Chair: Prof. Said El-Khamy, Alexandria Univ.

Conference Honorary Chair: Prof. Mohamed El Komy, MIU

Conference Co-Chair: Prof. Hassan El Ghitani, MIU

Conference Vice-Chair: Prof. El-Sayed Saad, Helwan Univ.

Conference Secretary General: Prof. Hesham El-Badawy, NTI

Conference Publications Chair: Assoc. Prof. Alemam Ragab, MIU

Local Organization Chair: Prof. Fawzy Ibrahim, MIU

NRSC Committee

Prof. Hamdy Al-Mikati, Mansoura Univ.

Prof. Hadia El Hennawy, Ain Shams Univ.

Prof. Mahmoud El-Hadidi, Cairo Univ.

Prof. Magdy El-Soudani, Cairo Univ.

Prof. Diah Khalil, Ain Shams Univ.

Prof. Saber Zainud-Deen, Menoufia Univ.

Prof. Khaled Shehata, AAST

Prof. Ahmed Attiya, ERI

Prof. Imbaby I. Mahmoud, AEA

Prof. Rowayda Sadek, Helwan Univ.

Dr. Hanaa Shaker, Zagazig Univ.

Dr. Ahmed El-Trass, Alexandria Univ.

Dr. Osama Marzouk, ASRT

Mr. Emad Emam, ASRT

Local Committee

Prof. Ayman Bahaa-Eldin

Dr. Nabil Hamdy

Dr. Ayman Nabil

Dr. Lamiaa Khashan

Dr. Mohamed Assad

Eng. Mehaseb Ahmed

Eng. Mostafa Rabie

Eng. Omar Morsy



3rd Indian URSI Regional Conference on Radio Science

A high-power 53 MHz mesosphere-stratosphere-troposphere (MST) radar was established in 1992 as a national facility for atmospheric research at the [National Atmospheric Research Laboratory \(NARL\)](#), Department of Space, Government of India Gadanki. The MST radar is a state-of-the-art instrument, capable of providing estimates of atmospheric parameters with very high resolution on a continuous basis. As part of the silver jubilee of the establishment of the MST Radar, NARL organized the third Regional Conference on Radio Science 2017 (URSI-RCRS 2017) during March 1-4, 2017, at Tirupati, jointly with the Indian Committee for URSI (INCURSI) under the Indian National Science Academy (INSA). Technical co-sponsorship was provided by the Institution of Electronics and Telecommunication Engineers (IETE), New Delhi, and the Hyderabad Section of the Institute of Electronic and Electrical Engineers (IEEE).

INCURSI started this series of conferences to encourage and promote radio-science research, as well as interdisciplinary interaction among researchers from the sub-fields of radio science, in the region encompassing Africa and South Asia, at a periodicity of about eighteen months. The first conference was organized in January 2014 at Symbiosis University, Pune. The second conference was held in November 2015 at Jawaharlal Nehru University, New Delhi. Over the years, the number of delegates has increased. The present conference had more than 280 registered participants.

The third URSI-RCRS was inaugurated by Dr. A. S. Kiran Kumar, Chair of the Indian Space Research



Figure 2. (l-r) Prof. Kazuya Kobayashi, Prof. S. Ananthkrishnan, Dr. A. S. Kiran Kumar, Prof. A. Jayaraman, Dr. T. V. Chandrasekhar Sarma, releasing the silver jubilee video of NARL.

Organisation (ISRO), on March 1, 2017, at Tirupati (Figures 1 and 2). He elaborated on the emerging opportunities in semiconductors, remote sensing, frontline propulsion systems, nano and micro satellites. He gave a call to the serious researchers, young scientists, and students to take up the challenging problems in these emerging areas, and reiterated the strong support and commitment of ISRO to the advancement of radio science. There were four general lectures, by Prof. Toshitaka Tsuda, Kyoto University, Japan (Figure 3); Dr. Gaetano Mileti, University of Neuchatel, Switzerland (Figure 4); Dr. Rajeev Jyoti, SAC, ISRO, India (Figure 5); and Prof. V. Chandrasekar, Colorado



Figure 1. (l-r) Prof. Kazuya Kobayashi, URSI Assistant Secretary (AP-RASC); Dr. A. S. Kiran Kumar, Chair ISRO; Prof. A. Jayaraman, Director NARL; Dr. T. V. Chandrasekhar Sarma, Convener URSI RCRS 2017. Prof. S. Ananthkrishnan, Vice President URSI, is addressing the participants.



Figure 3. The general lecture “Study of the Coupled Solar-Earth System with Large Atmospheric Radars, Ground-Based Observation Network, and Satellite Data” by Prof. Toshitaka Tsuda, Research Institute for Sustainable Humanosphere, Kyoto University, Japan.



Figure 4. The general lecture “High Performance and Miniature Laser-Pumped Vapor-Cell Frequency Standards” by Dr. Gaetano Mileti, University of Neuchatel, Neuchatel, Switzerland.



Figure 5. The general lecture “Scatsat-1: A Globally Significant Weather and Climate Mission” by Shri Rajeev Jyoti, Space Applications Center, Indian Space Research Organisation, Ahmedabad, India.

State University, USA (Figure 6). A total of 200 papers from all ten URSI Commissions were presented during URSI-RCRS 2017. Out of these, 26 were invited talks, 79 were contributed talks, and 95 were poster presentations. The conference was well attended by INCURSI members. Figure 7 shows a section of the participants, and Figure 8 shows the poster sessions.

A special session to mark the beginning of the silver jubilee year of the Indian MST Radar was organized at the conference. Talks about the origin, design, development, installation, and utilization of the radar were presented by the engineers and scientists associated with it. A detailed exposition of the initiation of the idea of ground-based remote sensing of the Earth’s atmosphere under the Indian Middle Atmosphere Programme was provided during the conference. Intricacies and challenges of low radio-noise site selection, project design, implementation, and operational phases over the past 25 years were described by the associated senior and young scientists and engineers.

Young Scientist (YSA) and Student Paper Competition (SPC) awards are a special feature of URSI-RCRS. Young scientists under the age of 35 years and students registered as



Figure 6. The general lecture “Urban Radar Network for Disaster Mitigation: Observations and Warnings of Floods, Tornadoes, Hail and Lightning in Dallas-Fort Worth Using X-band Radar Network” by Prof. V. Chandrasekar, Colorado State University, Boulder, Colorado, USA.

PhD or MTech students with some research experience are encouraged to participate in the conference by submitting good-quality papers, and prizes are given. There were 21

Table 1. The Young Scientist Award winners.

Position	Author Name	Paper
1	Vamsi Krishna Velidi	“Development of High Performance Microwave On-Board Diplexing Network for ASTROSAT Telemetry Tracking & Command Application,” V. K. Velidi, B. Gowrish, D. Sivareddy, A. V. G. Subramanyam, V. Senthil Kumar, Chitra Ramamurthy, and V. V. Srinivasan
2	Sneha Yadav	“The Impact of the 17 March 2015 St. Patrick’s Day Storm on the Evolutionary Pattern of Equatorial Ionization Anomaly Over the Indian Longitudes Using High Resolution Spatio-Temporal TEC Maps-New Insights,” Sneha Yadav, S. Sunda, and R. Sridharan
3	V. L. Narayanan	“Optical and Radio Observations of Electrified Medium Scale Traveling Ionospheric Disturbances Observed Near the Indian Dip Equatorial Region,” V. L. Narayanan, P. P. Chaitanya, S. Gurubaran, and A. K. Patra
Honorable Mention	R. Chakraborty	“Planetary Boundary Layer Anomalies During Convective Rain,” R. Chakraborty and A. Maitra
Honorable Mention	Sujith Raman	“Microwave Based Non-Invasive Diagnosis Technique for Analyzing Skin Burn Depth,” Sujith Raman, Jacob Velandar, Fredrik Huss, and Robin Augustine



Figure 7 (a), (b). Scenes of the conference participants.

YSA entries, out of which eight were short-listed for final presentation. Five YSA prizes were awarded (first, second, third, and two honorable mentions). For the SPC, there were 25 entries, out of which 10 were short-listed for final

presentations. Five SPC prizes were awarded (first, second, third, and two honorable mentions). Their names and their paper titles are given in Tables 1 and 2.



Figure 8(a)-(f). Poster sessions were organized on March 2 and 3.

Table 2. The Student Paper Competition winners.

Position	Author Name	Paper
1	Jitendra K. Pradhan	“Wavelength Selective Dual-Band Mid-Infrared Metamaterial Absorber/Emitter,” J. K. Pradhan, S. A. Ramakrishna, V. G. Achanta, and A. K. Agrwal
2	Latheef A. Shaik	“Coplanar Waveguide Fed Tapered Slot Antenna with Multi-Functional Characteristics,” L. A. Shaik, C. Saha and J. Y. Siddiqui
3	Mugundhan V.	“Long-Baseline Interferometric Observations of Sub-Arc Minute Structures in the Solar Corona,” Mugundhan V., R. Ramesh, G. V. S. Gireesh, C. Kathiravan, I. V. Barve, P. Kharb, and A. Misra
Honorable Mention	R. Rubia	“Evolution of Electrostatic Solitary Waves in the Lunar Wake,” R. Rubia, S. V. Singh, and G. S. Lakhina
Honorable Mention	Ajay Lotekar	“Fluid Simulation of the Effects of Super Thermal Electrons on the Wave Processes in Space Plasmas,” A. Lotekar, A. Kakad, and B. Kakad

The conference sessions during the first three days were held at the Fortune Select Grand Ridge Hotel, Tirupati. The final day’s sessions were organized at NARL Gadanki, to give the participants an exposure to the experimental facilities of NARL. In the valedictory session, it was mentioned by the general chairs that the third URSI-RCRS had given a tremendous boost to radio science. It would

now serve as an excellent impetus to the forthcoming URSI Asia Pacific Radio Science Conference (AP-RASC 2019), to be held in New Delhi during March 9-15, 2019. The Commission Chairs appreciated the participation of many new young scientists, apart from distinguished scientists from India and abroad, and the excellent organization of the conference.

Report on the Egyptian 34th National Radio Science Conference (NRSC2017)

The 2017 34th National Radio Science Conference (NRSC 2017) was held in Alexandria, Egypt, March 13-16, 2017. The conference was jointly organized by the National Radio Science Committee of the Egyptian Academy of Science and Scientific Research & Technology, and the Arab Academy for Science, Technology, and Maritime Transport (AASTMT) (main campus at Abo-Qir, Alexandria, Egypt). The following are some of the NRSC2017 conference highlights.

The opening session of NRSC2017 was held in the historical conference hall of the AASTMT main branch in Abo-Qir, Alexandria. The VIP guests included Prof. Mahmoud Sakr, President of Egypt's Academy of Scientific Research & Technology (ASRT), Gen. Magdy Mohamadeen, Assistant to the Minister of Military Production, and Prof. Ismail Abdel-Ghafar, President of AASTMT. A photo of the main desk during the formal opening is shown in Figure 1. Figure 2 shows some of the main speakers at the opening session.

During the formal opening ceremony, Prof. Hesham El-Badawy, General Secretary of NRSC, introduced the event (Figure 2a). Prof. El-Khamy, Chair of NRSC2017, gave a briefing of the efforts that had been made during the whole past year to enable the conference in its distinguished form for the 34th time (Figure 2b). Prof. Ismail Abdel Ghafar,

AASTMT President, provided a briefing on the efforts and facilities that had been presented by AASTMT to support the NRSC2017 (Figure 2c).

The President of ASRT praised the efforts of the National Radio Science Committee, NRSC, especially in maintaining the NRSC for 34 consecutive times in different universities and research institutes in Egypt. After his talk, Prof. Sakr was honored by the conference Chair and AASTMT Chair, as shown in Figure 3.

Following the tradition of the NRSC conference series, three pioneers of radio science in Egypt were honored, and their contributions to radio theory and practice were acknowledged. They were Prof. Nabil Eldaib (Figure 4a, Military Technical College), Prof. Onsy Abd Alim (Figure 4b, Alexandria University), and Prof. Ahmed Soliman (Figure 4c, Cairo University). In addition, for the first time in the NRSC conference series, one of the logistics and administration directors of radio science in Egypt, Mr. Emad Emam (Figure 4d), technical secretary of the Egyptian NRSC, was honored for his contributions to the support of the administration procedures for more than 20 years. Figure 5 is a photo of the honored radio-science pioneers with the organizing committee of NRSC2017 and VIP guests.

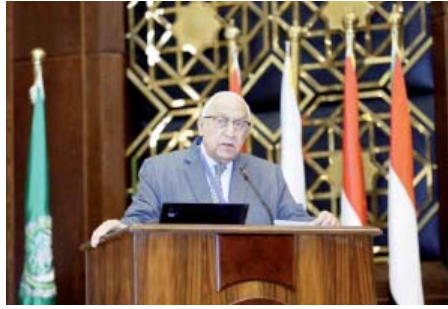


Figure 1. The formal opening ceremony of NRSC 2017. (l-r) Top row: Prof. El-Sayed Saad Conference Vice-Chair; Prof. Said El-Khamy, Conference Chair and President of Egypt's NRSC; Gen. Magdy Mohamadeen Assistant to the Minister of Military Production; Prof. Ismail Abdel Ghafar, AASTMT President; Prof. Mahmoud Sakr, President of ASRT; Prof. Allaa Abdel-Bary Vice President of AASTMT for Scientific Research; Prof. AttaAllah Hashad, Chairman of the Local Organization Committee. Front row: Prof. AbelMonem Abdel El-Bary, Local Committee member, and Prof. Khaled Shehata Conference Co-Chair.

Figure 2. Speeches at the opening ceremony:



**(a) Prof. Hesham El-Badawy,
General Secretary of NRSC**



(b) Prof. Said El-Khamy



(c) Prof. Ismail Abdel-Ghafar.

The conference attracted researchers, students, and academic staff from different universities and research institutes in Egypt. The authors came to participate and attend this highly prestigious scientific gathering. NRSC2017 was attended by more than 200 scientists and specialists. The contributors in NRSC2017 not only included Egyptian researchers, but NRSC2017 also had some papers coauthored by those from universities from Arab countries such as the Kingdom of Saudi Arabia. The Université Paris Pahad contributed one of the papers in the conference.

To the pleasant surprise of the conference organizers, a good turn out of contributions was achieved, with a total of 124 technical research papers being submitted. The selection of the papers was a challenging and difficult task. The program committee members put in a significant effort in order to provide useful feedback to the authors, with an acceptance ratio of 47.6% from the valuable submitted works. Following a rigorous refereeing process, whereby each submitted paper was blindly evaluated by three independent reviewers, only 59 papers were chosen for inclusion in the conference program.

According to the NRSC conference inspection criteria, all submitted papers were subjected to a plagiarism check with the IEEE similarity checker. After justifications of the reviewer comments and/or modifications, the accepted papers were then checked again before they were included

in the final accepted group. The final 59 accepted papers were distributed among URSI Commissions as follows:

Figure 4. Egyptian radio-science pioneers receiving honors:



(a) Prof. Nabil Eldaib



(b) Prof. Onsy Abd Alim



**(c) Prof. Mohamed Abol-Dahab,
representing Prof. Ahmed Soliman**



**(d) Mr. Emad Emam, Technical
Secretary of the Egyptian NRSC.**



Figure 3. (l-r) Honoring the ASRT President: Prof. El-Khamy, Prof. Sakr, and Prof. Abdel-Gahafar.



Figure 5. The radio scientists honored with the organizing committee of the NRSC2017 and the VIP guests.

Commission B, 18 papers; Commission C, 28 papers; Commission D, 8 papers; Commission H, 2 papers; and Commission K, 3 papers. For the second time in the NRSC conference series, all accepted papers (59 papers) were presented and no absences were recorded.

The NRSC and the IEEE Conference Publication Department have determined that the proceedings of our conference are appropriate for inclusion in the IEEE Book Broker Program and has assigned IEEE catalogue numbers for these publications. The conference proceedings are now available on IEEE Xplore.

Following the tradition of the NRSC conference series, two invited talks by distinguished keynote speakers were presented. The first keynote speaker was Prof. Said El-Khamy (Figure 6a; President of Egypt's URSI National Radio Science Committee, NRSC, and at Alexandria University). The title of his talk was "Recent Research Trends in Wireless Multimedia Communications." The second keynote speaker was Prof. Diao Khalil (Figure 6b;

Ain Shams University and Si-War Systems). His talk was entitled "MEMS Based Swept Laser Source for IR Imaging."

To encourage students and young radio scientists, 26 graduation-project posters and three Master-of-Science posters were selected for presentation at the conference. All of these students were exempted from conference fees, and some of them (from outside Alexandria) received free accommodation. The poster sessions were very crowded by the conference participants, session chairs, NRSC committee members, and other students from AASTMT, Alexandria University, and other educational institutes. Snapshots from the poster session are shown in Figure 7.

Following the NRSC tradition, five papers received awards: there were two best paper awards, in addition to three best student paper awards. As usual, URSI contributed 500 Euros towards the best student paper awards. It is worth noting that all of the papers that received awards were coauthored and presented by graduate students or young scientists. Figures 8a-8e show the awardees receiving their awards. The winning papers were as follows:

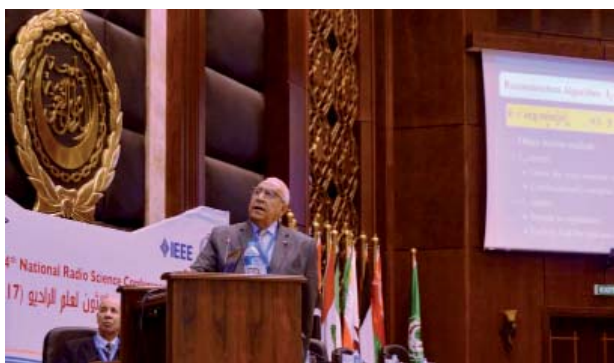


Figure 6. The keynote speakers: (a) Prof. Said El-Khamy; (b) Prof. Diao Khalil.



Figure 7. (a)-(d): Snapshots from the poster sessions.

Best Paper Awards:

1. “Multilayer Graphene-Only Transmit Array Antenna (MGOT) for Terahertz Applications,” by Dr. Walaa Hassan, Electronic Research Institute (ERI), Cairo, Egypt.
2. “Distortion of Gaussian Beams Reflected Off-Axis on Curved Mirrors in the MEMS Scale,” Eng. Yasser Sabry, Prof. Diaan Khalil, and Dr. Tarik Bourouina, Faculty of Engineering, Ain Shams University, Cairo, Egypt and Université Paris.

Figure 8. Prof. El-Sayed M. Saad, Chair of the Awards Committee; Prof. Said El-Khamy; Prof. Khaled Shehata, conference co-Chair; and Prof. Amro Ali, Dean of AASTM Alexandria College of Engineering, handling the awards to:



(a) Dr. Walaa Hassan



(b) Prof. Diaan Khalil (for Eng. Yasser Sabry)



(c) Eng. Marwa El-Sherif



(d) Eng. Ahmed Abdelaziz Salem

Figure 9. Some of the winning student-poster teams. At the left of the stage is Prof. Mohamed Hassan, coordinator of the poster sessions. The winning teams were from:



(a) Alexandria University,



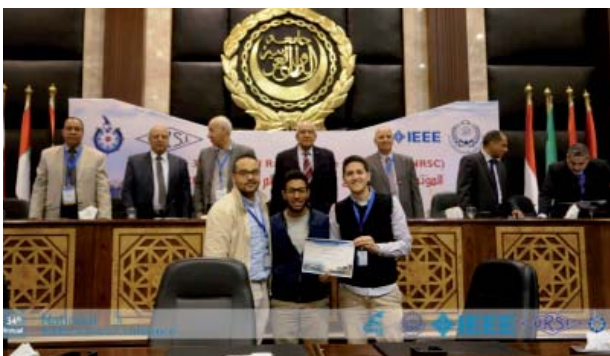
(b) AASTMT (Cairo)



(c) AASTMT (Port Said)



(d) AASTMT (Alexandria)



(e) AASTMT (Alexandria)



(f) Helwan University.

Best Student Paper Awards:

1. "Robust Image Hiding in Audio Based on Integer Wavelet Transform and Chaotic Maps Hopping," Eng. Marwa H. El-Sherif, Prof. Said E. El-Khamy, Prof. Noha O. Korany, Faculty of Engineering, Alexandria University.
2. "Game Theoretic Utility Optimization Based Power Control on Cognitive Sensor Network," Eng. Ahmed Abdelaziz Salem and Prof. Mona Shokair, Faculty of Electronic Engineering, Menoufia University, Menouf, Egypt.
3. "Low Complexity MIMO Detection Technique For 1-Bit ADC MIMO-CEM Using Adaptive Sphere Decoding," Eng. Doaa Abdelhameed, Eng. Hany S. Hussien, Prof.

Ehab Mahmoud Mohamed, Faculty of Engineering, Aswan University, Aswan, Egypt

Finally, NRSC 2017 embraced some new activities that were not typical in previous years. In particular:

Five invited talks were presented by members of the NRSC committee, about new trends:

1. "Asymmetric Double-Grating-Gated Plasmonic for Terahertz Detection," Prof. Ahmed M. Attiya, Electronics Research Institute, Giza, Egypt
2. "Optimization Algorithms: A Survey," Prof. El Sayed M. Saad, Faculty of Engineering, Helwan University



Figure 10. All winning student-poster teams with their advisors, and members of the Awards Committee.

3. "Internet of Things Technologies: A Survey," Prof. Rowayda Sadek, Faculty of Computer and Information Technology, Helwan University
4. "Fabrication and Characterization of Nano-Sensors," Prof. Abdelmoneim A. Nasser, Arab Academy for Science, Technology and Maritime Transport, Port Said, Branch
5. "WSNs for Nuclear Material Detection and Localization," Prof. Imbaby I. Mahmoud, Engineering Dept., NRC, Egyptian Atomic Energy Authority

A special session was held on "ITU: Academia Activity," by ITU Team and ITU-ASRT committee members. The session was chaired by Prof. Hadia El-Hennawy and Prof. Mohamed Aboul-Dahab.

For the second time at the NRSC conferences, student graduation projects were evaluated, and 12 of them received recognition awards. Figures 9a-9e show some of the winning student teams. Figure 10 is a memorial photo of all winning student teams with their advisors and members of the Awards Committee.

Prof. Hesham El-Badawy
Secretary General of the NRSC

Prof. Said El-Khamy
President of Egypt's NRSC
E-mail: said.elkhamy@gmail.com

September 2017

RADIO 2017

IEEE Radio and Antenna Days of the Indian Ocean

Cape Town, South Africa, 25-28 September 2017

Contact: IEEE RADIO 2017 Conference Secretariat, Email: radio2017@radiosociety.org, <http://www.radiosociety.org/radio2017/index.php>

October 2017

ISAP 2017

Phuket, Thailand, 30 October - 2 November

Contact: Dr. Titipong Lertwiriayaprapa, King Mongkut's University of Technology North Bangkok, 1518 Pracharat 1 Rd., Bangsue, Bangkok, Thailand 10800, E-mail: secretary@isap2017.org, <http://www.isap2017.org>

December 2017

International Workshop on Metamaterials-by-Design: Theory, Methods and Applications to Communications and Sensing

Madrid, Spain, 14-15 December 2017

Contact: Prof. Francisco Medina-Mena, Universidad de Sevilla, Avenida Reina Mercedes s/n, 41012 Sevilla, Spain, E-mail: medina@us.es

January 2018

USNC-URSI National Radio Science Meeting 2018

Boulder, CO, USA, 4-7 January 2018

Contact: Dr. David R. Jackson, Department of ECE, University of Houston, Houston, TX 77204-4005, USA, Fax: 713-743-4444, E-mail: djackson@uh.edu; Logistics: Christina Patarino, E-mail: christina.patarino@colorado.edu, Fax: 303-492-5959, <https://nrsmboulder.org/>

March 2018

Gi4DM 2018

Istanbul, Turkey, 18-21 March 2018

Contact: K2 Conference and Event Management Kosuyolu Mh. Ali Nazime Sk. No: 45 Kosuyolu 34718 Kadikoy / Istanbul Phone: +90 (216) 428 95 51 - Fax: +90 (216) 428 95 91 E-mail: gi4dm@k2-events.com, <http://www.gi4dm2018.org>

May 2018

AT-RASC 2018

Second URSI Atlantic Radio Science Conference

Gran Canaria, Spain, 28 May – 1 June 2018

Contact: Prof. Peter Van Daele, URSI Secretariat, Ghent University – INTEC, Technologiepark-Zwijnaarde 15, B-9052 Gent, Belgium, Fax: +32 9-264 4288, E-mail address: peter.vandaele@intec.ugent.be, <http://www.at-rasc.com>

July 2018

COSPAR 2018

42nd Scientific Assembly of the Committee on Space Research (COSPAR) and Associated Events

Pasadena, CA, USA, 14 - 22 July 2018

Contact: COSPAR Secretariat (cospar@cosparhq.cnes.fr) <http://www.cospar-assembly.org>

March 2019

C&RS “Smarter World”

18th Research Colloquium on Radio Science and Communications for a Smarter World

Dublin, Ireland, 8-9 March 2019

Contact: Dr. C. Brennan (Organising Cttee Chair) http://www.ursi2016.org/content/meetings/mc/Ireland-2017-CRS_Smarter_World_CFP.pdf

AP-RASC 2019

2019 URSI Asia-Pacific Radio Science Conference

New Delhi, India, 9-15 March 2019

Contact: Prof. Amitava Sen Gupta, E-mail: sengupto53@yahoo.com

May 2019

EMTS 2019

2019 URSI Commission B International Symposium on Electromagnetic Theory

San Diego, CA, USA, 27-31 May 2019

Contact: Prof. Sembiam R. Rengarajan, California State University, Northridge, CA, USA, Fax +1 818 677 7062, E-mail: srengarajan@csun.edu

URSI cannot be held responsible for any errors contained in this list of meetings

Information for Authors

Content

The *Radio Science Bulletin* is published four times per year by the Radio Science Press on behalf of URSI, the International Union of Radio Science. The content of the *Bulletin* falls into three categories: peer-reviewed scientific papers, correspondence items (short technical notes, letters to the editor, reports on meetings, and reviews), and general and administrative information issued by the URSI Secretariat. Scientific papers may be invited (such as papers in the *Reviews of Radio Science* series, from the Commissions of URSI) or contributed. Papers may include original contributions, but should preferably also be of a sufficiently tutorial or review nature to be of interest to a wide range of radio scientists. The *Radio Science Bulletin* is indexed and abstracted by INSPEC.

Scientific papers are subjected to peer review. The content should be original and should not duplicate information or material that has been previously published (if use is made of previously published material, this must be identified to the Editor at the time of submission). Submission of a manuscript constitutes an implicit statement by the author(s) that it has not been submitted, accepted for publication, published, or copyrighted elsewhere, unless stated differently by the author(s) at time of submission. Accepted material will not be returned unless requested by the author(s) at time of submission.

Submissions

Material submitted for publication in the scientific section of the *Bulletin* should be addressed to the Editor, whereas administrative material is handled directly with the Secretariat. Submission in electronic format according to the instructions below is preferred. There are typically no page charges for contributions following the guidelines. No free reprints are provided.

Style and Format

There are no set limits on the length of papers, but they typically range from three to 15 published pages including figures. The official languages of URSI are French and English: contributions in either language are acceptable. No specific style for the manuscript is required as the final layout of the material is done by the URSI Secretariat. Manuscripts should generally be prepared in one column for printing on one side of the paper, with as little use of automatic formatting features of word processors as possible. A complete style guide for the *Reviews of Radio Science* can be downloaded from <http://www.ips.gov.au/IPSHosted/NCRS/reviews/>. The style instructions in this can be followed for all other *Bulletin* contributions, as well. The name, affiliation, address, telephone and fax numbers, and e-mail address for all authors must be included with

All papers accepted for publication are subject to editing to provide uniformity of style and clarity of language. The publication schedule does not usually permit providing galleys to the author.

Figure captions should be on a separate page in proper style; see the above guide or any issue for examples. All lettering on figures must be of sufficient size to be at least 9 pt in size after reduction to column width. Each illustration should be identified on the back or at the bottom of the sheet with the figure number and name of author(s). If possible, the figures should also be provided in electronic format. TIF is preferred, although other formats are possible as well: please contact the Editor. Electronic versions of figures *must* be of sufficient resolution to permit good quality in print. As a rough guideline, when sized to column width, line art should have a minimum resolution of 300 dpi; color photographs should have a minimum resolution of 150 dpi with a color depth of 24 bits. 72 dpi images intended for the Web are generally *not* acceptable. Contact the Editor for further information.

Electronic Submission

A version of Microsoft *Word* is the preferred format for submissions. Submissions in versions of T_EX can be accepted in some circumstances: please contact the Editor before submitting. *A paper copy of all electronic submissions must be mailed to the Editor, including originals of all figures.* Please do *not* include figures in the same file as the text of a contribution. Electronic files can be sent to the Editor in three ways: (1) By sending a floppy diskette or CD-R; (2) By attachment to an e-mail message to the Editor (the maximum size for attachments *after* MIME encoding is about 7 MB); (3) By e-mailing the Editor instructions for downloading the material from an ftp site.

Review Process

The review process usually requires about three months. Authors may be asked to modify the manuscript if it is not accepted in its original form. The elapsed time between receipt of a manuscript and publication is usually less than twelve months.

Copyright

Submission of a contribution to the *Radio Science Bulletin* will be interpreted as assignment and release of copyright and any and all other rights to the Radio Science Press, acting as agent and trustee for URSI. Submission for publication implicitly indicates the author(s) agreement with such assignment, and certification that publication will not violate any other copyrights or other rights associated with the submitted material.

Become An Individual Member of URSI

The URSI Board of Officers is pleased to announce the establishment of Individual Fellowship (FURSI), Individual Membership (MURSI), and Individual Associate Membership (AMURSI). By joining URSI, Individual Associate Members, Individual Members, and Fellows secure recognition with their peers, are better connected to URSI Headquarters, and are better connected to their National Committees. Each can then better provide support to the other. Other benefits include discounted registration fees at URSI conferences (beginning with the 2018 URSI AT RASC) and at some conferences cosponsored by URSI (beginning with some conferences run by IEEE AP-S), a certificate of membership, and e-mail notification of the availability of the electronic edition of the URSI *Radio Science Bulletin*.

Fellowship is by invitation only. Membership and Associate Membership can be applied for through the online forms available at www.ursi.org/membership.php, or at www.ursi.org